Dissertations and Theses in Biological Sciences   Biological Sciences, School of

12-2015

A Lipidomics Approach to the Viral-Host Dynamics of the Unicellular, Eukaryotic Alga *Chlorella variabilis* and its Viral Pathogen, PBCV-1

Suzanne Rose
University of Nebraska-Lincoln, suzannerose220@gmail.com

A LIPIDOMICS APPROACH TO THE VIRAL-HOST DYNAMICS OF THE

UNICELLULAR, EUKARYOTIC ALGA *CHLORELLA VARIABILIS* AND ITS

VIRAL PATHOGEN, PBCV-1

by

Suzanne L. Rose

A DISSERTATION

Presented to the Faculty of

The Graduate College at the University of Nebraska

In Partial Fulfillment of Requirements

For the Degree of Doctor of Philosophy

Major: Biological Sciences

(Genetics, Cell, and Molecular Biology)

Under the Supervision of Professors James L. Van Etten

and Jennifer E. Markham

Lincoln, Nebraska

December, 2015

A LIPIDOMICS APPROACH TO THE VIRAL-HOST DYNAMICS OF THE

UNICELLULAR, EUKARYOTIC ALGA *CHLORELLA VARIABILIS* AND ITS

VIRAL PATHOGEN, PBCV-1

Suzanne L. Rose, Ph.D.

University of Nebraska, 2015

Advisors: James L. Van Etten and Jennifer E. Markham

This thesis focuses on the sterol and sphingolipid composition in the unicellular, green alga *Chlorella variabilis* and the lipidomic changes that occur during viral infection. Using lipid analysis by mass spectrometry, we have identified the major sterol, ergosterol and sphingolipid, glucosyl inositol phosphoceramide (GIPC) as constituents of *C. variabilis* cell membranes. Sterols and sphingolipids have essential biological functions such as hormone-based signaling, plant defense, and apoptosis as well as critical roles in structural components of the cell and organelle membranes. In chapters two and three, we focus on the characterization of sterol composition among both freshwater and marine alga and the GIPC structure among *Chlorophytes*, respectively, and the divergence of these lipids between fungi and plants. It is evident, given the current research in pathogenic lipidomics, that lipids play significant roles at many junctures of host-pathogen interactions. Viruses have been shown to exploit host membranes and their components such as sterols and sphingolipids during their infection cycle including attachment and entry, replication, protein sorting, viral assembly, and

budding. We conclude with chapter four, describing the lipid composition of the host-acquired PBCV-1 internal membrane and the effect of viral infection on lipid biogenesis in *C. variabilis*.

Table of Contents

1.0 Introduction

Using a lipidomics approach, this research sets out to define the virion lipidome of PBCV-1 as well as provide insight into algal lipid metabolic changes that occur during viral infection and viral acquisition of a host bilayer membrane to viral factories.

1.1 Eukaryotic, unicellular algae. Microalgae are unicellular, photosynthetic, eukaryotic organisms inhabiting both freshwater and marine ecosystems throughout the world. Evolving from the primary endosymbiotic event of green-algal-derived plastids, *Chlorella variabilis*, *Chlorella sorokiniana*, *Chlamydomonas reinhardtii* and *Coccomyxa subellipsoidea*, are examples of freshwater green microalgae (Kodner et al., 2008). The marine algae *Emiliania huxleyi*, a coccolithophore, and *Thalassiosira pseudonana*, a diatom, have evolved from a secondary endosymbiotic event involving red-algal-derived plastids (Kodner et al., 2008). Microalgae are of special interest in research involving novel metabolic pathways, biofuels, global net primary production and host-virus interactions. Genomes from these 6 algal species and several other green-, red- and brown-algal species have been sequenced allowing insight into important cell structure and function as well as biosynthetic pathways.

Green algae (Chlorophytes). *Chlorella variabilis* is a unicellular green alga and normally exists as a photosynthetic endosymbiont in the unicellular protozoan *Paramecium bursaria*; *P. bursaria* and its symbiont can be found in freshwater around the world. This symbiotic relationship affords *C. variabilis* protection against viral infection by the chloroviruses and it supplies sugar(s) to *P. bursaria*

(Van Etten, 2002; Van Etten, 2003; Hoshina et al., 2010; Yashchenko et al., 2012). *C. variabilis* (phylum *Chlorophyta*) has a single chloroplast and is ~ 6 µm in diameter. Its characteristic rigid cell wall contains the glucosamine polymers, chitin and chitosan, instead of cellulose found in the cell walls of land plants (Kapaun and Reisser, 1995). *C. variabilis* has a 46.2 Mb genome size with 9791 protein-encoding genes (Blanc et al., 2010). Homologs of receptors and biosynthetic enzymes of land plant hormones were identified (Blanc et al., 2010). The free-living *Chlorella sorokiniana UTEX1230*, isolated in 1953 by Sorokin and Myers, genome was recently sequenced and annotated (Cerutti et al., manuscript in preparation). *C. sorokiniana* are free-living and range in diameter from 3 – 8 µm (Morita et al., 2000). C. sorokiniana has become an important microalgae in the areas of CO_2 conversion and more recently, generation of biofuels because of its ability to grow at higher temperatures (38° – 41°C) (Morita et al., 2000). *Coccomyxa subellipsoidea* C-169 (hereafter *Coccomyxa*), a polar eukaryotic microalga, was originally classified as *Chlorella vulgaris (Holm-Hanson, 1964; Blanc et al., 2012).* Among the other sequenced algae, *Coccomyxa* is most closely related to *C. variabilis* and *C. reinhardtii.* Although a free-living, small (3 – 9 µm), non-motile alga, *Coccomyxa* contains putative genes not present in other algae which are attributed to its ability to adapt to polar climates (Blanc et al., 2012). *C. reinhardtii* (hereafter *Chlamydomonas*) is a unicellular soil algae with an alternate life cycle; possessing two flagella for motility and sensory transduction and a non-motile reproductive phase (Merchant, 2007; Miller, 2010). *Volvox carteri* (hereafter *Volvox*), a close relative

of *Chlamydomonas*, evolved motility and reproduction into two distinct cell types becoming a multicellular green alga (Miller, 2010).

Marine algae (Haptophyte). *Emiliania huxleyi* (Lohmann) Hay & Mohler (Prymnesiophyceae, Haptophyta) and *Thalassiosira pseudonana* (Hustedt) Hasle et Heimdal (Coscinodiscophyceae, Heterokontophyta), a coccolithophore and centric diatom, respectively, are unicellular marine alga (Jordan and Chamberlain, 1997; Armbrust, 2004; Alverson et al., 2011). These phytoplankton share commonalities in their evolutionary history and ecological importance and because their genomes have been sequenced they have become model algae in oceanographic research (Armbrust, 2004; Read et al., 2013). Haptophytes and heterokonts are derived from a secondary endosymbiotic event (engulfment of red-algal-derived plastids), form the base of the ocean's food web, and play an important role in biogeochemical cycles (Jordan and Chamberlain, 1997; Armbrust, 2004; von Dassow et al., 2009).

1.2 Paramecium bursaria Chlorella Virus (PBCV-1) and Chlorella variabilis as a viral-host model system. The *Phycodnaviridae* family of algal-infecting viruses encompass six genera; Chlorovirus, Coccolithovirus, Prasinovirus, Prymnesiovirus, Phaeovirus and Rhaphidovirus (ICTV, 2012). The phycodnaviruses are proposed to share a common evolutionary ancestor with a group of viruses known as nucleocytoplasmic large DNA viruses (NCLDVs) (Koonin and Yutin, 2001). The Chlorovirus PBCV-1 is probably the most studied phycodnavirus. PBCV-1 is a large (190 nm), double-stranded (ds) DNA virus with a linear, 331-kb genome predicted to encode about 416 proteins (Dunigan et

al., 2012). Its genome is enclosed in an internal lipid single bilayered membrane surrounded by an icosahedral, glycoprotein-containing outer capsid (Fig. 1) (Van Etten and Dunigan, 2012). Microarray analysis of PBCV-1 transcription during virus replication was reported in 2010 (Yanai-Balser et al., 2010). The functional characterization of gene expression delineated early, early-late and late viral transcripts as those disappearing prior to initiation of virus DNA synthesis, transcripts still detected after synthesis, and those detected only after viral DNA synthesis begins, respectively (Fig. 2) (Yanai-Balser et al., 2010). In 2012, a newly revised PBCV-1 genome, annotation, and proteomic analyses was released highlighting capsid structure and viral lifecycle. The major capsid protein (MCP) Vp54 complexes with itself to form homotrimeric capsomers responsible for the planar features of the capsid (Fig. 1) (Dunigan et al., 2012).
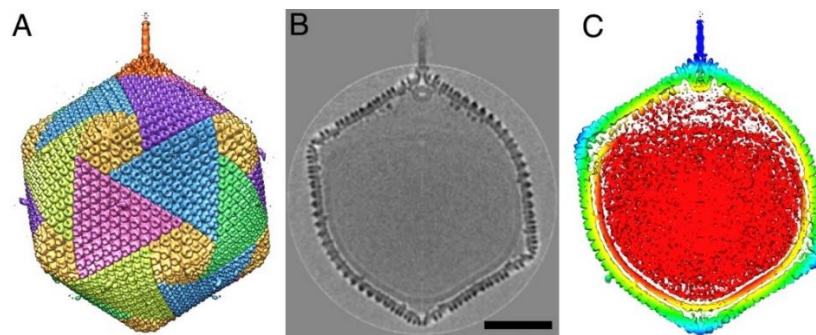
Figure 1. The five-fold-averaged cryoEM structure of PBCV-1 viewed down a quasi-2-fold axis. A) Hexagonal arrays of major capsomers form trisymmetrons and pentasymmetrons (yellow). The unique vertex with its spike structure is at the top. B) Central cross-section of the cryoEM density. (Scale bar: 500 Å) C) The same view as in B but colored radially, with red density being within 680 Å, yellow between 680 and 745 Å, green between 745 and 810 Å, light blue between 810 and 880 Å, and dark blue greater than 880 Å. Note the typical lipid low-density gap surrounding the red nucleocapsid density (Cherrier et al., 2009).

At each of the 11 icosahedral vertices are pentameric capsomers and a twelfth vertex is unique with a 560-Å-long bacteriophage-like spike structure which protrudes 340 Å from the surface of the virus (Fig. 1) (Cherrier et al., 2009; Zhang et al., 2011; Van Etten and Dunigan, 2012). PBCV-1 attaches specifically to its host *C. variabilis* which is thought to be mediated by the spike structure and external fibers extending from the surface of the virus.

Immediately upon PBCV-1 attachment, the cell wall is degraded at the site of attachment. PBCV-1 virions contain cell wall-degrading activity; the virus encodes two putative chitinase genes and one chitosanase gene, which degrade chitin (Sun et al., 1999; Chuchrid et al., 2001). Within the first minutes of infection, following cell wall degradation, the viral internal membrane presumably fuses with the host membrane, causing depolarization of the cell membrane, potassium ion efflux and an increased cytoplasmic pH (Fig. 2) (Chuchrid et al., 2001; Frohns et al., 2006; Blanc et al., 2014). PBCV-1 was the first virus discovered to encode a functional potassium ion channel (Plugge et al., 2000). The viral potassium ion channel Kcv is present in the virion internal membrane (Romani et al., 2013) the virus membrane presumably fuses with the host plasma membrane during infection, which results in depolarization of the host membrane (Fig. 2A-B) (Frohns et al., 2006). This 94 amino acid potassium ion channel protein is the smallest known potassium ion channel protein (Plugge et al., 2000) and it is essential for viral replication (Gazzarrini et al., 2003). During infection viral DNA and virion-associated proteins are predicted to migrate to the nucleus where in the first 5 minutes of infection, host chromatin begins to be degraded

(Agarkova et al., 2006). Synthesis of early viral transcripts begins at 5 – 10 min post infection (p.i) (Van Etten, 2003; Blanc et al., 2014). Viral DNA replication begins 60 – 90 min p.i. (Van Etten et al., 1984) followed by transcription of late genes (Fig. 2) (Schuster et al., 1986; Yanai-Balser et al., 2010). At about 2 – 3 h p.i. assembly of virus capsids begins in localized regions in the cytoplasm at viral assembly centers or viral factories, which become prominent by 3 – 4 h p.i. (Fig. 2C) (Meints et al., 1986; Milrot et al., 2015).
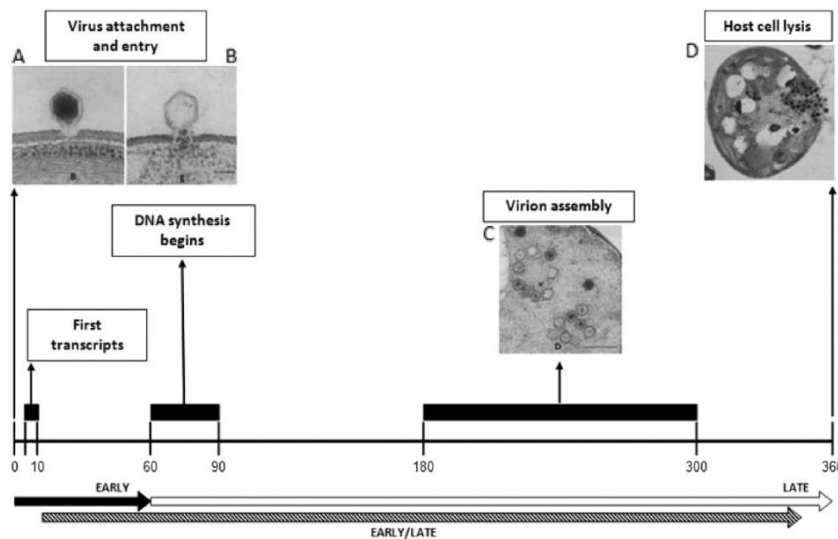
Figure 2. Timeline representing the PBCV-1 life cycle in *Chlorella* strain NC64A. Numbers represent minutes after infection. CDSs expressed before viral DNA synthesis begins were classified as early (black arrow), CDSs expressed after DNA synthesis begins were classified as late (white arrow), and CDSs expressed before and after DNA synthesis begins were classified as early/late (arrow with diagonal lines) (Meints et al., 1984; Meints et al., 1986; Yanai-Balser et al., 2010).

At 5 – 6 h after PBCV-1 infection, the cytoplasm fills with infectious progeny virus particles and localized lysis of the host cell releases progeny at 6 – 8 h p.i. (Fig. 2D). Typical burst sizes are about 1,000 virus particles/cell, of which ~25% of the particles form plaque (Van Etten and Dunigan, 2012; Blanc et al., 2014).

During the last phase of a lytic infection the products of DNA replication, procapsid assembly, and DNA packaging machinery converge at viral assembly centers to form infectious particles (Milrot et al., 2015). However, how this is accomplished by the chloroviruses is unknown. The viral DNA packaging machinery and mechanism for nucleic acid translocation into viral capsids has been described in detail for the bacteriophage PRD1, an internal-membrane containing dsDNA virus infecting bacteria (Bamford et al., 1995). Mechanisms for viral DNA packaging through a portal protein aided by an ATPase motor are numerous and have been described in detail in bacteriophage (Bamford et al., 1995; Rao and Feiss, 2008). Key to successful viral progeny production in internal membrane containing viruses is the ability to package genomes into a membrane containing procapsid. The lipid composition of the viral internal membrane that surrounds the virus PBCV-1 dsDNA within the procapsid is unknown and is the subject of Chapter 4 in this thesis. PBCV-1 viral assembly centers viewed by Cryo-Electron Microscopy (cryo-EM) show viral production occurring close to host organelles: nucleus, endoplasmic reticulum, and Golgi (Milrot et al., 2015). Recent studies of the internal-membrane-containing *Mimivirus*, an evolutionary relative of PBCV-1, describe the acquisition of host lipid membrane sheets from the endoplasmic reticulum (ER) (Kuznetsov et al., 2013; Mutsafi et al., 2013). The acquisition of the PBCV-1 internal bilayered single membrane also is derived from the host ER (Milrot et al., 2015).

1.3 Sterols

Sterols belong to a large family of over 30,000 known compounds classified as isoprenoids (Dhar et al., 2013). This group of molecules, which also include dolichols, triterpenes and ubiquinone, have important biological functions such as hormone-based signaling, plant defense, apoptosis, meiosis, protein degradation and prenylated proteins as well as serve critical roles in structural components of the cell and organelle membranes (Hunter, 2007; Dhar et al., 2013). As major structural components of plasma membranes, sterols partner with sphingolipids to form lipid raft domains creating a platform for membrane-bound proteins functioning as receptors, channels, and in host cell defense (Mercer, 1993; Rahier and Taton, 1997; Porsbring et al., 2009).

Sterols are synthesized from squalene which are cyclized to either lanosterol (fungi and animals) or cycloartenol (higher plants). Eukaryotic membranes can be characterized by the presence of C_{28}- to C_{30}- steroidal compounds containing a variable C_{24}-alkyl group side chain (Miller et al., 2012). Three pathways for isoprenoid-sterol biosynthesis have been described in detail; cholesterol (C_{24}-H) in animals, ergosterol (C_{24}-β-methyl) in fungi, and phytosterols (C_{24}-α-ethyl) in land plants (Miller et al., 2012). Assembly of sterols can be divided into three stages: production of isopentenyl diphosphate (IPP), IPP to squalene, and squalene conversion to an array of sterols. In yeast, there are 11 enzymatic steps in the squalene to ergosterol pathway, known collectively as the ergosterol (ERG) genes (Rahier and Taton, 1997). Ergosterol, also known as provitamin D_2, is found in both fungal and protozoal cell membranes and is important in the formation and source of vitamin D_2 with exposure to UV light (Veen et al., 2003).

Sterol biosynthetic pathways and effects of SBIs. Sterols are considered to be important in the regulation of biological processes, as well as in the formation and stabilization of the cell membrane. The biosynthetic pathway for sterol synthesis can be divided into three stages: 1) isopentenyl pyrophosphate isomerase (IPP) production, 2) cyclization of squalene, and 3) squalene to final sterol composition. In all eukaryotes, IPP is used as the precursor for all sterol biosynthesis. This occurs utilizing the mevalonate or methylerythritol phosphate (MEP) pathway (Fig. 3). The pathway from IPP to squalene cyclization is common to all sterol producing organisms with profound differences occurring after.
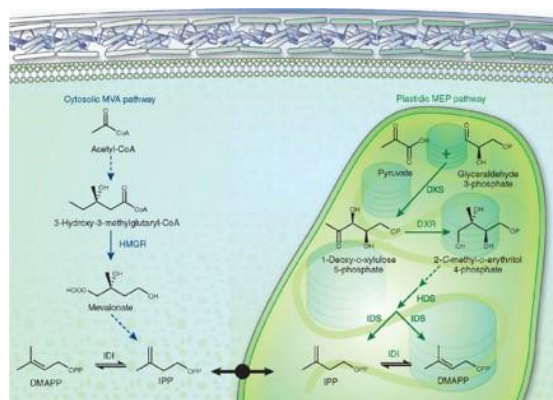
Figure 3. Compartmentalized biosynthesis of IPP and DMAPP. (Left) Via the cytosolic mevalonate (MVA) pathway. HMGR, 3-hydroxy-3-methylglutaryl coenzyme A reductase; IDI, isopentenyl diphosphate isomerase. (Right) Via the plastidic MEP pathway. DXS, 1-deoxy-D-xylulose-5-phosphate synthase; DXR, 1-deoxy-D-xylulose-5-phosphate reductoisomerase; HDS, hydroxy-2-methyl-2-(*E*)-butenyl 4-diphosphate synthase; IDS, isopentenyl diphosphate:dimethylallyl diphosphate synthase; IDI, isopentenyl diphosphate isomerase. Dashed arrows indicate more than one step (Roberts, 2007).

Mevalonate vs. non-mevalonate pathway. The universal precursors for all isoprenoids are isopentenyl diphosphate (IPP) and its isomer dimethylallyl

pyrophosphate (DMAPP) (Hunter, 2007). The cytosolic, mevalonate (MVA) pathway of non-photosynthetic organisms and the plastidal, non-mevalonate or MEP pathway, found only in photosynthetic organisms, are two nonhomologous and independent pathways, yet both produce the homologous sterol precursors IPP and DMAPP (Suzuki and Muranaka, 2007). The major route of isoprenoid biosynthesis in eukaryotes and archaea is the MVA pathway. The MEP pathway is employed by photosynthetic eukaryotes and most bacteria; however, in plants genes exist for both pathways (Lombard and Moreira, 2011). The presence of the MEP pathway in plastid containing eukaryotes are suggestive of a horizontal gene transfer (HGT) event having occurred from the first cyanobacterial plastidal endosymbiont (Lombard and Moreira, 2011).

MVA pathway. The MVA pathway begins with condensation reactions of three molecules of acetyl-Coenzyme A (CoA) to form 3-hydroxy-3-methylglutaryl coenzyme A (HMG-CoA), the last reaction being catalyzed by HMG-CoA synthase (HMGS) (Hunter, 2007). HMG-CoA reductase (HMGR), an NADPH-dependent enzyme, subsequently reduces HMG-CoA to mevalonate (Dhar et al., 2013). Mevalonate is then phosphorylated and decarboxylated by ATP-driven enzymes to yield IPP (Lombard and Moreira, 2011). Statins are a class of lipid-lowering drugs used to inhibit HMGR in the mevalonate pathway resulting in a decrease in sterol production. Therefore, statins are used to treat various human health diseases (i.e. fungal infections, high cholesterol, and cardiovascular disease) caused by non-photosynthetic pathogens (Istvan and Deisenhofer, 2001a, b; Malhotra and Goa, 2001; Hunter, 2007). Animals, fungi and higher

plants produce mevalonic acid from acetyl-CoA and acetoacetyl-CoA via the intermediate HMG-CoA (Istvan and Deisenhofer, 2001b). Therefore by targeting HMGR, statins competitively inhibit and block the first committed enzyme of isoprenoid precursor biosynthesis (Malhotra and Goa, 2001; Chugh et al., 2003). This study used the synthetic statin Atorvastatin, also known commercially as Lipitor (Pfizer), for the inhibition of HMGR. On the molecular level, statins occupy the catalytic pocket of HMGR, blocking the ability of HMG-CoA to bind and reducing the rate of mevalonate production (Istvan and Deisenhofer, 2001b; Chugh et al., 2003).

MEP pathway. The plastidal, MEP pathway of photosynthetic organisms consists of 9 enzymatic steps to produce IPP. Beginning with the condensation of pyruvate and glyceraldehyde-3-phosphate (GP3) by 1-deoxy-D-xylulose-5-phosphate synthase (DXS) to produce 1-deoxy-D-xylulose-5-phosphate (DOXP), MEP is produced by the subsequent reductoisomerase reaction by 1-deoxy-D-xylulose-5-phosphate-reductoisomerase (DXR)(Hunter, 2007; Roberts, 2007). A further six reactions take MEP to the final product and the universal isoprenoid intermediate, IPP.

The enzyme isopentenyl-diphosphate isomerase (IDI), present in both the MVA and MEP pathways is homologous, producing chemically identical molecules of IPP and its isomer DMAPP independent of the pathway used (Kuzuyama, 2002). Isomerization of the double carbon bond of IPP to create DMAPP provides downstream diversity for the vast isoprenoid biosynthetic routes branching off these two paths (Kuzuyama, 2002; Hunter, 2007). IPP and DMAPP from the

cytosolic MVA pathway are used in the isoprenoid biosynthesis of primary

metabolites such as triterpenoids, sterols, and ubiquinones where as those made

in the chloroplast are involved in the synthesis of chlorophylls, phytols, and

plastidic secondary metabolites (Dhar et al., 2013).   As the MEP pathway is

present only in photosynthetic eukaryotes and many pathogenic bacteria, the

enzymes of this pathway are therefore attractive targets in the development of

sterol biosynthesis inhibitor drugs for treatment and prevention of serious human

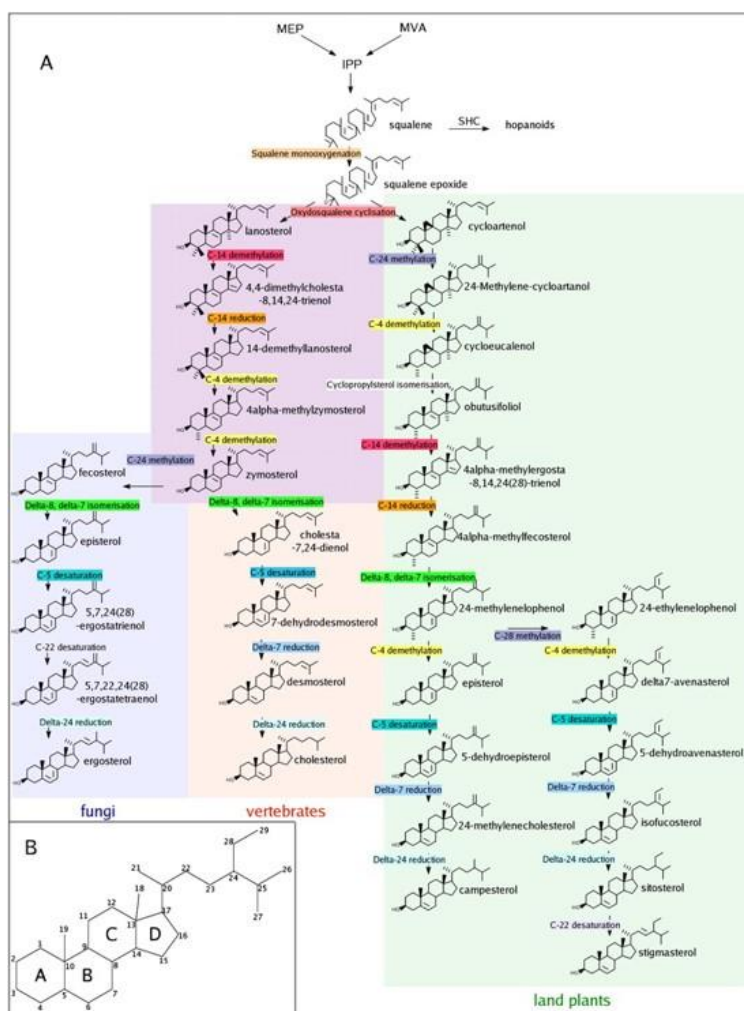and plant diseases (Kuzuyama, 2002; Hunter, 2007).

Figure 4A-B. Canonical pathways of sterol synthesis leading to land plants, fungi, and vertebrate sterols. (*A*) Canonical pathways of sterol synthesis leading to land plants, fungi, and vertebrate sterols. Upstream of squalene, the mevalonate (MVA) and 2-C-methyl-D-erythrol 4-phosphate (MEP) ways leading to IPP are shown. Downstream of squalene, the bacterial pathway of hopanoid synthesis *via* SHC is also indicated. (*B*) Numbering of carbons and cycles of steroids.

IPP to 2,3-oxidosqualene. The sterol biosynthetic pathway from IPP to 2,3-oxidosqualene (OS) is the same among all eukaryotes with significant differences occurring post-OS in both enzymatic steps and final sterol composition (Fig. 4) (Benveniste, 2004). The enzyme farnesyl pyrophosphate synthase (FPPS) mediates the chain elongation reaction by the sequential condensation of two molecules of IPP (C5) to DMAPP (C5), resulting in 15-carbon farnesyl pyrophosphate (FPP) (Dhar et al., 2013). Present in the chloroplast, cytoplasm, mitochondrion, and peroxisomes, FPPS is a key regulation enzyme of isoprenoid biosynthesis (Dhar et al., 2013). The first committed step in sterol biosynthesis is the catalysis of FPP, which is shuttled to the ER and bound by squalene synthase (SS). Through condensation of two molecules of FPP, SS catalyzes the formation of the 30 carbon, linear molecule squalene (Devarenne et al., 2002). Several studies have reported a drastic decrease in SS activity in the presence of pathogens or elicitor molecules thereby suppressing sterol biosynthesis, which supports a regulatory role of this key branch point in the isoprenoid pathway (Robinson et al., 1993; Kennedy and Bard, 2001; Devarenne et al., 2002; Rossard et al., 2010). In yeast, the production of squalene marks the beginning of committed ergosterol (ERG) biosynthesis (Alcazar-Fuoli et al., 2008). The conversion of squalene to 2,3-oxidosqualene is catalyzed by the

secondary rate limiting enzyme squalene epoxidase (SQE; ERG1) (Vago et al., 1994; Chugh et al., 2003). Terbinafine hydrochloride is a synthetic allylamine designed as a fungicidal drug which inhibits the activity of SQE (Ryder, 1992). The blocking of sterol biosynthesis at this stage in the pathway leads to an accumulation of squalene and a decrease in sterol production (Ryder, 1992; Chugh et al., 2003). Although an increase in intracellular squalene is known to be stable and non-toxic, it is the deficiency in cell membrane sterols that is suggested as contributing to the cidal action of these compounds (Ryder, 1992).

2,3-oxidosqualene to algal sterols. 2,3-oxidosqualene is a substrate for and cyclized by a wide range of oxidosqualene cyclases (OSC) including lanosterol synthase (LAS/ERG7) which produces lanosterol, a precursor for ergosterol in yeast and cholesterol in mammals and cycloartenol synthase (CAS), producing cycloartenol which enters the phytosterol pathway of plants (Benveniste, 2004; Abe, 2007). The demethylation of C-14 of lanosterol by 14α-demethylase is immediately followed by the reduction of the resulting C-14 double bond to give the precursor 14-dimethllanosterol. Present in all phyla, 14α-demethylases contain the conserved CYP450 domain, inhibition of which interferes with ergosterol production, which alters cell membrane production, fluidity and permeability leading to cell leakage and eventual cell death (Bodey, 1992; Porsbring et al., 2009; Crowley and Gallagher, 2014). A structurally diverse and broad spectrum group of fungicidal drugs, the azoles block sterol synthesis through inhibition of the 14α-demethylases (Porsbring et al., 2009; Crowley and

Gallagher, 2014). Clotrimazole and ketoconazole are both cytochrome P450

(CYP450) dependent enzyme inhibitors.

14-demethyllanosterol enters the two-cycle enzymatic process in which both C-4

methyl groups are removed consisting of C-4 demethylation (ERG25),

decarboxylation (ERG26) and 3-ketoreductase (ERG27), a complex bound to the

ER membrane by a sterol scaffold protein (ERG28) (Mo and Bard, 2005).

Recent studies in *S. cerevisiae* have shown protein-protein interactions between

the OSC (ERG7) and 3-ketoreductase (ERG27) wherein the deletion of 3-

ketoreductase inactivates the OSC (Teske et al., 2008; Taramino et al., 2010).

Although OSC is not considered a regulation enzyme of the pathway, indirectly it

is thought to be regulated by enzymes within the complex as well as other

enzymes within the pathway (Mo and Bard, 2005).

The C_{24}-side chain transmethylation reaction, catalyzed by sterol C24-methyl

transferase (24-SMT/ERG6), requires the methyl donor S-adenosyl-L-methionine

(SAM) giving 24-methylene-ergost-8,22-dienol (Miller et al., 2012). This is

followed by the isomerization of the delta8-delta7 bond (ERG2) and C-5

desaturase (ERG3) resulting in the substrate 5,7,22,24-ergostatetraenol. The

last step in the production of ergosterol is the reduction of C-24 by a reductase

(ERG4). In animals and plants, a delta 7 reduction of the substrate is required by

C-7 reductase (ERG5) as the last biosynthetic step, an enzyme not present in

Saccharomyces cerevisiae or *C. variabilis*.

Sterol biosynthesis inhibitors (SBIs) target enzymes in the sterol biosynthetic

pathway. Used commercially as fungicides in the field of agronomy and as

antimycotic drugs in human health, these compounds obstruct sterol production, disrupting the homeostasis of microbial pathogens (Burden et al., 1989; Song and Nes, 2007).   Fungicidal SBIs are designed to kill fungal pathogens whereas those that inhibit pathogenic growth are considered fungistatic drugs (Graybill et al., 1997; Lewis and Graybill, 2008). Inhibition at various stages of the sterol pathway can elucidate the importance, functionality and different roles of sterols as well as a useful tool in the investigation of as yet undescribed eukaryotic sterol biosynthetic pathways (Burden et al., 1989; Rahier and Taton, 1997).

1.4 Sphingolipids

The site of structural lipid synthesis begins in the endoplasmic reticulum (ER); producing the majority of the sterols, phospholipids, and ceramide precursors for complex sphingolipids (Fig. 5) (Van Meer et al., 2008). Ceramide precursors follow the secretory pathway to the Golgi where they are synthesized to glucosyl inositol phosphoceramide (GIPC) sphingolipids before joining their sterol partners in lipid raft formation at the plasma membrane (Fig. 5) (Xu et al., 2001; Van Meer et al., 2008; Guan et al., 2009; Gulati et al., 2010). Sphingolipids can be distinguished by distinct classes: 1) Long chain sphingoid bases (LCBs) 2) ceramides and 3) glycosylated sphingolipids (Cacas et al., 2012). Representing the conserved precursors for all other sphingolipid classes, LCBs are long chain aliphatic amines containing two or three hydroxyl groups and are either saturated or mono-unsaturated (Fig. 6) (Cacas et al., 2012).
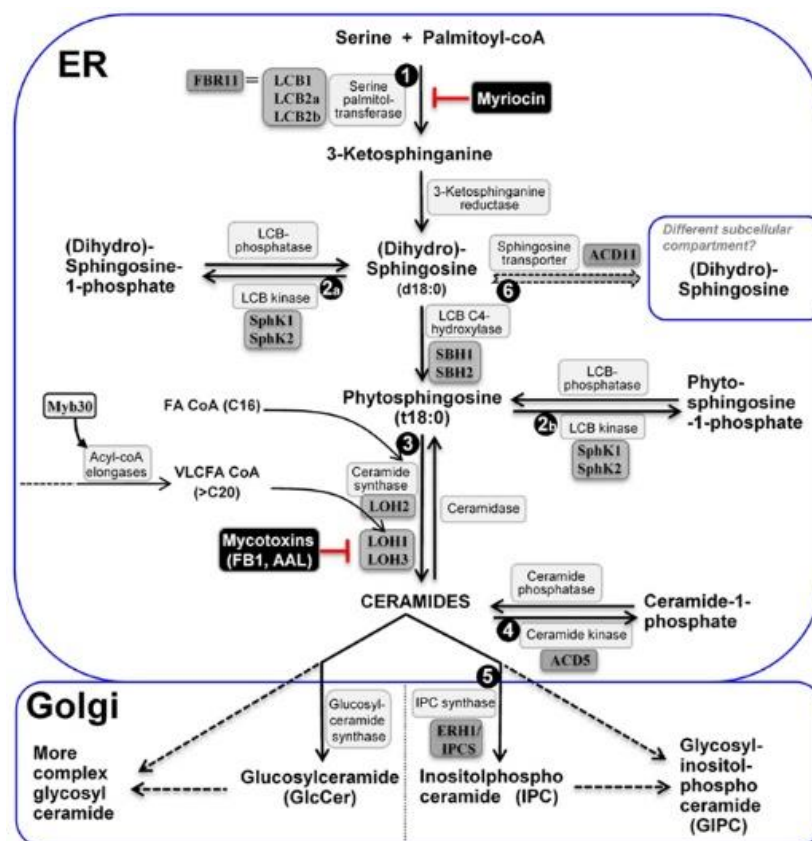
Figure 5. The major steps of sphingolipid metabolism in plants. De novo ceramide synthesis occurs in the ER and synthesis of more complex sphingolipids occurs in the Golgi apparatus. The metabolic steps genetically characterized to be critical for plant PCD regulation are enumerated 1 – 6; Name of enzymes are in white boxes, and genetically characterized ones in gray boxes; Uncharacterized steps are linked with dashed lines (Berkey et al., 2012).

Nomenclature is used to define these variations in LCBs and hydroxy fatty acids (see below); the prefix 'd' or 't' denotes di- or trihydroxy bases and is followed by chain length and number of double bonds (Bure et al., 2014). Major LCBs have been identified in all three kingdoms; fungi t18:0, plants t18:1 and animals d18:1 (Markham et al., 2006; Bure et al., 2014). Ceramides are composed of an LCB to which a fatty acyl chain has been amidified (Fig. 6) (Cacas et al., 2012) The structural differences of ceramides – length, unsaturation, and degree of

hydroxylation of both the LCB and the fatty acyl chain – are recognized as

determining the biophysical and biochemical effects of membrane properties

(Marques et al., 2015).

Glycosylated sphingolipids (GSLs) are considered the most diverse class of

lipids. The esterification of one or multiple sugar moieties either directly to

ceramide or through an intermediate inositol phosphate (IP) group linked to the

ceramide (IPC) via an ester bond results in glucosyl inositol phosphoceramides

(GIPCs), found only in fungi and plants (Cacas et al., 2012; Han et al., 2015).
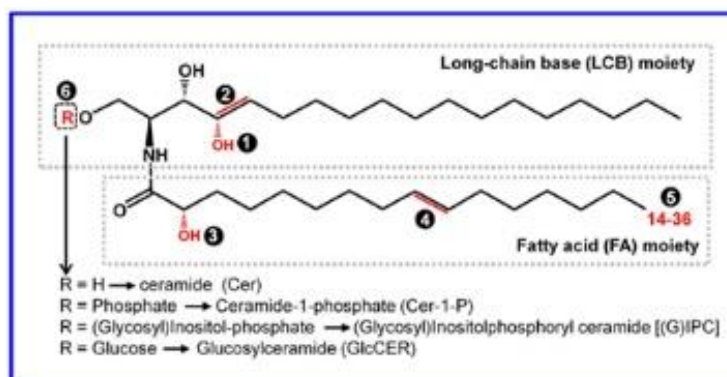
Figure 6. The basic structure, building blocks, and sources for structural diversity of sphingolipids. All the structural variables are highlighted in red and indicated by a number in a shaded circle. Ceramide (Cer) is the fundamental unit of all complex sphingolipids. The Cer core consists of two structural moieties: the sphingoid long-chain base (LCB) and the fatty acid (FA) chain linked via an amide bond. The typical LCB has a chain length of 18 carbons, which may be hydroxylated at 4-position (1), or have a double bond at the 4 or 8 carbon (2). The FA chain may be hydroxylated at the α-position (3), and/or have a double bond at ω9-position (4). The FA chain length may vary from 14 to 36 (if > 20, it is referred to as very long-chain FA, i.e., VLCFA) (5). The structurally diverse ceramides can be converted to more complex sphingolipids via substitution of the head group designated R at the 1-position of the LCB (6). Additional sugar residues may be further added to IPCs and GlcCERs, resulting in more complex sphingolipids (Berkey et al., 2012).

The addition of a hexuronic acid between the IPC and the sugar moieties has been described in plants, but not seen in fungi. The head group modifications as well as the core ceramide structure of GSLs enable their diverse and unique functions in eukaryotic cells (Breslow and Weissman, 2010).

1.5 Lipidomics

Lipidomics among animals, plants, fungi and bacteria have been studied in detail; however, it is understudied in microalgal cells (Markham et al., 2006; Gross and Han, 2007; Kumari et al., 2012; Bure et al., 2014). Development of biofuels and implications of algae as a renewable resource has triggered current algal lipidomic research. The amphipathic nature of lipids are responsible for the creation of bilayer membranes and maintain the fluidity and selective permeability of cell membranes (Van Meer et al., 2008). From the basic building blocks, ketoacyl and isoprene groups, the structural diversity of all possible combinations of lipid molecular species is estimated to be over 200,000 (Seppanen-Laakso and Oresic, 2009). Phospholipids (PL) make up approximately 10-20% of total lipids present in algal membranes; phosphatidylcholine (PC), phosphatidylglycerol (PG), phosphatidylethanolamine (PE), phosphatidylinositol (PI), phosphatidylserine (PS), and phosphatidic acid (PA) (Kumari et al., 2012). In addition to phospholipids are glycolipids; monogalactosyldiacylglycerol (MGDG), digalactosyldiacylglycerol (DGDG), and sulfoquinovosyldiacylglycerol (SQDG) and the non-polar or neutral glycerolipids, diacylglycerol (DAG) and triacylglycerol (TAG). Within algae, TAGs are the predominant neutral lipid. Stored as lipid bodies within the cytosol as both a

product and energy reservoir, TAGs are reutilized for fatty acids (FAs) and acyl

group donation for lipid biosynthesis under adverse conditions (Kumari et al.,

2012). The use of mass spectrometric analytic techniques has furthered the field

of lipidomics and the ability to classify organisms based on their lipid content.

Mass spectrometry. The aim of lipidomic research is to identify and quantitate

the complete profile of lipid molecules in cells, tissues or organisms – the

lipidome – as well as study their structure, function, interactions and cellular

dynamics (Wenk, 2005; Seppanen-Laakso and Oresic, 2009). Lipidomic

analysis relies on mass spectrometry (MS), an analytical technique which allows

the study of intact lipid species – quantitative (concentration or molecular mass)

and qualitative (structure) (Han and Gross, 2005; Bou Khalil et al., 2010; Han

and Christie, 2010). Methods used to extract lipids from a sample are dependent

on the class of lipids targeted or analytical method to be used.

Detection of a fatty acid by LC-MS/MS
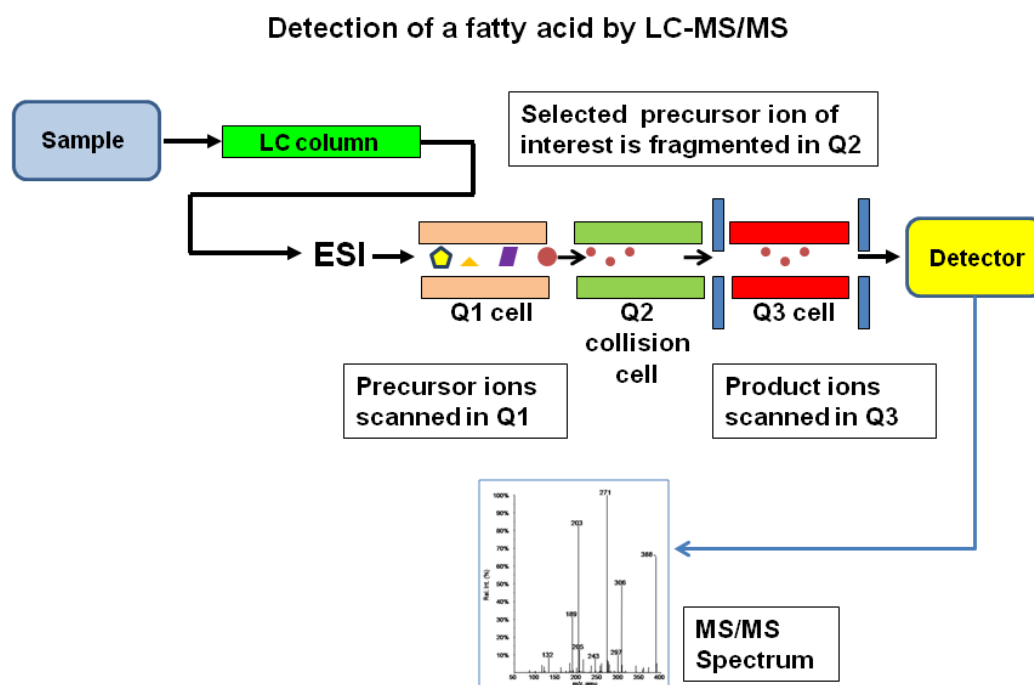
Figure 7. Scheme showing detection of a fatty acid by LC-MS/MS using a linear ion-trap instrument and an electrospray (ESI) ion source (Tandem ms by Lmaps).

Gas Chromatography – Mass Spectrometry (GC-MS) is a common method used for the analysis of sterols and hydroxyl fatty acid methyl esters, whereas fatty acid analysis requires Liquid Chromatography – Mass Spectrometry (LC-MS) (Fig. 7). Total lipid extracts can be introduced to MS after separation by gas chromatography (GC), high performance liquid chromatography (HPLC or LC) or by direct infusion into the MS – "shotgun lipidomics" (Ho et al., 2003; Han and Gross, 2005; German et al., 2007). Flame ionization detection (FID) is used to measure the concentration of organic species (i.e. hydrocarbons) of a sample in a gas stream and is most commonly used as a detector in gas chromatography (GC) (Ackman and Sipos, 1964). HPLC is used extensively for lipid separation of extracts prior to mass analysis; separation of different lipid classes as groups such as sterol esters, fatty acids, free sterol, phospholipids, glycerolipids and ceramides (Seppanen-Laakso and Oresic, 2009). For detection by MS, analytes require the acquisition of a positive or negative ionic charge. Electrospray ionization (ESI), a common ionization technique, is a soft ionization method which does not cause extensive fragmentation prior to mass analysis and is applicable for complex solutions with the advantage of high accuracy, sensitivity, and reproducibility (Fenn et al., 1989; Ho et al., 2003; Seppanen-Laakso and Oresic, 2009). ESI can be used in positive ion mode (ESI+) enabling analysis of diverse lipid classes (i.e. sphingolipids, phospholipids, and acylglycerols) or in negative ion mode (ESI-) (i.e. phosphatidylinositol, phosphatidic acid, and

phosphatidylserine) (Seppanen-Laakso and Oresic, 2009; Brugger, 2014). Ions arrive at a detector after traveling through a quadrupole mass analyzer, their ionic movement through a magnetic or electrical field is affected by their mass to charge ratio (m/z) (Fig. 7) (Ho et al., 2003). Typically, a tandem quadrupole system has a series of three linear quadrupoles where the first (Q1) and third (Q3) are mass spectrometers where the second, center quadrupole (Q2) is a collision cell (Murphy et al., 2001). Analyte ions entering the collision cell collide with a collision gas and undergo further fragmentation, a process called collision-induced dissociation (CID). The detector collects the data and displays the signals graphically as a mass spectrum, reflecting the relative abundance of the ion signals according to their m/z ratio (Ho et al., 2003; German et al., 2007). Several modes of data acquisition are used: 1) precursor scan (parent scan) where ions are scanned in Q1 over a range of precursor ions and Q3 focuses on one product ion resulting from CID of a lipid class, 2) product scan (daughter scan) in which an ion of specific m/z ratio is allowed to pass through and Q3 scans the product ions from CID, and 3) neutral loss where both Q1 and Q3 scan at a constant difference in m/z ratio in conjunction to monitor the loss of a neutral fragment after CID for a class of lipids (Fig. 7) (Ho et al., 2003).

1.6 Summary

Sterols are essential molecules found in nearly every eukaryotic cell membrane. Having the unique ability to partner with sphingolipids, together they maintain the integrity, fluidity and permeability of cell membranes through the formation of detergent-resistant lipid rafts. Most eukaryotes and some

prokaryotes encode the enzymatic genes required for sterol biosynthesis. Non-photosynthetic eukaryotes, animals and fungi, follow a different biosynthetic pathway than that found in plants or photosynthetic eukaryotes. The major sterols produced in non-photosynthetic organisms are cholesterol and ergosterol, animals and fungi, respectively. The phytosterols stigmasterol, campesterol, and beta (β)-sitosterol have been reported in various combinations and concentrations in plants. Prior studies on the unicellular, photosynthetic alga *C. reinhardtii* have reported a combination of both a phytosterol and ergosterol as sterol components within its cellular membranes; their production has been proposed to use the classical phytosterol biosynthetic pathway. Belonging to the same phylum as *C. reinhardtii*, our research goal was to identify and characterize the sterol genes and sterol biosynthetic pathway in the genus *Chlorella.* Through the use of gene gazing, targeted inhibition of the sterol biosynthetic pathway with sterol biosynthesis inhibitors (SBIs) – statin, terbinafine, and azoles – and GC/MS analysis, we identified ergosterol as the major sterol in *C. variabilis* cell membranes. Moreover, we describe a hybrid ergosterol biosynthetic pathway that is unique to this unicellular, photosynthetic alga. In Chapter 2 of this thesis we illustrate the use of the photosynthetic, non-mevalonate, sterol precursor pathway by *C. variabilis* in the formation of isopentenyl disphosphate (IPP), which then crosses over and is fed into the non-photosynthetic, fungal-like, sterol pathway to produce ergosterol.

The identification and characterization of glycosyl inositol phosphoceramides (GPICs) in plants is a current topic of interest in lipid

research; however, little information exists on the prevalence of this sphingolipid class in algae. Advances in mass spectrometric methods provides the tools for the structural analysis of GIPCs. The main goal of this research focuses on the characterization and structure analysis of the major sphingolipid, GIPCs, of the unicellular green algae (division *Chlorophyta*). Given the ecological and evolutionary divergence among algae we anticipated variances in their overall GIPC structure. In chapter 3 of this thesis, Liquid Chromatography- and Gas Chromatography-Mass Spectrometry was used in the analysis of long chain base (LCB) and fatty acid (FA) composition, respectively, to identify the major ceramide structure of *Chlorophytes* as having a trihydroxylated, 18-carbon LCB (t18:0) and a 24-carbon hydroxy FA (h24:0), both either saturated or monounsaturated. GIPC profiling was performed for *C. variabilis*, *C. sorokiniana*, *C. reinhardtii*, and *C. subellipsoidea*. Complete structure analysis of the major GIPCs was successfully determined using HPLC-ESI-MS. GIPC-fragment ions were detected and, based on fragmentation patterns, final structures were characterized regarding fatty acyl chain, long chain base and polar head groups. Variance among the Chlorophytes was observed in the presence or absence of hexuronic acid in their GIPCs. This research will provide the foundation for future research in elucidating the role of algal GIPC sphingolipids as components of specialized microdomains, or lipid rafts, in the cell membrane. Enriched in GIPC sphingolipids, sterols and membrane-associated proteins, substantial evidence supports these specialized microdomains play a central role in regulating cellular processes, stress response and viral infection. To date, little is known on the role

sphingolipids play in unicellular algae, the characterization of which is integral to understanding the vast array of cell dynamics, which is the main focus of Chapter 3 of this thesis.

PBCV-1 is the type member of the *Chlorovirus* genus. PBCV-1 is a lytic, double-strand (ds) DNA virus with a 331-kb genome enclosed in an internal, single bilayered membrane surrounded by an icosahedral outer capsid containing a spike structure at one vertex. Its fresh-water host, *C. variabilis*, is a unicellular, eukaryotic green alga and an endosymbiont of *Paramecium bursaria*. PBCV-1 has a 6 to 8 h life cycle with DNA synthesis starting at 60 – 90 min p.i. Virus assembly centers are visible in the cytoplasm at 2 to 5 h p.i. followed by localized lysis and release of infectious progeny at 6 to 8 h p.i. Viral DNA packaging is the culminating step in virion assembly leading to the production of infectious progeny inside the cell. In this study we describe the lipid composition of the PBCV-1 internal membrane and the effect of viral infection on lipid biogenesis in *C. variabilis*. The increased levels of ergosterol, long chain bases and hydroxy fatty acid methyl esters change very little during viral infection. There is an increase in mRNAs involved in sphingolipid biosynthesis and a decrease in sterol biosynthetic mRNAs during PBCV-1 replication. Electrospray Ionization-Mass Spectrometry of the PBCV-1 internal membrane detected diacylglycerol, ceramide, phospholipids, cardiolipin, and several unidentified peaks indicating that new lipid species were present in the virion that might result from viral lipid-modification proteins. Chapter 4 of this thesis is a culmination of

our research on sterol and sphingolipid metabolism in *C.variabilis* and its

application in pathogenic lipidomics.

1.7 References

Abe, I. (2007). Enzymatic synthesis of cyclic triterpenes. Natural Product Reports 24, 1311-1331.

Ackman, R., and Sipos, J. (1964). Application of specific response factors in the gas chromatographic analysis of methyl esters of fatty acis with flame ionization detectors. Journal of the American Oil Chemists Society 41, 377-378.

Alcazar-Fuoli, L., Mellado, E., Garcia-Effron, G., Lopez, J.F., Grimalt, J.O., Cuenca-Estrella, J.M., and Rodriguez-Tudela, J.L. (2008). Ergosterol biosynthesis pathway in Aspergillus fumigatus. Steroids 73, 339-347.

Alverson, A.J., Beszteri, B., Julius, M.L., and Theriot, E.C. (2011). The model marine diatom Thalassiosira pseudonana likely descended from a freshwater ancestor in the genus Cyclotella. BMC Evolutionary Biology 11.

Armbrust, E.V.e.a. (2004). The Genome of the Diatom Thlassiosira Pseudonana: Ecology, Evolution, and Metabolism. Science 306.

Bamford, D., Caldentey, J., and Bamford, J. (1995). Bacteriophage PRD1: a broad host range dsDNA tectivirus with an internal membrane. Advances in Virus Research 45, 281-319.

Benveniste, P. (2004). Biosynthesis and Accumulation of Sterols. Annual Review of Plant Biology 55, 429-457.

Berkey, R., Bendigeri, D., and Xiao, S. (2012). Sphingolipids and plant defense/dis3ease: the "death" connection and beyond. Frontiers in Plant Science 3.

Blanc, G., Mozar, M., Agarkova, I., Gurnon, J., Yanai-Balser, G.M., Rowe, J.M., Xia, Y., Riethoven, J.-J., Dunigan, D.D., and Van Etten, J.L. (2014). Deep RNA sequencing reveals hidden features and dynamics of early gene transcription in Paramecium bursaria Chlorella Virus 1. PLoS ONE 9.

Blanc, G., Duncan, G., Agarkova, I., Borodovsky, M., Gurnon, J., Kuo, A., Lindquist, E., Pangilinan, J., Polle, J., Salamov, A., Terry, A., Yamada, T., Dunigan, D.D., Grigoriev, I.V., Claverie, J.-M., and Van Etten, J.L. (2010). The Chlorella variabilis NC64A genome reveals adaptation to photosymbiosis, coevolution with viruses, and cryptic sex. Plant Cell 22, 2943-2955.

Blanc, G., Agarkova, I., Grimwood, J., Kuo, A., Bruegeman, A., Dunigan, D.D., Gurnon, J., Ladunga, I., Lindquist, E., Lucas, S., Pangilinan, J., Proschold, T., Salamov, A., Schmutz, J., Weeks, D., Yamada, T., Lomsadze, A., Borodovsky, M., Claverie, J.-M., Grigoriev, I.V., and Van Etten, J.L. (2012). The genome of the polar eukaryotic microalgo Coccomyxa subellipsoidea reveals traits of cold adaptation. Genome Biology 13.

Bodey, G. (1992). Azole antifungal agents. Clinical infectious diseases: An official publication of the Infectious Diseases Society of America 14, S161-169.

Bou Khalil, M., Hou, W., Zhou, H., Elisma, F., Swayne, L., Blanchard, A., Yao, Z., Bennett, S., and Figeys, D. (2010). Lipidomics era: accomplishments and challenges. Mass Spectrometry Reviews 29, 877-929.

Breslow, D.K., and Weissman, J.S. (2010). Membranes in Balance: Mechanisms of Sphingolipid Homeostasis. Molecular Cell 40.

Brugger, B. (2014). Lipidomics: Analysis of the lipid composition of cells and subcellular organelles by electrospray ionization mass spectrometry. Annual Review of Biochemistry 83, 79-98.

Burden, R.S., Cooke, D.T., and Carter, G.A. (1989). Inhibitors of Sterol Biosynthesis and Growth in Plants and Fungi. Phytochemistry 28, 1791-1804.

Bure, C., Cacas, J.-L., and Mongrand, S. (2014). Characterization of glycosyl inositol phosphoryl ceramides from plants and fungi by mass spectrometry. Analytical and Bioanalytical Chemistry 406, 995-1010.

Cacas, J.-L., Melser, S., Domergue, F., Joubes, J., Bourdeux, B., Schmitter, J.-M., and Mongrand, S. (2012). Rapid nanoscale quantitative analysis of plant sphingolipid long-chain bases by GC-MS. Analytical and Bioanalytical Chemistry 403, 2745-2755.

Cherrier, M.V., Kostyuchenko, V.A., Xiao, C., Bowman, V.D., Battisti, A.J., Yan, X., Chipman, P.R., Baker, T.S., Van Etten, J.L., and Rossmann, M.G. (2009). An icosahedral algal virus has a complex unique vertex decorated by a spike. PNAS 106, 11085-11089.

Chuchrid, N., Hiramatsu, S., Sugimoto, I., Fujie, M., Usami, S., and Yamada, T. (2001). Digestion of Chlorella cells by Chlorovirus-encoded polysaccharide degrading enzymes. Microbes and Environments 16, 206-212.

Chugh, A., Ray, A., and Gupta, J. (2003). Squalene epoxidase as hypercholesterolemic drug target revisted. Progress in Lipid Research 42, 37-50.

Crowley, P.D., and Gallagher, H.C. (2014). Clotrimazole as a pharmaceutical: past, present and future. Journal of Applied Microbiology 117, 611-617.

Devarenne, T.P., Ghosh, A., and Chappell, J. (2002). Regulation of Squalene Synthase, a Key Enzyme of Sterol Biosynthesis, in Tobacco. Plant Physiology 129, 1095-1106.

Dhar, M.K., Koul, A., and Kaul, S. (2013). Farnesyl pyrophosphate synthase: a key enzyme in isoprenoid biosynthetic pathway and potential molecular target for drug development. New Biotechnology 30.

Dunigan, D.D., Cerny, R.L., Bauman, A.T., Roach, J.C., Lane, L.C., Agarkova, I., Wulser, K., Yanai-Balser, G.M., Gurnon, J., Vitek, J.C., Kronschnabel, B.J., Jeanniard, A., Blanc, G., Upton, C., Duncan, G.A., McClung, O.W., Ma, F., and Van Etten, J.L. (2012). Paramecium bursaria Chlorella Virus 1 proteome reveals novel architectural and regulatory features of a giant virus. Journal of Virology 86, 8821-8834.

Fenn, J., Mann, M., Meng, C., Wong, S., and Whitehouse, C. (1989). Electrospray ionization for mass spectrometry of large biomolecules. Science 246, 64-71.

Frohns, F., Kasmann, A., Kramer, D., Schafer, B., Mehmel, M., Kang, M., Van Etten, J., Gazzarrini, S., Moroni, A., and Thiel, G. (2006). Potassium ion channels of Chlorella viruses cause rapid depolarization of host cells during infection. Journal of Virology 80, 2437-2444.

Gazzarrini, S., Severino, M., Lombardi, M., Morandi, M., DiFrancesco, D., Van Etten, J.L., Thiel, G., and Moroni, A. (2003). The viral postassium channel Kcv: structural and functional features. FEBS Letters 552, 12-16.

German, J., Gillies, L., Smilowitz, J., Zivkovic, A., and Watkins, S. (2007). Lipidomics and lipid profiling in metabolomics. Current Opinion in Lipidology 18, 66-71.

Graybill, J., Burgess, D., and Hardin, T. (1997). Key issues concerning fungistatic versus fungicidal drugs. European Journal of Clinical Microbiology and Infectious Dieseases 16, 42-50.

Gross, R., and Han, X. (2007). Lipidomics in diabetes and the metabolic syndrome. Methods in Enzymology 433, 73-90.

Guan, X.L., Souza, C.M., Pichler, H., Dewhurst, G., Schaad, O., Kajiwara, K., Wakabayashi, H., Ivanova, T., Castillon, G.A., Piccolis, M., Abe, F., Loewith, R., Funato, K., Wenk, M.R., and Riezman, H. (2009). Functional Interactions between Sphingolipids and Sterols in Biological Membranes Regulating Cell Physiology. Molecular Biology of the Cell 20, 2083-2095.

Gulati, S., Munkacsi, A.B., Wilcox, L., and Sturley, S.L. (2010). Sterols and sphingolipids: Dynamic duo or partners in crime? Progress in Lipid Research 49, 353-365.

Han, X., and Gross, R. (2005). Shotgun lipidomics: electrospray ionization mass spectrometric analysis and quantitation of cellular lipidomes directly from crude extracts of biological samples. Mass Spectrometry Reviews 24, 367-412.

Han, X., and Christie, W.W. (2010). Lipid Analysis: Isolation, Separation, Identification and Lipidomic Analysis. (Bridgewater, England: The Oily Press).

Han, Y.-B., Wu, L., Rich, J.R., Huang, F.-T., Withers, S.G., Feng, Y., and Yang, G.-Y. (2015). Comprehensive characterization of sphingolipid ceramide N-deacylase for the synthesis and fatty acid remodeling of glycosphingolipids. Applied Microbiology and Biotechnology 99, 6715-6726.

Ho, C., Lam, C., Chan, M., Cheung, L., Law, L., Lit, L., Ng, K., Suen, M., and Tai, H. (2003). Electrospray ionisation mass spectrometry: principles and clinical applications. Clinical Biochemistry Review 24, 3-12.

Holm-Hanson, O. (1964). Isolation and culture of terrestrial and fresh-water algae of Antartica. Phycologia 4, 43-51.

Hoshina, R., Iwataki, M., and Imamura, N. (2010). Chlorella variabilis and Micractinium reisseri sp. nov. (Chlorellaceae, Trebouxiophyceae): Redscription of the endosymbiotic green algae of Paramecium bursaria

(Peniculia, Oligohymenophorea) in the 120th year. Phycological Research 58, 188-201.

Hunter, W.N. (2007). The Non-mevalonate Pathway of isoprenoid Precursor Biosynthesis. The Journal of Biological Chemistry 282, 21573-21577.

ICTV. (2012). Virus taxonomy: Classification and nomenclature of viruses: Ninth Report of the International Committee on Taxonomy of Viruses, A. King, M. Adams, E. Carstens, and E. Lefkowitz, eds (San Diego: Elsevier Academic Press).

Istvan, E.S., and Deisenhofer, J. (2001a). The structure of the catalytic portion of human HMG-CoA reductase. Biochimica et Biophysica Acta 1529, 9-18.

Istvan, E.S., and Deisenhofer, J. (2001b). Structural mechanism for statin inhibition of HMG-CoA reductase. Science 292, 1160-1164.

Jordan, R.W., and Chamberlain, A.H.L. (1997). Biodiversity among haptophyte algae. Biodiversity Conservation 6, 131-152.

Kapaun, E., and Reisser, W. (1995). A chitin-like glycan in the cell wall of a Chlorella sp. (Chlorococcales, Chlorophyceae). Planta 197, 577-582.

Kennedy, M., and Bard, M. (2001). Positive and negative regulation of squalene synthase (erg9), an ergosterol biosynthetic gene, in Saccromyces cerevisiae. Biochimica et Biophysica Acta 1517, 177-189.

Kodner, R.B., Pearson, A., Summons, R.E., and Knoll, A.H. (2008). Sterols in red and green algae: quantification, phylogeny, and relevance for the interpretation of geologic steranes. Geobiology 6, 411-420.

Koonin, E.V., and Yutin, N. (2001). Nucleo-cytoplasmic Large DNA Viruses (NCLDV) of Eukaryotes. In eLS (John Wiley & Sons, Ltd.

Kumari, P., Kumar, M., Reddy, C., and Jha, B. (2012). Algal lipids, fatty acids and sterols. In Functional ingredients from algae for foods and nutraceuticals, H. Dominguez, ed (Woodhead Publishing Ltd.), pp. 87-134.

Kuznetsov, Y., Klose, T., Rossmann, M.G., and McPherson, A. (2013). Morphogenesis of Mimivirus and its viral factories: an atomic force microscopy study of infected cells. Journal of Virology 87, 11200-11213.

Kuzuyama, T. (2002). Mevalonate and Nonmevalonate Pathways for the Biosynthesis of Isoprene Units. Bioscience Biotechnology Biochemistry 66, 1619-1627.

Lewis, J., and Graybill, J. (2008). Fungicidal versus fungistatic: What's in a word? Expert opinion on pharmacotherapy 9, 927-935.

Lombard, J., and Moreira, D. (2011). Origins and Early Evolution of the Mevalonate Pathway of isoprenoid Biosynthesis in the Three Domains of Life. Molecular Biology and Evolution 28, 87-99.

Malhotra, H., and Goa, K. (2001). Atorvastatin: an updated review of its pharmacological properties and use in dyslipidemia. Drugs 61, 1835-1881.

Markham, J.E., Li, J., Cahoon, E.B., and Jaworski, J.G. (2006). Separation and Identification of Major Plant Sphingolipid Classes from Leaves. The Journal of Biological Chemistry 281, 22684-22694.

Marques, J.T., Cordeiro, A.M., Viana, A.S., Herrmann, A., Marinho, H.S., and de Almeida, R.F. (2015). Formation and Properties of Membrane-Ordered

Domains by Phytoceramide: Role of Sphingoid Base Hydroxylation. In ACS Publications - Langmuir, pp. 12.

Mehmel, M., Rothermel, M., Meckel, T., Van Etten, J.L., Moroni, A., and Thiel, G. (2003). Possible function for virus encoded K+ channel Kcv in the replication of chlorella virus PBCV-1. FEBS Letters 552, 7-11.

Meints, R.H., Lee, K., and Van Etten, J.L. (1986). Assembly site of the virus PBCV-1 in a Chlorella-like green alga: ultrastructural studies. Virology 154, 240-245.

Meints, R.H., Lee, K., Burbank, D.E., and Van Etten, J.L. (1984). Infection of a chlorella-like alga with the virus, PBCV-1: Ultrastructural studies. Virology 138, 341-346.

Mercer, E. (1993). Inhibitors of sterol biosynthesis and their applications. Progress in Lipid Research 32, 357-416.

Merchant, S.S.e.a. (2007). The Chlamydomonas Genome Reveals the Evolution of Key Animal and Plant Functions. Science 318.

Miller, M.B., Haubrich, B.A., Wang, Q., Snell, W.J., and Nes, D. (2012). Evolutionarily conserved delta 25(27)-olefin ergosterol biosynthesis pathway in the alga Chlamydomonas reinhardtii. Journal of Lipid Research 53, 1636-1645.

Miller, S.M. (2010). Volox, Chlamydomonas, and the Evolution of Multicellularity. Nature Education 3, 65.

Milrot, E., Mutsafi, Y., Fridmann-Sirkis, Y., Shimoni, E., Rechav, K., Gurnon, J., Van Etten, J.L., and Minsky, A. (2015). Virus-host interactions: insights from the replication cycle of the large Paramecium bursaria Chlorella virus. Cellular Microbiology.

Mo, C., and Bard, M. (2005). A systematic study of yeast sterol biosynthetic protein-protein interactions using the split-ubiquitin system. Biochemical and Biophysical Acta 1737, 152-160.

Morita, M., Watanabe, Y., and Saiki, H. (2000). High photosynthetic productivity of green microalga Chlorella sorokiniana. Applied Biochemistry and Biotechnology 87, 203-218.

Murphy, R., Fiedler, J., and Hevco, J. (2001). Analysis of nonvolatile lipids by mass spectrometry. Chemical Reviews 101, 479-526.

Mutsafi, Y., Shimoni, E., Shimon, A., and Minsky, A. (2013). Membrane assembly during the infection cycle of the giant Mimivirus. PlOS Pathogens 9.

Plugge, B., Gazzarrini, S., Nelson, M., Cerana, R., Van Etten, J.L., Derst, C., DiFrancesco, D., Moroni, A., and Thiel, G. (2000). A potassium channel protein encoded by chlorella virus PBCV-1. Science 287.

Porsbring, T., Blanck, H., Tjellstrom, H., and Backhaus, T. (2009). Toxicity of the pharmaceutical clotrimazole to marine microalgal communities. Aquatic toxicology 91, 203-211.

Rahier, A., and Taton, M. (1997). Fungicides as Tools in Studying Postsqualene Sterol Synthesis in Plants. Pesticide Biochemistry and Physiology 57, 1-27.

Rao, V., and Feiss, M. (2008). The bacteriophage DNA packaging motor. Annual Review Genetics 42, 647-681.

Read, B.A., Kegel, J., Klute, M.J., Kuo, A., Lefebvre, S.C., Maumus, F., Mayer, C., Miller, J., Monier, A., Salamov, A., Young, J., Aguilar, M., Claverie, J.-M., Frickenhaus, S., Gonzalez, K., Herman, E.K., Lin, Y.-C., Napier, J., Ogata, H., Sarno, A.F., Shmutz, J., Schroeder, D., de Vargas, C., Verret, F., von Dassow, P., Valentin, K., Van de Peer, Y., Wheeler, G., Emiliania huxleyi Annotation, C., Dacks, J.B., Delwiche, C.F., Dyhrman, S.T., Glockner, G., John, U., Richards, T., Worden, A.Z., Zhang, X., and Grigoriev, I.V. (2013). Pan genome of the phytoplankton Emiliania underpins its global distribution. Nature 499, 209-213.

Roberts, S.C. (2007). Production and engineering of terpenoids in plant cell culture. Nature Chemical Biology 3, 387-395.

Robinson, G., Tsay, Y., Kienzle, B., Smithmonroy, C., and Bishop, R. (1993). Conservation between human and fungal squalene synthetases: similarities in structure, function, and regulation. Molecular Cell Biology 13, 2706-2717.

Rossard, S., Roblin, G., and Atanassova, R. (2010). Ergosterol triggers characteristic elicitation steps in Beta vulgaris leaf tissues. Journal of Experimental Botany 61, 1807-1816.

Ryder, N. (1992). Terbinafine: mode of action and properties of the squalene epoxidase inhibition. The British Journal of Dermatology 126, 2-7.

Schuster, A., Girton, L., Burbank, D.E., and Van Etten, J.L. (1986). Infection of a Chlorella-like alga with the virus PBCV-1: Transcriptional studies. Virology 148, 181-189.

Seppanen-Laakso, T., and Oresic, M. (2009). How to study lipidomes. Journal of Molecular Endocrinology 42, 185-190.

Song, Z., and Nes, D. (2007). Sterol biosynthesis inhibitors: potential for transition state analogs and mechanism-based inactivators targeted at sterol methyltransferase. Lipids 42, 15-33.

Sun, L., Adams, B., Gurnon, J., Ye, Y., and Van Etten, J.L. (1999). Characterization of two chitinase genes and one chitosanase gene encoded by Chlorella virus PBCV-1. Virology 263, 376-387.

Suzuki, M., and Muranaka, T. (2007). Molecular Genetics of Plant Sterol Backbone Synthesis. Lipids 42, 47-54.

Taramino, S., Valachovic, M., Oliaro-Bosso, S., Viola, F., Teske, B., Bard, M., and Balliano, G. (2010). Interactions of oxidosqualene cyclase (Erg7p) with 3-keto reductase (Erg27p) and other enzymes of sterol biosynthesis in yeast. Biochimica et Biophysica Acta 1801.

Teske, B., Taramino, S., Bhuiyan, M.S.A., Kumaraswarmi, N.S., Randall, S.K., Barbuch, R., Eckstein, J., Balliano, G., and Bard, M. (2008). Genetic analyses involving interactions between the ergosterol biosynthetic enzymes, lanosterol synthase (Erg7p) and 3-ketoreductase (Erg27p), in the yeast Saccromyces cerevisiae. Biochemical and Biophysical Acta 1781, 359-366.

Vago, T., Baldi, G., Colombo, D., Barbareschi, M., Norbiato, G., Dallegri, F., and Bevilacqua, M. (1994). Effects of Naftifine and Terbinafine, Two Allylamine

Antifungal Drugs, on Selected Functions of Human Polymorphonuclear Leukocytes. Antimicrobial Agents and Chemotherapy 38, 2605-2611.

Van Etten, J.L. (2003). Unusual life style of giant Chlorella viruses. Annual Review Genetics 37, 153-195.

Van Etten, J.L., and Dunigan, D.D. (2012). Chloroviruses: Not your everyday plant virus. Trends in Plant Science 17, 1-8.

Van Etten, J.L., Burbank, D.E., Joshi, J., and Meints, R.H. (1984). DNA synthesis in a chlorella-like alga following infection with the virus PBCV-1. Virology 134, 443-449.

Van Etten, J.L.G., MV; Muller, DG; Boland, W; Delaroque, N. (2002). Phycodnaviridae -- large DNA algal viruses. Archives of Virology 147, 1479-1516.

Van Meer, G., Voelker, D.R., and Feignson, G.W. (2008). Membrane lipids: where they are and how they behave. Nature Reviews Molecular Cell Biology 9.

Veen, M., Stahl, U., and Lang, C. (2003). Combined overexpression of genes of the ergosterol biosynthetic pathway leads to accumulation of sterols in Saccharamomyces cerevisiae. FEMS Yeast Research 4, 87-95.

von Dassow, P., Ogata, H., Probert, I., Wincker, P., Da Silva, C., Audic, S., Claverie, J.-M., and de Vargas, C. (2009). Transcriptome analysis of functional differentiation between haploid and diploid cells of Emiliania huxleyi, a globally significant photosynthetic calcifying cell. Genome Biology 10, R114.

Wenk, M. (2005). The emerging field of lipidomics. Nature Reviews Drug Discovery 4, 594-610.

Xu, X., Bittman, R., Duportail, G., Heissler, D., Vilcheze, C., and London, E. (2001). Effect of the Structure of Natural Sterols and Sphingolipids on the Formation of Ordered Sphingolipid/Sterol Domains (Rafts). The Journal of Biological Chemistry 276, 33540-33546.

Yanai-Balser, G.M., Duncan, G., Eudy, J.D., Wang, D., Li, X., Agarkova, I., Dunigan, D.D., and Van Etten, J.L. (2010). Microarray analysis of Paramecium bursaria Chlorella Virus 1 transcription. Journal of Virology 84, 532-542.

Yashchenko, V.V., Gavrilova, O.V., Rautian, M.S., and Jakobsen, K. (2012). Association of Paramecium bursaria Chlorella viruses with Paramecium bursaria cells: Ultrastructural studies. European Journal of Protistology 48, 149-159.

Zhang, X., Xiang, Y., Duncan, G., Klose, T., Chipman, P.R., Van Etten, J.L., and Rossmann, M.G. (2011). Three-dimensional structure and function of the Paramecium bursaria chlorella virus capsid. PNAS 108, 14837-14842.

1.8 Appendix: acronyms

CAS	Cycloartenol synthase
CL	Cardiolipin
DAG	Diacylglycerol
ER	Endoplasmic reticulum
ERG	Ergosterol
ESI-MS	Electrospray Ionization-Mass Spectrometry
FA	Fatty acid
GC-MS	Gas Chromatography-Mass Spectrometry
GIPC	Glucosylinositolphosphorylceramide
Hex	Hexose
HexA	Hexuronic acid
hFAME	Hydroxy fatty acid methyl ester
IPC	Inositolphosphorylceramide
LAS	Lanosterol synthase
LCB	Long chain base
LC-MS	Liquid Chromatography-Mass Spectrometry
MS	Mass Spectrometry
m/z	Mass to charge
PC	Phosphatidylcholine
PI	Phosphatidylinositol
PM	Plasma membrane
SBI	Sterol biosynthesis inhibitor
TAG	Triacylglycerol
VF	Viral factory

CHAPTER 2

Hybrid Ergosterol Biosynthetic Pathway Designed By *Chlorella*

Suzanne L. Rose[1,2], Nakierah Christie[1], Adam Voshall[1,5], Wayne R. Riekhof[1,5], James L. Van Etten[2,3,5], Jennifer E. Markham[4,5], Ken Nickerson[1]

[1]School of Biological Sciences, University of Nebraska, Lincoln, NE 68588-0118

[2]Nebraska Center for Virology, University of Nebraska, Lincoln, NE, 68583-0900

[3]Department of Plant Pathology, University of Nebraska, Lincoln, NE 68582-0722

[4]Department of Biochemistry, University of Nebraska, Lincoln, NE 68588-0664

[5]Center for Plant Science Innovation, University of Nebraska, Lincoln, NE 68588

Corresponding author: Ken Nickerson

Abstract

Sterols are essential molecules found in nearly every eukaryotic cell membrane. Having the unique ability to partner with sphingolipids, together they maintain the integrity, fluidity and permeability of cell membranes through the formation of detergent-resistant lipid rafts. Most eukaryotes and some prokaryotes encode the enzymatic genes required for sterol biosynthesis. Non-photosynthetic eukaryotes, animals and fungi, follow a different biosynthetic pathway than that found in plants or photosynthetic eukaryotes. The major sterols produced in non-photosynthetic organisms are cholesterol and ergosterol, in animals and fungi, respectively. The phytosterols stigmasterol, campesterol, and β-sitosterol have been reported in various combinations and concentrations in plants. Prior studies on the unicellular, photosynthetic alga *Chlamydomonas reinhardtii* have reported a combination of both a phytosterol and ergosterol as sterol components within its cellular membranes; their production has been proposed to use the classical phytosterol biosynthetic pathway. Belonging to the same phylum as *C. reinhardtii*, our research goal was to identify and characterize the sterol genes and sterol biosynthetic pathway in the genus *Chlorella.* Through the use of gene gazing, targeted inhibition of the sterol biosynthetic pathway with sterol biosynthesis inhibitors (SBIs) – statin, terbinafine, and azoles – and GC/MS analysis, we identified ergosterol as the major sterol in *C. variabilis* cell membranes. Moreover, we describe a hybrid ergosterol biosynthetic pathway that is unique to this unicellular, photosynthetic alga. *C. variabilis* uses the photosynthetic, non-mevalonate, sterol precursor pathway to form isopentenyl

disphosphate (IPP), which then crosses over into the non-photosynthetic, fungal-like, sterol pathway to produce ergosterol.

Introduction

Lipids, essential biological compounds present in all organisms, play key roles in cellular functions and membrane stability (He et al., 2003). Within the class of lipids, sterols are critical to and present in distinctly different compositions within cell membranes among animals, fungi and plants; cholesterol, ergosterol and phytosterols, respectively. Sterol biosynthesis occurs in the endoplasmic reticulum (ER) through a functional complex of enzymes that display specific protein-protein interactions. This complex of enzymes, described as the ergosterol (ERG) proteins in fungi, has been coined the "ergosome" (Mo and Bard, 2005). The sterol biosynthetic pathway present in plants differs from fungi and animals in its production of a wide variety of phytosterols and intermediates in the phytosterol pathway. Sterols are found in many forms; free sterols, sterol esters (acylated), sterol alkyl ethers (alkylated), sterol sulfate (sulfated) or linked to a glycoside moiety, steryl glycosides (Benveniste, 2004). As integral components of the cell membrane, free sterols are crucial for the integrity, fluidity and permeability of the lipid bilayer (Benveniste, 2004). In addition to their importance for cell membrane stability, they affect membrane-bound protein composition and influence the functionality of enzymes, receptors and channels (Porsbring et al., 2009). Inhibitors of the sterol biosynthetic pathway, sterol biosynthetic inhibitors (SBIs) – statins, allylamines, and azoles – are known inhibitors which block sterol production, lead to accumulation of sterol precursors,

or create a different suite of sterols changing the composition, stability, and the integrity of the lipid cell membrane.

In addition to having key regulatory roles in membrane fluidity and permeability, sterols play an important role in host defense during viral infection. Therefore, it is important to understand the sterol biosynthetic pathway and sterol composition of eukaryotic, unicellular algae, which until now has been understudied. In our attempt to identify and characterize the sterol composition and the sterol biosynthetic pathway in *C. variabilis*, we employed genome gazing, phylogenetic analysis, inhibition of sterol biosynthesis, and GC/MS analysis. The sterol biosynthetic pathways and identified enzymes of *Arabidopsis thaliana* and *Saccharomyces cerevisiae* were used as representative plant and fungi models, respectively.   Here we report that ergosterol, an ergosterol derivative, and stigmasterol are the major sterols in most freshwater green algae, in the coccolithophore *Emiliania huxlyei*, and in the diatom *Thalassiosira pseudonana*, respectively. Using Gas Chromatography-Mass Spectrometry (GC-MS) analysis of sterol biosynthetic inhibited algal cultures and bioinformatics we describe a unique ergosterol biosynthetic pathway that is present in *C. variabilis* and distinct from that found in fungi and plants.

Materials and Methods

Cell cultures and growth conditions. Chlorella variabilis and *Coccomyxa subellipsoidea* cultures were grown in Modified Basal Broth Medium (MBBM) under constant shaking of 100 RPM, 22°C and light intensity [30 µmol m^{-2}s^{-1} (µE)]. *Chlorella sorokiniana* UTEX 1230 was obtained from the University of

Texas Culture Collection. *C. sorokiniana* cultures were grown in liquid Basal

Broth Medium (BBM) media, shaken at 115 RPM, 25°C, and a light intensity of

58 uE. *Chlamydomonas reinhardtii* CC124, obtained from Dr. Don Weeks'

laboratory, was grown in Tris-Acetate-Phosphate (TAP) media, under constant

shaking of 100 RPM, 22°C and light intensity (30 µE).

Sequence retrieval. The completed *C. variabilis* genome assembly

[http://genome.jgi.psf.org/ChlNC64A_1/ChlNC64A_1.home.html;v1.0; (Blanc et

al., 2010)] was used to search and identify sterol biosynthetic pathway genes.

The recently sequenced and annotated *Chlorella sorokiniana* UTEX 1230

genome was accessed (Cerutti et al., manuscript in preparation). The

Arabidopsis thaliana (NCBI taxon ID: 3702), *Chlamydomonas reinhardtii* (NCBI

taxon ID: 3055) and *Coccomyxa subellipsoidea* (NCBI taxon ID: 574566)

genomes were accessed through the National Center for Biotechnology

Information (http://www.ncbi.nlm.nih.gov/). *Saccharomyces cerevisiae* (NCBI

taxon ID: 4932) ergosterol (ERG) genes were used to identify homologues and

elucidate the ergosterol pathway in *C. variabilis.*

Phylogenetic analysis. The 2,3-oxidosqualene cyclase sequences used for the

phylogenetic analyses were taken from the results of a BLASTp search (version

2.2.30) against the non-redundant protein database using default settings

(Altschul et al., 1990). Sequences from lanosterol producing vertebrates and

fungi, cycloartenol producing plants, and algae capable of producing both

lanosterol and cycloartenol were chosen to represent a broad representation of

each lineage and to have a roughly equal representation of lanosterol and

cycloartenol producing proteins. The squalene-hopene cyclase from *Acetobacter tropicalis* was included as an out-group. The protein sequences were globally aligned using version 7.215 of MAFFT, with a maxiumum of 1000 iterations (Katoh and Standley, 2013). The maximum likelihood phylogenic tree was produced with version 20120412 of PhyML with 1000 bootstrap replicates (Guindon et al., 2010).

Sterol Standards and Inhibitors. Plant sterols kit (cat. #1123) was used (Matreya, Pleasant Gap, PA) and kept at -20C. Cholestanol (1 mg/ml) was used as the sterol internal standard for GC-MS analysis. Antifungal inhibitors: Atorvastatin (A7658), Terbinafine (T1672), Clotrimazole (C4657), Ketoconazole (K1676), and Fluconazole (F4682) were purchased from LKT Laboratories (St. Paul, MN).

Inhibitory Concentration Kill Curve. To determine the inhibitory concentrations of Terbinafine and the azole drugs, a range of stock methanol (MeOH) solutions with drug concentrations ranging from 0 – 50 mM was made. A culture of *C. sorokiniana* was diluted with fresh BBM to a final cell density of $1x10^6$ cells/ml. The culture was partitioned into 5 mL volumes and treated with 5 µL of a given stock solution, which resulted in a 1:1000 dilution of the stock drug solution. Other samples were treated with 5 µL of MeOH as solvent controls. Trials were run in duplicate. After six days, the absorbance of light at 750 nm was measured via a Biotek Synergy H1 Hybrid reader (Winooski, VT). Inhibitory concentrations were determined by graphing absorbance vs. drug concentration and identifying the lowest concentrations at which growth was minimal.

Growth Curves. Growth curves were prepared similar to the above inhibitory concentration curves, however, absorbance of each sample trial was read every day and plotted over time (data not shown).

Sterol Inhibition Assays. Algal cultures were grown to mid-log phase (ca. $1x10^6$ cells/ml). Sterol inhibitor solutions were added to each culture in a final concentration equal to that of the inhibitory concentration; 100 µM statin, 4 µM terbinafine, 30 µM ketoconazole, and 5 µM clotrimazole. A concentration of 0.1% MeOH was added to control cultures.   Algal cultures were incubated for 48 h before cells were harvested via centrifugation. Pelleted algal cells were freeze dried and stored at -80°C for further analysis.

Sterol Extraction and Analysis by Gas Chromatography – Mass Spectrometry (GC-MS). Sterol extraction followed a modified version of the Bligh and Dyer (1959) chloroform-methanol protocol followed by GC/MS analysis of membrane sterol composition (Bligh and Dyer, 1959). One mg/ml of cholestanol standard (Matreya, Pleasant Gap, PA) was added to freeze dried algal pellets. Total sterols were extracted three times with chloroform:methanol (1:1, v:v), loaded onto silica SPE columns and eluted with 30% 2-propanol. Purified sterol extracts were dried under nitrogen at 37°C and then converted to trimethylsilyl ether (TMS-ether) derivatives using bis (trimethylsilyl) trifluoracetamide (BSFTA-TMCS 99:1) (Sigma, St. Louis, MO). Dried sterol samples were suspended in 100 µl hexane for GC/MS analysis. Initial gas chromatographic analysis was carried out using the Agilent 6890 Series Gas Chromatograph System equipped with a DB-5ms capillary column (30.0 m x 250.00 µm, 0.25 µm, J&W 122-5532, J&W

Scientific, Inc., Folsom, USA). Helium was used as the carrier gas at a linear velocity of 48 cm/sec and constant flow of 1.5 mL min^{-1}. A dual ramp temperature program was used with the oven heated from 250 to 270°C for 30 min and then from 270 – 280°C for 3.30 min. A detector temperature of 270°C was used. Sterols were initially identified using the *NIST98 library* (Scientific Instrument Services, Inc., Ringoes, USA) followed by comparisons based on their mass fragmentation pattern and retention time. Peak areas of identified sterols were quantified relative to the cholestanol standard.

Resuspensions. To determine if a given drug was algicidal (permanently and irreversibly killed the algal cultures) or algistatic (arresting cell growth and development without killing the algae), cultures in which growth had been inhibited were spun down at 4200 RPM for three minutes and transferred into 5 mL of fresh BBM media and allowed to grow. Absorbance was measured as mentioned above.

Results

The major sterols were identified in six species of microalgae, four freshwater and two marine, by GC/MS (Table 1). The major sterol found among the unicellular, green algae studied was ergosterol with the exception of *Coccomyxa*. The highest percentage of total sterols being ergosterol was found in both species of *Chlorella*, *C. variabilis* (97.6%) and *C. sorokiniana* (82%) (Table 1). Present only in both *Chlorella* species was the relatively uncharacterized sterol ergosta-5,8-dienol. Interestingly, only during azole inhibition of *Chlamydomonas* does ergosta-5,8-dienol appear as an intermediate (Table 5). *C. sorokiniana*

also contained two other minor sterols, stellasterol (ergosta-7,22-dienol) and ergost-7-ene (Table 1). *Coccomyxa* more closely resembled a plant rather than algae because it only had phytosterols – campesterol (45.2%), β-sitosterol (34%), and stigmasterol (20.8%) (Table 1). The similarity of sterol composition in *Chlamydomonas* and *Volvox*, ergosterol (62.1% and 68.4%) and the phytosterol 7-dehydroporiferasterol (35.5% and 31.6%), respectively, supported the idea that having an alternating life cycle or having two distinct cell types to carry out different functions requires sterol biosynthesis using both lanosterol and cycloartenol precursors (Table1). Even though one alga is a unicellular, soil alga and the other a multicellular, freshwater alga, *Chlamydomonas* and *Volvox* are phylogenetically closely related which we also found during comparision of the oxidosqualene cyclase enzyme (Fig. 2). *E. huxleyi* contained stellasterol, a derivative of ergosterol, whereas *T. pseudonana* produced the phytosterol, stigmasterol (Table 1).

Bioinformatics. Gene mining with the *Arabidopsis thaliana* sterol biosynthetic genes and *S. cerevisiae* ergosterol (ERG) pathway genes was used to blast against the *C. variabilis* genome in order to identify sterol gene homologs (Table 2). We further blasted these enzymatic genes against the recently sequenced *C. sorokiniana* genome. Both sets of homologs were then blasted back against the NCBI database for affirmation. Bioinformatic analysis of the *C. variabilis* NC64A annotated proteome revealed the absence of the last four enzymes (HMGR, MK, PMK, MVD) of the Stage I cytosolic MVA pathway (Table 2). The genes encoding these four enzymes were also absent in *C. sorokiniana*. However,

homologous genes for the complete plastidal MEP pathway were present in both *Chlorella* species, with high sequence identity to those of *A. thaliana* (Table 2). Stage II of sterol biosynthesis – IPP conversion to squalene – has three enzymatic steps of which homologous genes were present in *Chlorella*. Of the Stage III sterol biosynthesis genes, the conversion of squalene to the final sterol composition, homology to both *A. thaliana* and *S. cerevisiae* genes were detected. We identified one OSC within the *Chlorella* genome, CHLNCDRAFT 22200, which is homologous to both the CAS (At2g07050) and LAS (At3g45130) genes found in *Arabidopsis thaliana* with 60% and 54% identity, respectively, and 99% coverage (Table 2). One gene homologous to both cycloartenol and lanosterol synthase was present in *Chlorella* with a high sequence identity to both genes (Table 2). Interestingly, two sets of the desaturase and demethylase genes, ERG 5/11 and ERG 3/25, within the ergosterol pathway of *S. cerevisiae* and the corresponding functional genes in *A. thaliana*, 14DM1/2 and SMO/DWF7, exist as one, multi-domain gene in *Chlorella* for each of these gene pairs (Fig.1). Also notable was the absence of the delta 24 reductase (ERG24) in both *Chlorella* species (Table 2).

Minimal Inhibitory Concentration (MIC). Minimal inhibitory concentrations (MICs) were determined in *C. sorokiniana* cultures (1×10^6 cell/ml) subjected to various drug concentrations of the allylamine terbinafine, two imidazoles – ketoconazole and clotrimazole, and the triazole fluconazole. Absorbance, to track growth, was measured after six days. Terbinafine and both imidazoles inhibited *C. sorokiniana* growth. Cell cultures with a final concentration of 2 µM terbinafine

had an average absorbance of 0.42, but at 3 µM the average dropped to 0.11.

Likewise, cultures exposed to 2 µM clotrimazole had an average absorbance of

0.28, while at 3 µM the average was 0.03. Ketoconazole's MIC was much higher

at a final concentration of 25 µM, the culture's absorbance averaged 0.08,

whereas at a final concentration of 20 µM the cells reached 0.57 absorbance.

Fluconazole did not inhibit cell growth at any concentration. Cultures exposed to

a final concentration of 50 µM fluconazole averaged an absorption of 0.70

compared to the control average of 0.84. Therefore, fluconazole was not used

for further study.

Sterol Biosynthesis Inhibition. Using antifungal inhibitors of the sterol

biosynthetic pathway, statin (ST), terbinafine (TB), ketoconazole (KC) and

clotrimazole (CT), we analyzed the accumulation of sterol intermediates in *C.

variabilis* and *C. sorokiniana* (Tables 3-4) and azole inhibitors (KC and CT) in *C.

reinhardtii* and *Coccomyxa* (Tables 5-6) by gas chromatography/mass

spectrometry (GC/MS). Compared to controls (MeOH), *C. variabilis* and *C.

sorokiniana* cultures showed no significant change in ergosterol abundance in

the presence of statin (ST) (Tables 3-4). Terbinafine resulted in decreased

ergosterol levels. Inhibition of the pathway with two different azoles,

ketoconazole and clotrimazole resulted in a further decrease in ergosterol and

the appearance of the intermediate lanosterol (Tables 3-4). Two major peaks

appeared with azole inhibition, one of which had the same retention time and MS

fragmentation as lanosterol (data not shown). The intermediate 4,4-

dimethylcholesta-8, 22, 24-trienol was also present in *C. variabilis* (Table 3). An

uncommon sterol, ergosta-5,8-dienol, was present in *C. variabilis* as a minor

sterol which increased in abundance in the presence of both azoles, whereas, it

was not detected until azole inhibition in *C. sorokiniana* (Table 3-4). In the

presence of azoles, abundance levels of the two major sterols in

Chlamydomonas, ergosterol and 7-dehydroporiferasterol, were reduced with the

appearance of intermediates from both the lanosterol-cyclase pathway –

lanosterol, ergost-7-ene, lanost-8-ene and ergosta-5,8,22-trienol – and the

cycloartenol-cyclase pathway – stigma-4,7,22-trienol and stigmasterol (Table 5).

In the presence of azoles, *Coccomyxa,* which only synthesizes the phytosterols

campesterol, stigmasterol, and β-sitosterol, had intermediates appear from

mainly the cycloartenol pathway however, small amounts of lanosterol

intermediates were detected, lanosterol, 24-methylenelanost-8-ene,

cycloaudenol and 24-methylene-cycloartenol (Table 6).

Phylogenetic Analysis of 2,3-Oxidosqualene Cyclases (OSC). OSCs with

specificity to produce either lanosterol, cycloartenol, or both were used to

construct a phylogenetic tree (Fig. 2). OSCs that produce the sterol precursor

cycloartenol form the branch of higher plants whereas those producing the

lanosterol precursor constitute the Metazoa/Fungi group. The microalgae cluster

represents a group of organisms with an OSC that is thought to have a lower

specificity for producing one precursor over another and therefore is capable of

producing either or both lanosterol or cycloartenol. *Coccomyxa* only has

phytosterols, which suggests that cycloartenol is the preferred product (Table 6).

Chlamydomonas and *Volvox,* group together with its OSC as they both produce

the same sterol composition requiring both sterol OSC precursors (Fig.2).

Chlorella with its major sterol composition of ergosterol and exclusively lanosterol

intermediates suggests an OSC with lanosterol specificity.

Discussion

The biosynthesis of sterols differs among animals, fungi, and plants in

precursors, enzymatic steps, and final sterol composition. It is widely accepted

that the major sterol in animals is cholesterol and ergosterol in fungi and that

both employ the MVA pathway leading to the precursor lanosterol and that they

share the first few enzymatic steps. After lanosterol, a bifurcated pathway

produces their distinct sterols (Fig.3). Plants, with its sterol precursor

cycloartenol, follow a separate pathway to produce a wide array of phytosterols.

The goals of this research focused on 1) the characterization and comparison of

sterol compositions in microalgae and 2) the identification of the sterol

biosynthetic pathway and enzymes employed by *Chlorella species.*

Determination of algal sterol composition was achieved by GC/MS analysis. For

characterization and comparison analysis we selected four unicellular, freshwater

algae *C. variabilis*, *C. sorokiniana*, *Chlamydomonas*, and *Coccomyxa*; two

unicellular, marine algae, the coccolithophore *E. huxleyi* and diatom *T.

pseudonana*; and the multicellular *Volvox* alga species (Table 1). Previous

studies of sterol biosynthesis in *Chlamydomonas* reported the presence of

ergosterol and 7-deydroporiferasterol as the major sterols (Miller et al., 2012),

which agree with our results. Interestingly, this sterol composition is identical to

what we detected in the multicellular alga, *Volvox* (Table 1).

To elucidate the enzymatic pathway of *C. variabilis* ergosterol biosynthesis, the sequenced and well-studied *Chlamydomonas* and the sequenced, plant-like alga *Coccomyxa*, were selected for bioinformatic and GC/MS analysis of sterol biosynthesis inhibition studies. The recently sequenced and annotated genome of *C. sorokiniana* (Ceruitti et al., manuscript in preparation) was used for a species-specific comparison and the fungal ergosterol biosynthetic model of the ergosome provided a beneficial framework (Mo and Bard, 2005). We identified, through inhibition of key enzymes, the precursors involved in sterol biosynthesis allowing the generation of a putative ergosterol biosynthetic pathway in *C. variabilis* (Table 2; Fig.1).

Through gene mining we noticed the lack of a homologous HMGR enzyme in both *C. variabilis* and *C. sorokiniana* genomes (Table 2). Insignificant decreases in final sterol production in atorvastatin inhibited cultures substantiates the absence of a complete MVA pathway, suggesting that *Chlorella* only employs the plastidic MEP pathway to produce IPP (Table 2-3). The complete MVA pathway has either been lost or nonhomologous replacement enzymes have yet to be discovered in *Chlorella* species. As expected, inhibiting cell cultures with terbinafine led to a significant decrease in ergosterol levels in both *Chlorella* species (Table 3-4).

Prior studies have shown that in non-photosynthetic eukaryotes, the cyclization of 2,3-oxidosqualene by LAS/ERG7 produces lanosterol; however, single mutations in the CAS of the photosynthetic eukaryote *A. thaliana* have been reported to produce lanosterol instead of cycloartenol as the major product

(Segura et al., 2002; Benveniste, 2004). Considering ergosterol is the major sterol with the complete absence of phytosterols, having one gene homologous to both *CAS* and *LAS*, and the presence of lanosterol pathway intermediates, we predict the high probability of the *C. variabilis* OSC to preferentially produce lanosterol (Table 3; Fig.2).

With both ketoconazole and clotrimazole inhibition of the 14α-demethylase enzyme in *C. variabilis* cultures, we see a reduction of ergosterol and the appearance of the intermediate lanosterol (Table 3). Interestingly, 14-demethyllanosterol (4,4-dimethyl-5α-cholesta-8,24-dienol), a metabolite of lanosterol, was also detected as an intermediate with azole inhibition (Table 3) (Leonardsen et al., 2000; Chemler et al., 2006). The presence of the P450 superfamily domain, targeted by azole inhibitors, is present both as a CYP51 domain in 14α-demethylase (ERG11) and a CYPX domain in C22-desaturase (ERG5). Through gene mining and protein alignments we report a *C. variabilis* protein (CHLNCDRAFT 56217) as being a multi-domain protein having the dual activity of ERG11 and 5 (Table 2; Fig.1). We suggest the demethylase and desaturase activity occurs in tandem; therefore, incomplete inhibition of the demethylase is followed by further inhibition of the desaturase which would account for the presence of both intermediates (Table 3; Fig. 1).

The rapid removal of a C-14 methyl from 4,4-dimethylcholesta-8,14,22-trienol by a sterol reductase would be required before desaturation of C-22 in order for the intermediate 14-dimethyllanosterol to accumulate during azole inhibition. However, gene mining found no homologs for the C-14 sterol reductase

(ERG24), C-24 sterol reductase (ERG4), or C-7 sterol reductase. Although there

are approximately 150 reductases coded by *C. variabilis*, no sterol specific

reductases were identified; however, we suggest a possible reductase

(CHLNCDRAFT 136479) for C-14 and C-24 reduction, but having a low

percentage of both query coverage and percent identity with known homologs, its

function will require further study (Table 2). Therefore, we hypothesize that the

reductase functioning in the *C. variabilis* sterol pathway would have non-specific

enzymatic activity for the reduction of C-14 and C-24, the final enzymatic step of

ergosterol synthesis (Fig.1). The C-7 double bond is retained in ergosterol and a

homologous reductase is absent in both fungi and *C. variabilis*.

Azoles are a useful tool to inhibit key enzymes, leading to accumulation

and detection of intermediates, and the determination of sterol biosynthesis. The

initial class of azoles, which includes clotrimazole, along with second generation

azoles, such as ketoconazole, are capable of inhibition at additional steps during

sterol biosynthesis resulting in an accumulation of Δ^5 sterols (Berg et al., 1988).

The accumulation and appearance of the Δ^5 sterol ergosta-5,8-dienol was seen

during azole inhibition of all four algal species (Tables 3-6). Fluconazole, a third

generation of azoles, had no effect on the growth of *C. sorokiniana* (Berg et al.,

1988). Clotrimazole inhibited both fungal and *Chlorella* growth by replacing

ergosterol with the accumulation of lanosterol intermediates and it is also a

potent inhibitor of many different forms of cytochrome P450 enzymes in plants

and animals as well (Burden et al., 1989). We surmise that the inability to

desaturate C-22 blocks the activity of C-24 methyltransferase, and in turn

delta8/delta7 isomerase possibly through steric hindrance; therefore, blocking the formation of ergosterol. The substrate 14-dimethyllanosterol is still able to undergo two cycles of C-4 demethylation, decarboxylation and removal of each C-4 methyl group. The final action of C-5 desaturase and delta 24 reductase would result in the synthesis of ergosta-5,8-dienol.

Both lanosterol and 14-demethyllanosterol are intermediates of the fungal and *Chlorella* ergosterol pathway and not present in the cylcoartenol to phytosterol pathway in plants, further suggesting that Chlorella sterol biosynthesis more closely resembles fungi instead of plants (Fig.1). However, a key distinction between the ergosterol pathway of fungi and *Chlorella* is the presence of two multi-domain *Chlorella* genes (CHLNCDRAFT 56217 and 37407) that are homologous to the four fungal ERG genes (ERG11/5 and ERG3/25); therefore, we predict a change in the order of the enzymatic steps and presence of different intermediates not commonly found in fungi (Fig. 3). The erogsterol biosynthetic pathway is composed of membrane-associated enzymes assembled as a multi-enzyme complex. In yeast, the non-catalytic protein ERG28 functions as a scaffold, anchoring enzymes and creating a "hub" for enzymatic interactions with substrates (Mo and Bard, 2005; Winkel, 2009). We have identified the ERG28 homolog in *Chlorella* (CHLNCDRAFT 59539) as well as in other algae; however, no homolog was present in *A. thaliana*. Given that the enzymes of the sterol biosynthetic pathway form a membrane bound complex, and not physically arranged linearly, may explain the diversity of sterols produced by various algae and other organisms (Winkel, 2009). Currently, algae

have been grouped with plants as producing the precursor cycloartenol and utilizing the phytosterol biosynthetic pathway. Employing azole inhibitors, GC/MS analysis, gene mining and bioinformatics, we propose that a unique sterol biosynthetic pathway exists in *Chlorella* and other lanosterol-producing, unicellular alga (Fig. 1-3).

Conclusions

In our comparison of the sterols present in freshwater and marine algae, we speculate that factors influencing the differences among species in their sterol content are both ecological and evolutionary based. One such factor, specific water composition (i.e. temperature, salinity, nutrient and ionic composition) is highly variable among and between freshwater and marine ecosystems (Porsbring et al., 2009). Adaptation to changing environmental conditions, such as light and day length, has been shown to change the ratio of sterols to other membrane lipids and the percentages of sterols present (Rahier and Taton, 1997). As *C. sorokiniana* can grow at warmer temperatures and *Coccomyxa* at extreme polar temperatures we see distinct differences in the final sterol composition when compared to *C. variabilis* (Table 1). Unraveling the determining factors in the sterol composition in phytoplankton, *E. huxleyi* and *T. pseudonana*, may include a more complex combination of factors. *E. huxleyi* and *T. pseudonana* have evolved from a secondary, red plastid endosymbiotic event. The primary vs. secondary plastid endosymbiotic events along with obvious ecological differences between marine and freshwater algae may explain the differences in sterol composition.

Primitive orders of algae within the Class *Chlorophyceae* have many species that contain the major sterol ergosterol or other $\Delta^{5, 7}$- sterols not found in higher orders of algae and land plants (Patterson, 1991). The evolution from cell membrane $\Delta^{5, 7}$- sterols to Δ^5 - or Δ^7-sterols as major constituents is suggested to have taken place as earth's ozone developed, as $\Delta^{5, 7}$- sterols are more beneficial in the absorption of UV radiation (Patterson, 1991). With an increase in atmospheric oxygen, it has been hypothesized as the trigger for sterol evolution, providing an early defense mechanism against molecular oxygen, which in turn facilitated the appearance of eukaryotes (Chen et al., 2007; Brown and Galea, 2010). Hence, in the presence of ozone, these primitive sterols are thought to have become inferior to the phytosterols of higher plants. Research of other *Chlorella* species have been identified as having either Δ^5 or Δ^7 sterols which allows for the evolution within this genus to unfold and be characterized. Higher plants contain a cocktail of three Δ^5 sterols – campesterol (24-methyl), stigmasterol (24-ethyl) and β-sitosterol (24-ethyl) – in place of a single major sterol (Mercer, 1993; Holmberg et al., 2002). Surprisingly, we see this phytosterol composition in the unicellular alga *Coccomyxa* (Table 1). A phylogenetic marker in the evolution of sterol biosynthesis occurs during the C-24 methylation step. The size and direction of the 24-alkyl group placed by the sterol methyltransferase is indicative of either a primitive (24β-methyl) or advanced (24α-ethyl) organism (Nes and New, 1980; Zhou et al., 2006). As *C. variabilis* sterols are wholly 24β-methyl, this corroborates with other phylogenetic evidence of *Chlorella* having a primitive sterol biosynthetic pathway.

Due to an exclusively lanosterol-based pathway in *C. variabilis*, it is hypothesized

its sterol biosynthetic pathway origin evolved from a non-photosynthetic lineage,

has lost the capability to produce a wide range of sterols through enzyme

mutations, or as a natural endosymbiont of *Paramecium bursaria* the benefit of

synthesizing one sterol, ergosterol, outweighs the cost of the sterol complexity of

higher plants. In algae, the intricate roles and functions of sterols are not

completely understood; however, the composition and characterization of algal

sterols is essential in the study of phylogenetic comparisons, inter- and

intraspecies interactions, viral-host interactions, and ecological and

environmental issues (Patterson, 1991). Here we have characterized intra- and

interspecies-specific composition of cell membrane sterols among unicellular

algae and propose a unique sterol biosynthetic pathway in *C. variabilis*.

Acknowledgements

References

Abe, I. (2007). Enzymatic synthesis of cyclic triterpenes. Natural Product Reports 24, 1311-1331.

Ackman, R., and Sipos, J. (1964). Application of specific response factors in the gas chromatographic analysis of methyl esters of fatty acis with flame ionization detectors. Journal of the American Oil Chemists Society 41, 377-378.

Alcazar-Fuoli, L., Mellado, E., Garcia-Effron, G., Lopez, J.F., Grimalt, J.O., Cuenca-Estrella, J.M., and Rodriguez-Tudela, J.L. (2008). Ergosterol biosynthesis pathway in Aspergillus fumigatus. Steroids 73, 339-347.

Altschul, S., Gish, W., Miller, W., Myers, E., and Lipman, D. (1990). Basic local alignment search tool. Journal of Molecular Biology 215, 403-410.

Alverson, A.J., Beszteri, B., Julius, M.L., and Theriot, E.C. (2011). The model marine diatom Thalassiosira pseudonana likely descended from a freshwater ancestor in the genus Cyclotella. BMC Evolutionary Biology 11.

Armbrust, E.V.e.a. (2004). The Genome of the Diatom Thlassiosira Pseudonana: Ecology, Evolution, and Metabolism. Science 306.

Bamford, D., Caldentey, J., and Bamford, J. (1995). Bacteriophage PRD1: a broad host range dsDNA tectivirus with an internal membrane. Advances in Virus Research 45, 281-319.

Bennion, B., Park, C., Fuller, M., Lindsey, R., Momany, M., Jennemann, R., and Levery, S.B. (2003). Glycosphingolipids of the model fungus Aspergillus nidulans: characterization of GIPCs with oligo-a-mannose-type glycans. Journal of Lipid Research 44.

Benveniste, P. (2004). Biosynthesis and Accumulation of Sterols. Annual Review of Plant Biology 55, 429-457.

Berg, D., Plempel, M., Buchel, K.-H., Holmwood, G., and Stroech, K. (1988). Sterol Biosynthesis Inhibitors. Secondary effects and enhanced in vivo efficacy. Annals of the New York Academy of Sciences 544, 338-347.

Berkey, R., Bendigeri, D., and Xiao, S. (2012). Sphingolipids and plant defense/dis3ease: the "death" connection and beyond. Frontiers in Plant Science 3.

Blaas, N., and Humpf, H. (2013). Structural profiling and quantitation of glycosyl inositol phosphoceramides in plants with Fourier transform mass spectrometry. Journal of Agriculture and Food Chemistry 61, 4257-4269.

Blanc, G., Mozar, M., Agarkova, I., Gurnon, J., Yanai-Balser, G.M., Rowe, J.M., Xia, Y., Riethoven, J.-J., Dunigan, D.D., and Van Etten, J.L. (2014). Deep RNA sequencing reveals hidden features and dynamics of early gene transcription in Paramecium bursaria Chlorella Virus 1. PLoS ONE 9.

Blanc, G., Duncan, G., Agarkova, I., Borodovsky, M., Gurnon, J., Kuo, A., Lindquist, E., Pangilinan, J., Polle, J., Salamov, A., Terry, A., Yamada, T., Dunigan, D.D., Grigoriev, I.V., Claverie, J.-M., and Van Etten, J.L. (2010). The Chlorella variabilis NC64A genome reveals adaptation to photosymbiosis, coevolution with viruses, and cryptic sex. Plant Cell 22, 2943-2955.

Blanc, G., Agarkova, I., Grimwood, J., Kuo, A., Bruegeman, A., Dunigan, D.D., Gurnon, J., Ladunga, I., Lindquist, E., Lucas, S., Pangilinan, J., Proschold, T., Salamov, A., Schmutz, J., Weeks, D., Yamada, T., Lomsadze, A., Borodovsky, M., Claverie, J.-M., Grigoriev, I.V., and Van Etten, J.L. (2012). The genome of the polar eukaryotic microalgo Coccomyxa subellipsoidea reveals traits of cold adaptation. Genome Biology 13.

Blanc, M., Hsieh, W.Y., Robertson, K.A., Watterson, S., Shui, G., Lacaze, P., Khondoker, M., Dickinson, P., Sing, G., Rodriguez-Martin, S., Phelan, P.,

Forster, T., Strobl, B., Muller, M., Riemersma, R., Osborne, T., Wenk, M.R., Angulo, A., and Ghazal, P. (2011). Host Defense against Viral Infection Involves Interferon Mediated Down-Regulation of Sterol Biosynthesis. PLoS Biology 9.

Bligh, E.G., and Dyer, W.J. (1959). A rapid method for total lipid extraction and purification. Canadian Journal of Biochemistry and Physiology 37, 911-917.

Bodey, G. (1992). Azole antifungal agents. Clinical infectious diseases: An official publication of the Infectious Diseases Society of America 14, S161-169.

Bou Khalil, M., Hou, W., Zhou, H., Elisma, F., Swayne, L., Blanchard, A., Yao, Z., Bennett, S., and Figeys, D. (2010). Lipidomics era: accomplishments and challenges. Mass Spectrometry Reviews 29, 877-929.

Bratbak, G., Egge, J., and Heldal, M. (1993). Viral mortality of the marine alga Emiliania huxleyi (Haptophyceae) and termination of algal blooms. Marine Ecology Progress Series 93, 39-48.

Breslow, D.K., and Weissman, J.S. (2010). Membranes in Balance: Mechanisms of Sphingolipid Homeostasis. Molecular Cell 40.

Brown, A., and Galea, A. (2010). Cholesterol as an evolutionary response to living with oxygen. Evolution 64, 2179-2183.

Brugger, B. (2014). Lipidomics: Analysis of the lipid composition of cells and subcellular organelles by electrospray ionization mass spectrometry. Annual Review of Biochemistry 83, 79-98.

Brussard, C.P.D., Kempers, R., Kop, A., Riegman, R., and Heldal, M. (1996). Virus-like particles in a summer bloom of Emiliania huxleyi in the North Sea. Aquatic Microbial Ecology 10, 105-113.

Burden, R.S., Cooke, D.T., and Carter, G.A. (1989). Inhibitors of Sterol Biosynthesis and Growth in Plants and Fungi. Phytochemistry 28, 1791-1804.

Bure, C., Cacas, J.-L., and Mongrand, S. (2014). Characterization of glycosyl inositol phosphoryl ceramides from plants and fungi by mass spectrometry. Analytical and Bioanalytical Chemistry 406, 995-1010.

Cacas, J.-L., Melser, S., Domergue, F., Joubes, J., Bourdeux, B., Schmitter, J.-M., and Mongrand, S. (2012). Rapid nanoscale quantitative analysis of plant sphingolipid long-chain bases by GC-MS. Analytical and Bioanalytical Chemistry 403, 2745-2755.

Cacas, J.-L., Bure, C., Furt, F., Maalouf, J.-P., Badoc, A., Cluzet, S., Schmitter, J.-M., Antajan, E., and Mongrand, S. (2013). Biochemical survey of the polar head of plant glycosylinositolphosphoceramides unravels broad diversity. Phytochemistry 96, 191-200.

Castberg, T., Thyrhaug, R., Larsen, A., Sandaa, R.-A., Heldal, M., Van Etten, J., and Bratbak, G. (2002). Isolation and characterization of a virus that infects Emiliania huxleyi (Haptophyta). Journal of Phycology 38, 767-774.

Cazzaniga, S., Dalli'Osto, L., Szaub, J., Scibilia, L., Ballottani, M., Purton, S., and Bassi, R. (2014). Domestication of the green alga Chlorella: reduction of

antenna size improves light-use efficiency in a photobioreactor. Biotechnology for Biofuels 7, 13.

Chemler, J.A., Yan, Y., and Koffas, M.A. (2006). Biosynthesis of isoprenoids, polyunsaturated fatty acids, and favenoids in Saccromyces cerevisiae. Microbial Cell Factories 5.

Chen, L., Wang, G., and Zhang, H. (2007). Sterol biosynthesis and prokaryotes-to-eukaryotes evolution. Biochemical and Biophysical Research Communications 363, 885-888.

Cherrier, M.V., Kostyuchenko, V.A., Xiao, C., Bowman, V.D., Battisti, A.J., Yan, X., Chipman, P.R., Baker, T.S., Van Etten, J.L., and Rossmann, M.G. (2009). An icosahedral algal virus has a complex unique vertex decorated by a spike. PNAS 106, 11085-11089.

Chuchrid, N., Hiramatsu, S., Sugimoto, I., Fujie, M., Usami, S., and Yamada, T. (2001). Digestion of Chlorella cells by Chlorovirus-encoded polysaccharide degrading enzymes. Microbes and Environments 16, 206-212.

Chugh, A., Ray, A., and Gupta, J. (2003). Squalene epoxidase as hypercholesterolemic drug target revisted. Progress in Lipid Research 42, 37-50.

Cottrell, M., and Suttle, C. (1991). Wide-spread occurrence and clonal variation in viruses which cause lysis of a cosmopolitan, eukaryotic marine phytoplankton, Micromonas pusilla. Marine Ecology Progress Series 78, 1-9.

Crowley, P.D., and Gallagher, H.C. (2014). Clotrimazole as a pharmaceutical: past, present and future. Journal of Applied Microbiology 117, 611-617.

Darienko, T., Gustavs, L., Eggert, A., Wolf, W., and Proschold, T. (2015). Evaluating the species boundaries of green microalgae (Coccomyxa, Trebouxiophyceae, Chlorophyta) using integrative taxonomy and DNA barcoding with further implications for the species identification in environmental samples. PLoS ONE 10.

Devarenne, T.P., Ghosh, A., and Chappell, J. (2002). Regulation of Squalene Synthase, a Key Enzyme of Sterol Biosynthesis, in Tobacco. Plant Physiology 129, 1095-1106.

Dhar, M.K., Koul, A., and Kaul, S. (2013). Farnesyl pyrophosphate synthase: a key enzyme in isoprenoid biosynthetic pathway and potential molecular target for drug development. New Biotechnology 30.

Dunigan, D.D., Cerny, R.L., Bauman, A.T., Roach, J.C., Lane, L.C., Agarkova, I., Wulser, K., Yanai-Balser, G.M., Gurnon, J., Vitek, J.C., Kronschnabel, B.J., Jeanniard, A., Blanc, G., Upton, C., Duncan, G.A., McClung, O.W., Ma, F., and Van Etten, J.L. (2012). Paramecium bursaria Chlorella Virus 1 proteome reveals novel architectural and regulatory features of a giant virus. Journal of Virology 86, 8821-8834.

Eisenkolb, M., Zenzmaier, C., Leitner, E., and Schneiter, R. (2002). A Specific Structural Requirement for Ergosterol in Long-chain Fatty Acid Synthesis Mutants Important for Maintaining Raft Domains in Yeast. Molecular Biology of the Cell 13, 4414-4428.

Fenn, J., Mann, M., Meng, C., Wong, S., and Whitehouse, C. (1989). Electrospray ionization for mass spectrometry of large biomolecules. Science 246, 64-71.

Frohns, F., Kasmann, A., Kramer, D., Schafer, B., Mehmel, M., Kang, M., Van Etten, J., Gazzarrini, S., Moroni, A., and Thiel, G. (2006). Potassium ion channels of Chlorella viruses cause rapid depolarization of host cells during infection. Journal of Virology 80, 2437-2444.

Gamper, K., and Shapiro, M. (2007). Target-specific PIP2 signalling: how it might work. Journal of Physiology 582, 967-975.

Gazzarrini, S., Severino, M., Lombardi, M., Morandi, M., DiFrancesco, D., Van Etten, J.L., Thiel, G., and Moroni, A. (2003). The viral postassium channel Kcv: structural and functional features. FEBS Letters 552, 12-16.

German, J., Gillies, L., Smilowitz, J., Zivkovic, A., and Watkins, S. (2007). Lipidomics and lipid profiling in metabolomics. Current Opinion in Lipidology 18, 66-71.

Graybill, J., Burgess, D., and Hardin, T. (1997). Key issues concerning fungistatic versus fungicidal drugs. European Journal of Clinical Microbiology and Infectious Dieseases 16, 42-50.

Gross, R., and Han, X. (2007). Lipidomics in diabetes and the metabolic syndrome. Methods in Enzymology 433, 73-90.

Guan, X.L., Souza, C.M., Pichler, H., Dewhurst, G., Schaad, O., Kajiwara, K., Wakabayashi, H., Ivanova, T., Castillon, G.A., Piccolis, M., Abe, F., Loewith, R., Funato, K., Wenk, M.R., and Riezman, H. (2009). Functional Interactions between Sphingolipids and Sterols in Biological Membranes Regulating Cell Physiology. Molecular Biology of the Cell 20, 2083-2095.

Guindon, S., Dufayard, J., Lefort, V., Anisimova, M., Hordijk, W., and Gascuel, O. (2010). New algorithms and methods to estimate maximum-likelihood phylogenies: assessing the performance of PhyML 3.0. Systems Biology 59, 307-321.

Gulati, S., Munkacsi, A.B., Wilcox, L., and Sturley, S.L. (2010). Sterols and sphingolipids: Dynamic duo or partners in crime? Progress in Lipid Research 49, 353-365.

Han, X., and Gross, R. (2005). Shotgun lipidomics: electrospray ionization mass spectrometric analysis and quantitation of cellular lipidomes directly from crude extracts of biological samples. Mass Spectrometry Reviews 24, 367-412.

Han, X., and Christie, W.W. (2010). Lipid Analysis: Isolation, Separation, Identification and Lipidomic Analysis. (Bridgewater, England: The Oily Press).

Han, Y.-B., Wu, L., Rich, J.R., Huang, F.-T., Withers, S.G., Feng, Y., and Yang, G.-Y. (2015). Comprehensive characterization of sphingolipid ceramide N-deacylase for the synthesis and fatty acid remodeling of glycosphingolipids. Applied Microbiology and Biotechnology 99, 6715-6726.

Hannich, J.T., Umebayashi, K., and Riezman, H. (2011). Distribution and Functions of Sterols and Sphingolipids. Cold Spring Harbor Perspectives in Biology 3, a004762.

Harris, E. (2001). Chlamydomonas as a model organism. Annual Review of Plant Physiology and Plant Molecular Biology 52, 363-406.

He, J.-X., Fujioka, S., Li, T.-C., Kang, S.G., Seto, H., Takatsuto, S., Yoshida, S., and Jang, J.-C. (2003). Sterols Regulate Development and Gene Expression in Arabidopsis. Plant Physiology 131, 1258-1269.

Ho, C., Lam, C., Chan, M., Cheung, L., Law, L., Lit, L., Ng, K., Suen, M., and Tai, H. (2003). Electrospray ionisation mass spectrometry: principles and clinical applications. Clinical Biochemistry Review 24, 3-12.

Holm-Hanson, O. (1964). Isolation and culture of terrestrial and fresh-water algae of Antartica. Phycologia 4, 43-51.

Holmberg, N., Harker, M., Gibbard, C.L., Wallace, A.D., Clayton, J.C., Rawlins, S., Hellyer, A., and Safford, R. (2002). Sterol C-24 methyltransferase type 1 controls the flux of carbon into sterol biosynthesis in tobacco seed. Plant Physiology 130, 303-311.

Hoshina, R., Iwataki, M., and Imamura, N. (2010). Chlorella variabilis and Micractinium reisseri sp. nov. (Chlorellaceae, Trebouxiophyceae): Redscription of the endosymbiotic green algae of Paramecium bursaria (Peniculia, Oligohymenophorea) in the 120th year. Phycological Research 58, 188-201.

Hunter, W.N. (2007). The Non-mevalonate Pathway of isoprenoid Precursor Biosynthesis. The Journal of Biological Chemistry 282, 21573-21577.

ICTV. (2012). Virus taxonomy: Classification and nomenclature of viruses: Ninth Report of the International Committee on Taxonomy of Viruses, A. King, M. Adams, E. Carstens, and E. Lefkowitz, eds (San Diego: Elsevier Academic Press).

Istvan, E.S., and Deisenhofer, J. (2001a). Structural mechanism for statin inhibition of HMG-CoA reductase. Science 292, 1160-1164.

Istvan, E.S., and Deisenhofer, J. (2001b). The structure of the catalytic portion of human HMG-CoA reductase. Biochimica et Biophysica Acta 1529, 9-18.

Iyer, L., Balaji, S., Koonin, E., and Aravind, L. (2006). Evolutionary genomics of nucleo-cytoplasmic large DNA viruses. Virus Research 117, 156-184.

Jordan, R.W., and Chamberlain, A.H.L. (1997). Biodiversity among haptophyte algae. Biodiversity Conservation 6, 131-152.

Kapaun, E., and Reisser, W. (1995). A chitin-like glycan in the cell wall of a Chlorella sp. (Chlorococcales, Chlorophyceae). Planta 197, 577-582.

Katoh, K., and Standley, D. (2013). MAFFT multiple sequence alignment software version 7: improvements in performance and usability. Molecular Biology and Evolution 30, 772-780.

Kennedy, M., and Bard, M. (2001). Positive and negative regulation of squalene synthase (erg9), an ergosterol biosynthetic gene, in Saccromyces cerevisiae. Biochimica et Biophysica Acta 1517, 177-189.

Kodner, R.B., Pearson, A., Summons, R.E., and Knoll, A.H. (2008). Sterols in red and green algae: quantification, phylogeny, and relevance for the interpretation of geologic steranes. Geobiology 6, 411-420.

Koonin, E.V., and Yutin, N. (2001). Nucleo-cytoplasmic Large DNA Viruses (NCLDV) of Eukaryotes. In eLS (John Wiley & Sons, Ltd.

Kumari, P., Kumar, M., Reddy, C., and Jha, B. (2012). Algal lipids, fatty acids and sterols. In Functional ingredients from algae for foods and nutraceuticals, H. Dominguez, ed (Woodhead Publishing Ltd.), pp. 87-134.

Kuznetsov, Y., Klose, T., Rossmann, M.G., and McPherson, A. (2013). Morphogenesis of Mimivirus and its viral factories: an atomic force microscopy study of infected cells. Journal of Virology 87, 11200-11213.

Kuzuyama, T. (2002). Mevalonate and Nonmevalonate Pathways for the Biosynthesis of Isoprene Units. Bioscience Biotechnology Biochemistry 66, 1619-1627.

Lagace, T., and Ridgway, N. (2013). The role of phospholipids in the biological activty and structure of the endoplasmic reticulum. Biochemical and Biophysical Acta 1833, 2499-2510.

Leonardsen, L., Stromstedt, M., and Byskov, A. (2000). Effect of inhibition of sterol delta 14-reductase on accumulation of meiosis-activating sterol and meiotic resumption in cumulus-enclosed mouse oocytes in vitro. Journal of Reproduction and Fertility 118, 171-179.

Lewis, J., and Graybill, J. (2008). Fungicidal versus fungistatic: What's in a word? Expert opinion on pharmacotherapy 9, 927-935.

Lombard, J., and Moreira, D. (2011). Origins and Early Evolution of the Mevalonate Pathway of isoprenoid Biosynthesis in the Three Domains of Life. Molecular Biology and Evolution 28, 87-99.

Maier, I., Muller, D., and Katsaros, C. (2002). Entry of the DNA virus, Ectocarpus fasciculatus type 1 (Phycodnaviridae), into host cell cytosol and nucleus. Phycology Research 50, 227-231.

Malhotra, H., and Goa, K. (2001). Atorvastatin: an updated review of its pharmacological properties and use in dyslipidemia. Drugs 61, 1835-1881.

Malin, G., Wilson, W., Bratbak, G., Liss, P., and Mann, N. (1998). Elevated production of dimethylsulfide resulting from viral infection of cultures of Phaeocystis pouchetti. Limnology and Oceanography 43, 1389-1393.

Markham, J.E. (2013). Acyl-Lipid Metabolism. In The Arabidopsis Book 11.e0161 (The American Society of Plant Biologists.

Markham, J.E., Li, J., Cahoon, E.B., and Jaworski, J.G. (2006). Separation and Identification of Major Plant Sphingolipid Classes from Leaves. The Journal of Biological Chemistry 281, 22684-22694.

Marques, J.T., Cordeiro, A.M., Viana, A.S., Herrmann, A., Marinho, H.S., and de Almeida, R.F. (2015). Formation and Properties of Membrane-Ordered Domains by Phytoceramide: Role of Sphingoid Base Hydroxylation. In ACS Publications - Langmuir, pp. 12.

Mayer, J., and Taylor, F. (1979). A virus which lyses the marine nanoflagellate Micromonas pusilla. Nature 281, 299-301.

Mehmel, M., Rothermel, M., Meckel, T., Van Etten, J.L., Moroni, A., and Thiel, G. (2003). Possible function for virus encoded K+ channel Kcv in the replication of chlorella virus PBCV-1. FEBS Letters 552, 7-11.

Meints, R.H., Lee, K., and Van Etten, J.L. (1986). Assembly site of the virus PBCV-1 in a Chlorella-like green alga: ultrastructural studies. Virology 154, 240-245.

Meints, R.H., Lee, K., Burbank, D.E., and Van Etten, J.L. (1984). Infection of a chlorella-like alga with the virus, PBCV-1: Ultrastructural studies. Virology 138, 341-346.

Mercer, E. (1993). Inhibitors of sterol biosynthesis and their applications. Progress in Lipid Research 32, 357-416.

Merchant, S.S.e.a. (2007). The Chlamydomonas Genome Reveals the Evolution of Key Animal and Plant Functions. Science 318.

Miller, M.B., Haubrich, B.A., Wang, Q., Snell, W.J., and Nes, D. (2012). Evolutionarily conserved delta 25(27)-olefin ergosterol biosynthesis pathway in the alga Chlamydomonas reinhardtii. Journal of Lipid Research 53, 1636-1645.

Miller, S.M. (2010). Volox, Chlamydomonas, and the Evolution of Multicellularity. Nature Education 3, 65.

Milrot, E., Mutsafi, Y., Fridmann-Sirkis, Y., Shimoni, E., Rechav, K., Gurnon, J., Van Etten, J.L., and Minsky, A. (2015). Virus-host interactions: insights from the replication cycle of the large Paramecium bursaria Chlorella virus. Cellular Microbiology.

Mo, C., and Bard, M. (2005). A systematic study of yeast sterol biosynthetic protein-protein interactions using the split-ubiquitin system. Biochemical and Biophysical Acta 1737, 152-160.

Morita, M., Watanabe, Y., and Saiki, H. (2000). High photosynthetic productivity of green microalga Chlorella sorokiniana. Applied Biochemistry and Biotechnology 87, 203-218.

Murphy, R., Fiedler, J., and Hevco, J. (2001). Analysis of nonvolatile lipids by mass spectrometry. Chemical Reviews 101, 479-526.

Mutsafi, Y., Shimoni, E., Shimon, A., and Minsky, A. (2013). Membrane assembly during the infection cycle of the giant Mimivirus. PlOS Pathogens 9.

Nagasaki, K., and Yamaguchi, M. (1998a). Isolation of a virus infectious to the harmful bloom causing microalga Heterosigma akashiwo virus. Aquatic Microbial Ecology 15.

Nes, W.R., and New, W.D. (1980). Lipids in Evolution (New York: Plenum), pp. 157-197.

Paradies, G., Paradies, V., De Benedictis, V., Ruggiero, F.M., and Petrosillo, G. (2014). Functional role of cardiolipin in mitochondrial bioenergetics. Biochemical and Biophysical Acta 1837, 408-417.

Patterson, G.W. (1991). Physiology and Biochemistry of Sterols. (American Oil Chemists' Society).

Plugge, B., Gazzarrini, S., Nelson, M., Cerana, R., Van Etten, J.L., Derst, C., DiFrancesco, D., Moroni, A., and Thiel, G. (2000). A potassium channel protein encoded by chlorella virus PBCV-1. Science 287.

Porsbring, T., Blanck, H., Tjellstrom, H., and Backhaus, T. (2009). Toxicity of the pharmaceutical clotrimazole to marine microalgal communities. Aquatic toxicology 91, 203-211.

Rahier, A., and Taton, M. (1997). Fungicides as Tools in Studying Postsqualene Sterol Synthesis in Plants. Pesticide Biochemistry and Physiology 57, 1-27.

Rao, V., and Feiss, M. (2008). The bacteriophage DNA packaging motor. Annual Review Genetics 42, 647-681.

Raoult, D., La Scola, B., and Birtles, R. (2007). The discovery and characterization of Mimivirus, the largest known virus and putative pneumonia agent. Clinical Infectious Diseases 45, 95-102.

Read, B.A., Kegel, J., Klute, M.J., Kuo, A., Lefebvre, S.C., Maumus, F., Mayer, C., Miller, J., Monier, A., Salamov, A., Young, J., Aguilar, M., Claverie, J.-M., Frickenhaus, S., Gonzalez, K., Herman, E.K., Lin, Y.-C., Napier, J., Ogata, H., Sarno, A.F., Shmutz, J., Schroeder, D., de Vargas, C., Verret, F., von Dassow, P., Valentin, K., Van de Peer, Y., Wheeler, G., Emiliania huxleyi Annotation, C., Dacks, J.B., Delwiche, C.F., Dyhrman, S.T., Glockner, G., John, U., Richards, T., Worden, A.Z., Zhang, X., and Grigoriev, I.V. (2013). Pan genome of the phytoplankton Emiliania underpins its global distribution. Nature 499, 209-213.

Rennie, E., Ebert, B., Miles, G., Cahoon, R.E., Christiansen, K., Stonebloom, S., Khatab, H., Twell, D., Petzold, C., Adams, P., Dupree, P., Heazlewood, J., Cahoon, E.B., and Scheller, H. (2014). Identification of a sphingolipid alpha-glucuronosyltransferase that is essential for pollen function in Arabidopsis. Plant Cell 26, 3314-3325.

Rhee, S., Beavis, W., Berardini, T., Chen, G., Dixon, D., Doyle, A., Garcia-Hernandez, M., Huala, E., Lander, G., Montoya, M., Miller, N., Mueller, L., Mundodi, S., Tacklind, J., Weems, D., Wu, Y., Xu, I., Yoo, D., Yoon, J., and Zhang, P. (2003). The Arabidopsis Information Resource (TAIR): a model organism database providing a centralized, curated gateway to Arabidopsis biology, research materials and community. Nucleic Acids Research 31, 224-228.

Rice, G., Tang, L., Stedman, K., Roberto, F., Spuhler, J., Gillitzer, E., Johnson, J., Douglas, T., and Young, M. (2004). The structure of a thermophilic archaeal virus shows a double-stranded DNA viral capsid type that spans all domains of life. PNAS 101, 7716-7720.

Roberts, S.C. (2007). Production and engineering of terpenoids in plant cell culture. Nature Chemical Biology 3, 387-395.

Robinson, G., Tsay, Y., Kienzle, B., Smithmonroy, C., and Bishop, R. (1993). Conservation between human and fungal squalene synthetases: similarities in structure, function, and regulation. Molecular Cell Biology 13, 2706-2717.

Roine, E., and Bamford, D.H. (2012). Lipids of Archaeal Viruses. Archaea, 8.

Rossard, S., Roblin, G., and Atanassova, R. (2010). Ergosterol triggers characteristic elicitation steps in Beta vulgaris leaf tissues. Journal of Experimental Botany 61, 1807-1816.

Rowe, J.M., Jeanniard, A., Gurnon, J., Xia, Y., Dunigan, D.D., Van Etten, J.L., and Blanc, G. (2014). Global analysis of Chlorella variabilis NC64A mRNA profiles during the early phase of Paramecium bursaria Chlorella Virus-1 infection. PLoS ONE 9.

Ryder, N. (1992). Terbinafine: mode of action and properties of the squalene epoxidase inhibition. The British Journal of Dermatology 126, 2-7.

Schug, Z.T., and Gottlieb, E. (2009). Cardiolipin acts as a mitochondrial signalling platform to launch apoptosis. Biochemical and Biophysical Acta, 2022-2031.

Schuster, A., Girton, L., Burbank, D.E., and Van Etten, J.L. (1986). Infection of a Chlorella-like alga with the virus PBCV-1: Transcriptional studies. Virology 148, 181-189.

Segura, M., Lodeiro, S., Meyer, M., Patel, A., and Matsuda, S. (2002). Directed evolution experiments reveal mutations at cycloartenol synthase residue His477 that dramatically alter catalysis. Organic Letters 4, 4459-4462.

Seppanen-Laakso, T., and Oresic, M. (2009). How to study lipidomes. Journal of Molecular Endocrinology 42, 185-190.

Siaut, M., Cuine, S., Cagnon, C., Fessler, B., Nguyen, M., Carrier, P., Beyly, A., Beisson, F., Triantaphylides, C., Li-Beisson, Y., and Peltier, G. (2011). Oil accumulation in the model green alga Chlamydomonas reinhardtii: characterization, variability between common laboratory strains and relationship with starch reserves. BMC Biotechnology 11.

Song, Z., and Nes, D. (2007). Sterol biosynthesis inhibitors: potential for transition state analogs and mechanism-based inactivators targeted at sterol methyltransferase. Lipids 42, 15-33.

Sun, L., Adams, B., Gurnon, J., Ye, Y., and Van Etten, J.L. (1999). Characterization of two chitinase genes and one chitosanase gene encoded by Chlorella virus PBCV-1. Virology 263, 376-387.

Suzuki, M., and Muranaka, T. (2007). Molecular Genetics of Plant Sterol Backbone Synthesis. Lipids 42, 47-54.

Taramino, S., Valachovic, M., Oliaro-Bosso, S., Viola, F., Teske, B., Bard, M., and Balliano, G. (2010). Interactions of oxidosqualene cyclase (Erg7p) with 3-keto reductase (Erg27p) and other enzymes of sterol biosynthesis in yeast. Biochimica et Biophysica Acta 1801.

Teske, B., Taramino, S., Bhuiyan, M.S.A., Kumaraswarmi, N.S., Randall, S.K., Barbuch, R., Eckstein, J., Balliano, G., and Bard, M. (2008). Genetic analyses involving interactions between the ergosterol biosynthetic enzymes, lanosterol synthase (Erg7p) and 3-ketoreductase (Erg27p), in the yeast Saccromyces cerevisiae. Biochemical and Biophysical Acta 1781, 359-366.

Vago, T., Baldi, G., Colombo, D., Barbareschi, M., Norbiato, G., Dallegri, F., and Bevilacqua, M. (1994). Effects of Naftifine and Terbinafine, Two Allylamine Antifungal Drugs, on Selected Functions of Human Polymorphonuclear Leukocytes. Antimicrobial Agents and Chemotherapy 38, 2605-2611.

Van Etten, J.L. (2003). Unusual life style of giant Chlorella viruses. Annual Review Genetics 37, 153-195.

Van Etten, J.L., and Dunigan, D.D. (2012). Chloroviruses: Not your everyday plant virus. Trends in Plant Science 17, 1-8.

Van Etten, J.L., Burbank, D.E., Kuczmarski, D., and Meints, R.H. (1983). Virus infection of culturable Chlorella-like algae and development of a plaque assay. Science 219, 994-996.

Van Etten, J.L., Burbank, D.E., Joshi, J., and Meints, R.H. (1984). DNA synthesis in a chlorella-like alga following infection with the virus PBCV-1. Virology 134, 443-449.

Van Etten, J.L., Graves, M., Muller, D., Boland, W., and Delaroque, N. (2002). Phycodnaviridae - large DNA algal viruses. Archives of Virology 147, 1479-1516.

Van Etten, J.L.G., MV; Muller, DG; Boland, W; Delaroque, N. (2002). Phycodnaviridae -- large DNA algal viruses. Archives of Virology 147, 1479-1516.

Van Meer, G., Voelker, D.R., and Feignson, G.W. (2008). Membrane lipids: where they are and how they behave. Nature Reviews Molecular Cell Biology 9.

Veen, M., Stahl, U., and Lang, C. (2003). Combined overexpression of genes of the ergosterol biosynthetic pathway leads to accumulation of sterols in Saccharamomyces cerevisiae. FEMS Yeast Research 4, 87-95.

von Dassow, P., Ogata, H., Probert, I., Wincker, P., Da Silva, C., Audic, S., Claverie, J.-M., and de Vargas, C. (2009). Transcriptome analysis of functional differentiation between haploid and diploid cells of Emiliania huxleyi, a globally significant photosynthetic calcifying cell. Genome Biology 10, R114.

Weernink, P., Han, L., Jakobs, K., and Schmidt, M. (2007). Dynamic phospholipid signaling by G protein-coupled receptors. Biochemical and Biophysical Acta - Biomembranes 1768, 888-900.

Wenk, M. (2005). The emerging field of lipidomics. Nature Reviews Drug Discovery 4, 594-610.

Wilson, W., Van Etten, J., and Allen, M. (2009). "The Phycodnaviridae: the story how tiny giants rule the world". Current Topics in Microbiology and Immunology 328, 1-42.

Winkel, B.S.J. (2009). Multi-enzyme Complexes. In Plant-derived natural products: Synthesis, function and application, A.E. Osbourn and V. Lanzotti, eds (New York: Springer), pp. 195.

Xu, X., Bittman, R., Duportail, G., Heissler, D., Vilcheze, C., and London, E. (2001). Effect of the Structure of Natural Sterols and Sphingolipids on the Formation of Ordered Sphingolipid/Sterol Domains (Rafts). The Journal of Biological Chemistry 276, 33540-33546.

Yanai-Balser, G.M., Duncan, G., Eudy, J.D., Wang, D., Li, X., Agarkova, I., Dunigan, D.D., and Van Etten, J.L. (2010). Microarray analysis of Paramecium bursaria Chlorella Virus 1 transcription. Journal of Virology 84, 532-542.

Yashchenko, V.V., Gavrilova, O.V., Rautian, M.S., and Jakobsen, K. (2012). Association of Paramecium bursaria Chlorella viruses with Paramecium

bursaria cells: Ultrastructural studies. European Journal of Protistology 48, 149-159.

Zhang, X., Xiang, Y., Duncan, G., Klose, T., Chipman, P.R., Van Etten, J.L., and Rossmann, M.G. (2011). Three-dimensional structure and function of the Paramecium bursaria chlorella virus capsid. PNAS 108, 14837-14842.

Zhou, W., Lepesheva, G.I., Waterman, M.R., and Nes, D. (2006). Enzyme Catalysis and Regulation: Mechanistic Analysis of a Multiple Product Sterol Methyltransferase Implicated in Ergosterol Biosynthesis in Trypanosoma brucei. The Journal of Biological Chemistry 281, 6290-6296.

Table 1. Percentage* of major sterol composition in fresh water and marine microalgae.

	C. variabilis	C. sorokiniana	C. reinhardtii	Volvox	Coccomyxa	E. huxleyi	T. pseudonana
Erogosterol	97.6	82	62.1	68.4	0	0	0
Ergosta-5,8-dienol	2.4	6	0	0	0	0	0
Ergosta-7,22-dienol	0	5	0	0	0	100	0
Ergost-7-ene	0	7	0	0	0	0	0
Ergosta-5,8,22-trienol	0	0	2.4	0	0	0	0
7-dehydroporiferasterol	0	0	35.5	31.6	0	0	0
Campesterol	0	0	0	0	45.2	0	0
Stigmasterol	0	0	0	0	20.8	0	100
β-sitosterol	0	0	0	0	34	0	0
Total Sterols (nmol/mg dw)	2.5	3.2	3.4	1.9	3.6	1.4	1.0

*Percentage of total sterol.

Table 2. Sterol biosynthetic pathway genes

PATHWAY	FUNCTION (CHARACTERIZED OR PREDICTED)	ARABIDOPSIS THALIANA (Gene ID)	DESIGNATED GENE SYMBOL	CHLORELLA VARIABILIS (CHLNCDRAFT)	% QUERY COVERAGE	E-VALUE	% IDENTITY	CHLORELLA SOROKINIANA (scaffold)	E-VALUE	S. CEREVISIAE (homologue)
MEP PATHWAY STAGE I- PLASTID	1-deoxy-D-xylulose 5-phosphate synthase	At(Q38854)	DXPS	59788	90	0	68	185.g31	0	
	1-deoxy-D-xylulose 5-phosphate reductoisomerase	At5g62790	DXR	29723	89	0	68	79.g22	9e-156	
	2-C-methyl-D-erythritol 4-phosphate cytidyltransferase	At2g02500	MCT	141910	42	3e-22	66	11.g46	4e-37	
	4-diphosphocytidyl-2-C-methyl-D-erythritol kinase	At2g26930	CMK	33454	76	2e-95	54	85.g90	1e-170	
	2-C-methyl-D-erythritol 2,4-cyclo-diphosphate synthase	At1g63970	MCS	53457	68	6e-91	76	55.g46	4e-118	
	1-hydroxy-2-methyl-2E-butenyl-4-diphosphate synthase	At5g60600	HMB-PPS	144676	94	0	55	127.g4	0	
	4-hydroxy-3-methyl-2E-butenyl-4-diphosphate reductase	At4g34350	HMB-PPR	59658	86	6e-173	59	12.g126	0	
	Isopentenyl pyrophosphate isomerase	At5g16440/ At3g02780	IPI (iPPI1/iPPi2)	53578	76	2e-64	45	136.g51	5e-157	
MVA PATHWAY STAGE I- CYTOSOL	Acetoacetyl-CoA thiolase	At5g47720/ At5g48230	AACT (AAT1/AAT2)	27161	94	5e-159	59	243.g48	0	
	3-Hydroxy-3-methylglutaryl-CoA synthase	At4g11820	HMGS	138158	97	9e-116	41	110.g88	0	
	3-Hydroxy-3-methylglutaryl-CoA reductase	At1g76490/At2g17370	HMGR	NF				NF		
	Mevalonate kinase	At5g27450	MK	NF				NF		
	Phosphomevalonate kinase	At1g31910	PMK	NF				NF		
	Mevalonate diphosphate decarboxylase	At2g38700/At3g54250	MVD1/2	N				NF		
STAGE II- ER	Farnesyl pyrophosphate synthase	At5g47770/ At4g17190	FPS (FPS1/FPS2)	33543	89	2e-122	53	140.g5	0	ERG20
	Squalene synthase	At4g34640/ At4g34650	SQS (SQS1/SQS2)	18492 / 55669 (partial)	46 / 32	5e-64 / 8e-24	53 / 37	85.g33	9e-113	ERG9
	2,3-oxidosqualene	At1g58440	SQE (SQE1-7)	137251	82	1e-148	50	94.g19	0	ERG1
STAGE III- ER	Cycloarterol/Lanosterol Synthase	At2g07050/At3g45130	CAS/LAS	22200	99	0	60	81.g34	0	ERG7
	C14-alpha-demethylase/ C22-desaturase	At1g11680/At2g17330	14DM1/14DM2	56217	98	0	55	139.g2	0	ERG11/5
	Delta-14/24-reductase	At3g52940/ At3g19820	DIM	136479	16	6e-06	30	275.g2	0	ERG4/24
	C4-demethylase/ Delta7-SterolC5-desaturase	At NP_567669/At3g02580	SMO/DWF7	37407	49	4e-04	25	134.g50	8e-157	ERG25/3
	C4-decarboxylase/C3-dehydrogenase	At AAY28502		49861	95	5e-89	45	89.g160	3e-140	ERG26
	3-ketoreductase	At EE34688		56728	84	4e-72	41	89.g307	3e-146	ERG27
	S-AdoMet-C24-methyltransferase	At AAG28462	SMT1	37067	49	4e-21	35	15.g7	0	ERG6
	Delta8-delta7-sterol isomerase	At1g20050	HYDRA1	34496	100	2e-49	38	34.g25	5e-129	ERG2

Table 3. Antifungal inhibition of *Chlorella variabilis* sterol biosynthetic pathway. Methanol (MeOH), statin (ST), terbinafine (TB), ketoconazole (KC), and clotrimazole (CT).

	MeOH	ST	TB	KC	CT
Ergosterol	97.6	97.3	98.8	74.9	67.2
Ergosta-5,8-dienol	2.4	2.7	1.2	5.2	5.9
14-demethyllanosterol	0	0	0	6.9	18.4
Lanosterol	0	0	0	12.9	8.5
Total Sterols (nmol/mg dw)	4.3	4.1	2.5	4.0	3.5

Table 4. Antifungal inhibition of *Chlorella sorokiniana* sterol biosynthetic pathway. Methanol (MeOH), statin (ST), terbinafine (TB), ketoconazole (KC), and clotrimazole (CT).

	MeOH	ST	TB	KC	CT
Ergosterol	82.1	82.9	85.1	65.7	51.3
Ergosta-5,8-dienol	6.1	7.0	7.9	7.5	20.1
Ergosta-7,22-dienol	4.6	4.6	3.7	11.3	3.4
Ergost-7-ene	6.8	5.5	3.3	5.4	3.7
Lanosterol	0	0	0	8.4	14.9
24-methylene-cycloartenol	0	0	0	1.7	6.6
Total Sterols (nmol/mg dw)	3.2	2.7	2.0	2.6	2.6

Table 5. Antifungal inhibition of *Chlamydomonas reinhardtii* sterol biosynthetic pathway. Methanol (MeOH), ketoconazole (KC), and clotrimazole (CT).

	MeOH	*KC*	*CT*
Ergosterol	62.0	22.0	26.5
Ergosta-5,8,22-trienol	2.3	0	0.0
7-dehydroporiferasterol	35.7	0	0.0
Ergost-7-ene	0	5.9	11.7
Ergosta-5,8-dienol	0	2.5	1.3
Stigma-4,7,22-trienol	0	27.3	27.8
Lanost-3beta-ol	0	30.5	19.4
Stigmasterol	0	5.3	9.1
Lanost-8-ene	0	3.1	2.4
24-methylene	0	3.5	1.7
Total Sterols (nmol/mg dw)	3.4	3.2	3.0

Table 6. Antifungal inhibition of *Coccomyxa* sterol biosynthetic pathway.
Methanol (MeOH), ketoconazole (KC), and clotrimazole (CT).

	MeOH	KC	CT
Campesterol	45.4	32.9	40.5
Stigmasterol	20.7	19.2	15.9
B-Sitosterol	34.0	29.6	36.2
Lanosterol	0	2.8	3.4
Cycloartenol	0	0.8	1.0
24-methylene	0	8.0	1.4
25-methylene	0	11.6	0.9
14-dimethyllanosterol	0	0.7	0.8
Total Sterols (nmol/mg dw)	3.6	4.6	3.7

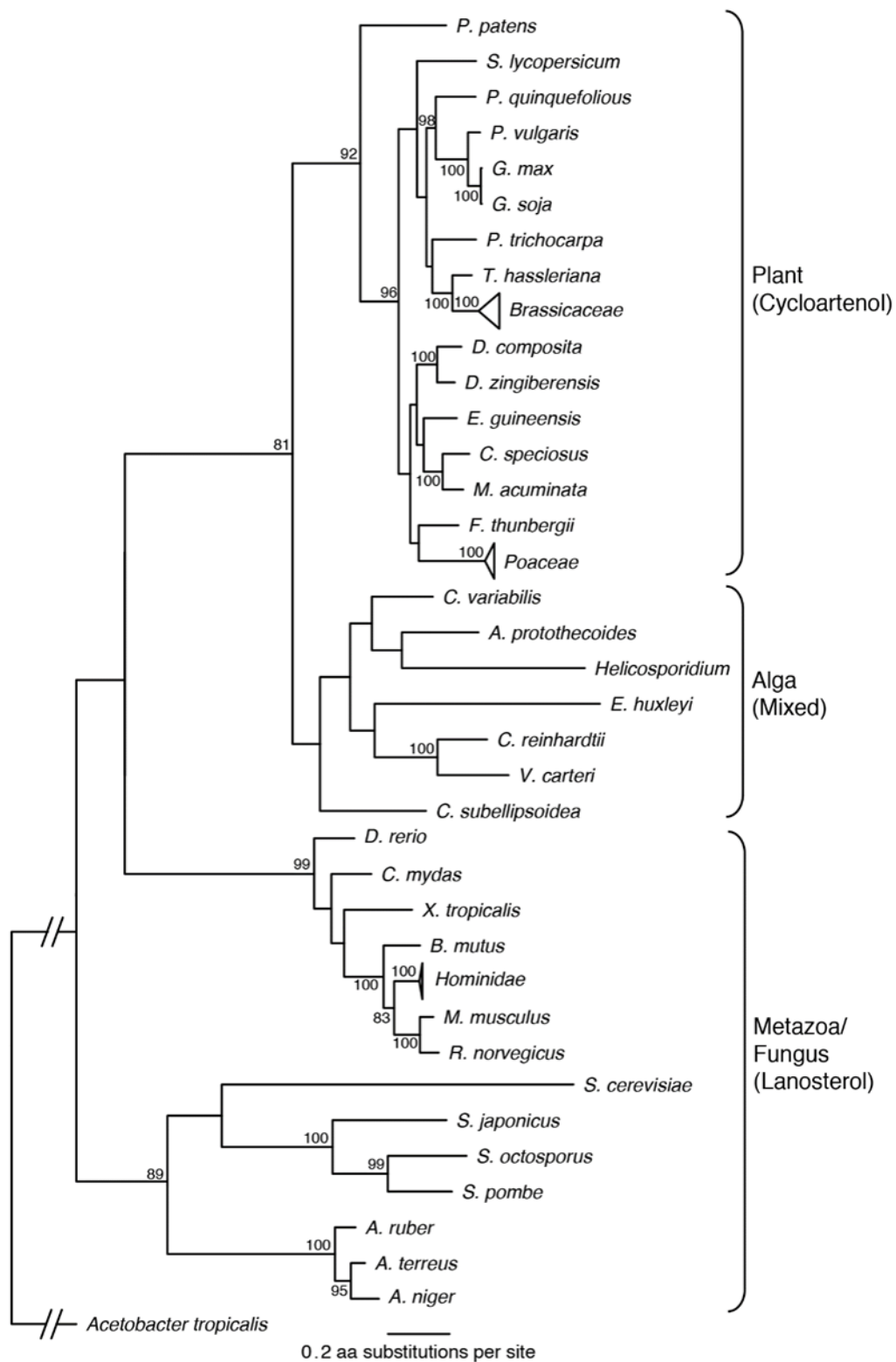Figure 1. Ergosterol biosynthetic pathway in *Chlorella variabilis*.
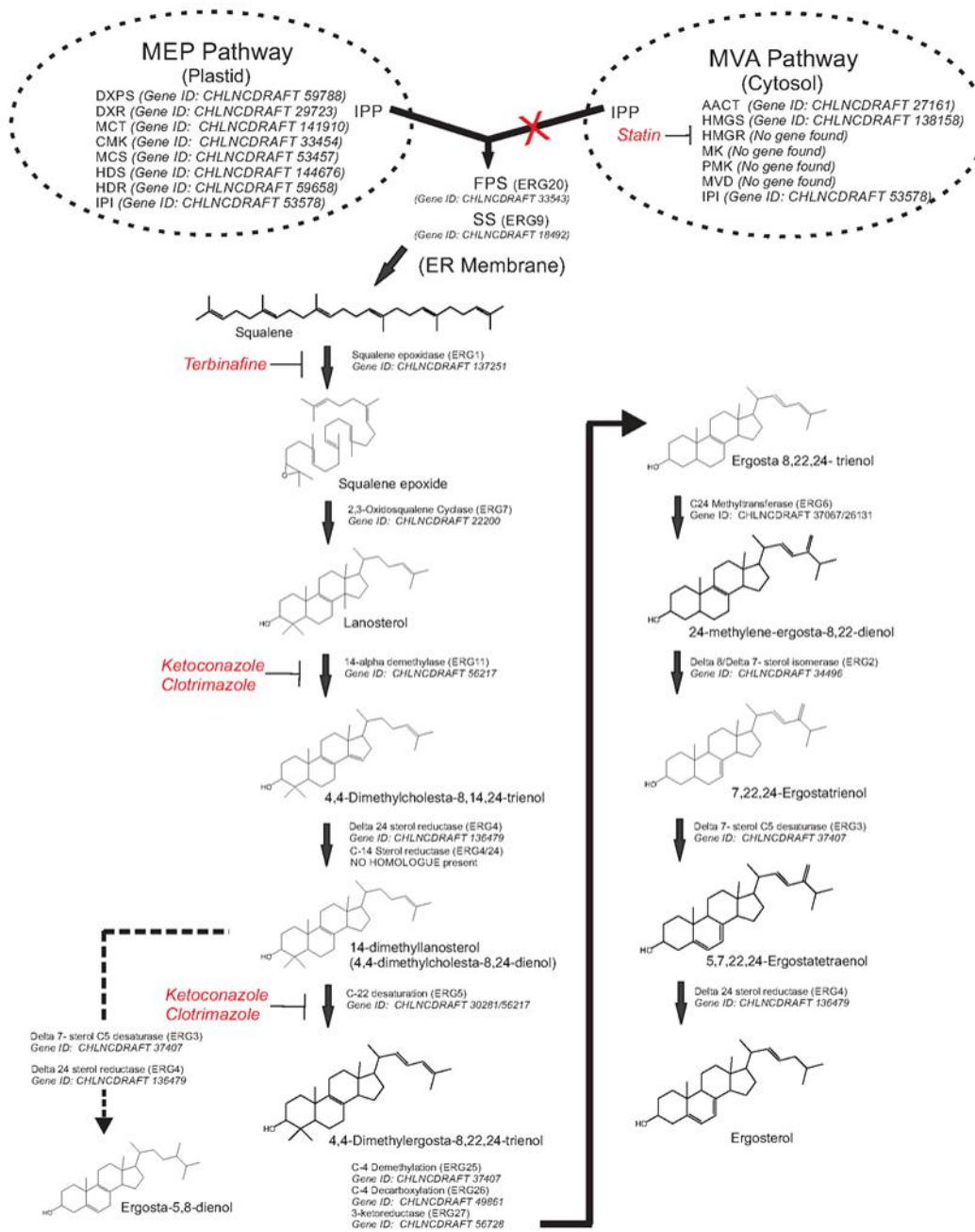
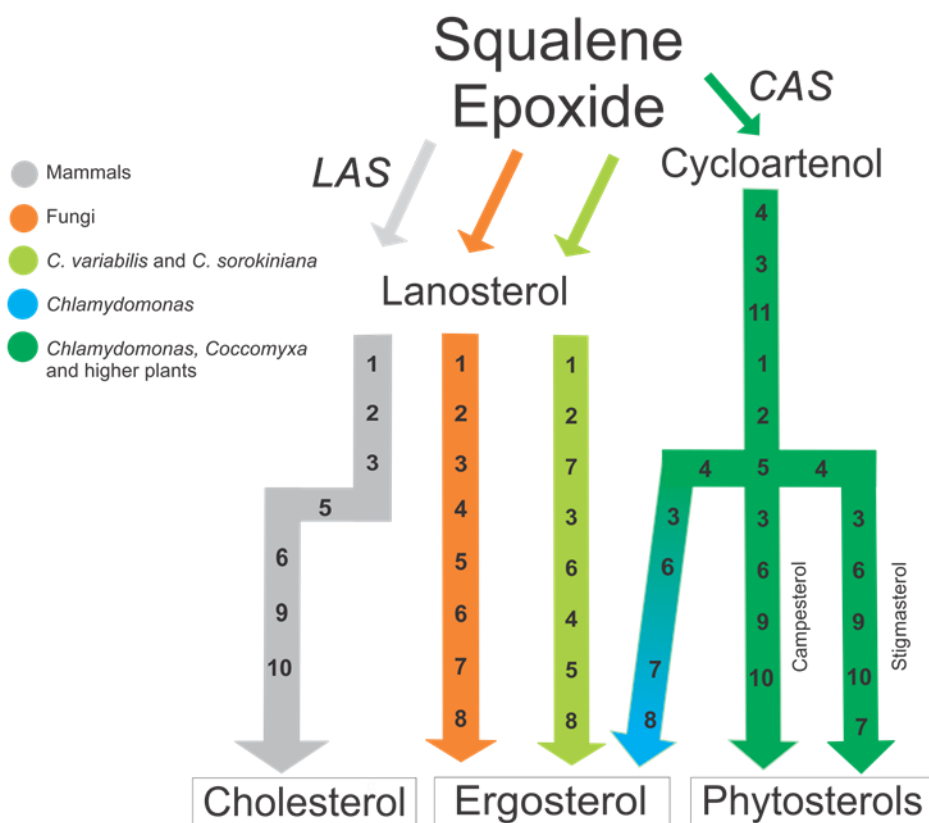Figure 2. Oxidosqualene Cyclase (OSC) phylogenetic tree.

Figure 3. Deduced pathway of sterol biosynthesis from squalene epoxide in *C. variabilis* in comparison with mammals, fungi, algae and higher plants. Numbers represent enzymatic steps of pathway as nomenclature due to different names and abbreviations between species. Enzymes present in each pathway catalyze equivalent reactions. *Chlorella* contains the same number of enzymatic steps in ergosterol biosynthesis as fungi; however, the order of the enzymatic steps differ. In mammals, fungi and *Chlorella*, step 3 is a combination of ERG 25-27 enzymes which is a C4 demethylation complex and cycles twice, whereas in other algae and higher plants each C4 methyl group removal occurs at different stages of synthesis. Lanosterol synthase (LAS) is present in higher plants but has a minor role. Enzyme abbreviations and function: LAS, lanosterol synthase; CAS, cycloartenol synthase 1) CYP51, ERG11, Sterol 14α-demethylase 2) FK, Fackel, ERG24, Sterol C-14 reductase 3) SMO, ERG 25-27, Sterol C4 demethylation complex 4) SMT1, ERG6, Sterol C-24 methyl-transferase 5) HYD1, ERG2, delta8, delta7 isomerase 6) DWF7, ERG3, delta7 sterol C5 desaturase 7) CYP710A, ERG5, Sterol C-22 desaturase 8) ERG4, sterol delta 24(28) reductase 9) DWF5, sterol C7 reductase 10) DHCR24/DWF1, dihydrocholesterol reductase/sterol C24(28) isomerase-reductase 11) CPI, cycloeucanol cycloisomerase.

CHAPTER 3

GIPC Sphingolipid Diversity: Composition, Structure and Function Among the *Chlorophytes*

Suzanne L. Rose[1,2], Trevor Rohmsdahl[4,5], James L. Van Etten[2,3,5], Jennifer E. Markham[4,5]

[1]School of Biological Sciences, University of Nebraska, Lincoln, NE 68588-0118

[2]Nebraska Center for Virology, University of Nebraska, Lincoln, NE 68583-0900

[3]Department of Plant Pathology, University of Nebraska, Lincoln, NE 68583-0722

[4]Department of Biochemistry, University of Nebraska, Lincoln, NE 68588-0664

[5]Center for Plant Science Innovation, University of Nebraska, Lincoln, NE 68588

Corresponding author: Jennifer E. Markham

Abstract

The identification and characterization of glycosyl inositol phosphoceramides (GPICs) in plants is a current topic of interest in lipid research; however, little information exists on the prevalence of this sphingolipid class in algae. Advances in mass spectrometric methods provide the tools for the structural analysis of GIPCs. The goal of this research focuses on the characterization and structure analysis of the major sphingolipid, GIPCs, of the unicellular green algae (division *Chlorophyta*). Given the ecological and evolutionary divergence among algae we anticipated variances in their overall GIPC structure. Liquid Chromatography- and Gas Chromatography-Mass Spectrometry analysis of long chain base (LCB) and fatty acid (FA) composition, respectively, identified the major ceramide structure of *Chlorophytes* as having a trihydroxylated, 18-carbon LCB (t18:0) and a 24-carbon hydroxy FA (h24:0), both either saturated or monounsaturated. GIPC profiling was performed for *Chlorella variabilis*, *Chlorellea sorokiniana*, *Chlamydomonas reinhardtii*, and *Coccomyxa subellipsoidea c-169*. Complete structure analysis of the major GIPCs was successfully determined using HPLC-ESI-MS. GIPC-fragment ions were detected and based on fragmentation patterns final structures were characterized regarding fatty acyl chain, long chain base and polar head groups. Variance among the Chlorophytes was observed in the presence or absence of hexuronic acid (HexA) in their GIPCs. This research will provide the foundation for future research in elucidating the role of algal GIPC sphingolipids as components of specialized microdomains, or lipid rafts, in the cell membrane. Enriched in GIPC

sphingolipids, sterols and membrane-associated proteins, substantial evidence supports these specialized microdomains play a central role in regulating cellular processes, stress response and viral infection.

Introduction

In eukaryotic organisms, the major structural lipids in cell membranes belong to the class sphingolipids. Together with sterols and glycerolipids, sphingolipids are essential for the formation, stability, and fluidity of cell membranes (Breslow and Weissman, 2010; Blaas and Humpf, 2013). With essential additional functions as signaling molecules and components of lipid rafts, they also play a crucial role in programmed cell death (PCD) and determining cell fate during viral infection (Breslow and Weissman, 2010; Cacas et al., 2013; Rennie et al., 2014).

The unique and complex functions of sphingolipids rely on the remarkably diverse modifications to their core structure. The key lipid building blocks, long-chain bases (LCBs) and fatty acids (FAs), are attached to a serine backbone creating the core structure ceramide, to which head-group modifications can be added (Breslow and Weissman, 2010). Glycosyl inositol phosphoceramides (GIPCs) represent the most abundant class of sphingolipids in higher plants, making up to 25% of the plasma membrane and having the general structure *(N-acetyl)* glucosamine-glucuronic acid-inositolphosphoceramide where either at the inositol or glucosamine residues diverse saccharides can be added (Markham et al., 2006; Cacas et al., 2013; Rennie et al., 2014).

The prevalence and occurrence of these inositol-containing glycosphingolipids, GIPCs in unicellular algae is relatively understudied. The focus of this comparative study is to: 1) Identify sphingolipid biosynthetic genes involved in synthesis, homeostasis and regulation of algal sphingolipids, 2) characterize the major GIPC structures among *Chlorophytes* and 3) compare their functional role in lipid raft formation. The freshwater, unicellular green algae *Chlorella variabilis*, *Chlorella sorokiniana*, *Chlamydomonas reinhardtii*, and *Coccomyxa subellipsoidea* were chosen to address these issues because of their *Chlorophyta* classification, the availability of sequenced genomes, and their status as model organisms used by the scientific community in research involving cell and molecular biology, ecology, evolutionary biology, pharmacology, and most recently biofuels.

Structural information regarding GIPC sphingolipids and their polar head groups in algae is scarce and remains poorly characterized. With advances in methodology, our mass spectrometry analysis of algal GIPCs was an attempt to characterize this branch of the plant kingdom. In addition, two unanswered questions will be addressed. How diverse are GIPCs within algae? Are there any significant differences in GIPC polar head's between algae, fungi and higher plants? The proposed GIPC structures in *Saccharomyces cerevisiae* are oligo-α-mannose GIPCs with the core structure mannose-inositolphosphoceramide (Man-IPC) and ceramide structure t18:0/h24:0 (Bennion et al., 2003; Cacas et al., 2013; Bure et al., 2014). In comparision, GIPCs in *Arabidopsis thaliana* are slightly more complex having a ceramide structure of t18:1/h24:0 with a polar

head group with glycan moieties attached to a hexuronic acid-inositolphosphoceramide (Hex-HexA-IPC) (Markham, 2013; Bure et al., 2014). Here we report variability in GIPC composition among algae in the division *Chlorophyta*, wherein *Chlorella* species contain fungal-like GIPCs and *Chlamydomonas reinhardtii* and *Coccomyxa subellipsoidea* resemble plant GIPCs.

Materials and Methods

Algal cell cultures and growth conditions.

Chlorella variabilis NC64A and *Coccomyxa* cultures were obtained from James Van Etten. Cultures were grown in Modified Basal Broth Medium (MBBM) under constant shaking of 100 RPM, 22°C and light intensity 30 µmol m^{-2}s^{-1} (µE). *Chlorella sorokiniana* UTEX 1230 was obtained from the University of Texas Culture Collection. *C. sorokiniana* cultures were grown in liquid Basal Broth Medium (BBM) media, shaken at 115 RPM, 25°C, and light intensity of 58 uE. *Chlamydomonas reinhardtii* was obtained from Don Weeks and grown in Tris-Acetate-Phosphate (TAP) media, under constant shaking of 100 RPM, 22°C and light intensity 30 µE.

Bioinformatics: sequence retrieval and alignment.

The identified sphingolipid biosynthetic enzymes from *A. thaliana* (taxid: 3702) were used for the identification of homologs in the genomes of the four algal species; *Chlorella variabilis* (taxid: 554065), *Chlorella sorokiniana*, *Chlamydomonas reinhardtii* (taxid: 3055), and *Coccomyxa* sp. C-169 (taxid:

574566). The completed *Chlorella variabilis* NC64A genome assembly

[http://genome.jgi-psf.org/ChlNC64A_1/ChlNC64A_1.home.html; v1.0; (Blanc et

al., 2010)] was used to search and identify sterol biosynthetic pathway genes.

The newly sequenced and annotated *Chlorella sorokiniana* UTEX 1230 genome

was accessed (Cerutti et al., manuscript in preparation). The *Arabidopsis*

thaliana (NCBI taxon ID: 3702), *Chlamydomonas reinhardtii* (NCBI taxon ID:

3055) and *Coccomyxa* (NCBI taxon ID: 574566) genomes were accessed

through the National Center for Biotechnology Information

(http://www.ncbi.nlm.nih.gov/). The *Arabidopsis thaliana* (NCBI taxon ID: 3702)

sphingolipid biosynthesis genes were used to identify homologues and elucidate

the pathway in *Chlorella varaibilis*.

LCB purification and analysis by LC-MS.

Long chain base samples were obtained through sphingolipid hydrolysis. To

freeze dried pellets (mentioned above), 0.1 nmol/µL of the d16:0 standard, 1 ml

dioxane and 1 ml $Ba(OH)_2$ was added and hydrolysis allowed to proceed

overnight at 110°C. To cooled samples, 2 ml of both 2% ammonium sulphate

and diethylether was added, vortexed then centrifuged at 500 x g for 10 min.

The upper phase was collected in a glass tube and dried under N_2. The samples

were allowed to derivatize at room temperature for 20 min following the addition

of o-phthalaldehyde (OPA) reagent. OPA diluent was added and samples were

run on HPLC/MS (C18 HPLC column). Sphingolipid hydrolysis and LCB analysis

was run in triplicate for each time point.

hFAME purification and analysis by GC-MS.

Analysis of 2-hydroxy fatty acids was achieved through the production of TMS-derivatives of hydroxy fatty acid methyl esters for GC/MS. Hydrolysis with 2 ml methanolic HCL (Fluka 17935) added to freeze dried pellets was allowed to proceed overnight at 75°C. Hexane extractions of the cooled hydrolysis reaction were done in triplicate, the upper phase from each collected and combined into a clean tube and dried under N_2. Extracts were purified on a silica acid column and hFAMEs eluted with hexane:ethyl acetate (6:1, v:v). TMS-derivatives of hFAMEs, using BSFTA +TMCS 99:1 (Supelco, 33154-U), were analyzed by GC/MS. Hydrolysis and production of hFAMEs were run in triplicate for each time point.

Sphingolipid extraction, preparative HPLC, and ESI-MS of algal GIPCs.

All chemicals were of high performance liquid chromatography (HPLC) grade from Sigma. Hexanes were optima grade, propan-2-ol was HPLC grade, both from Fisher. Tetrahydrofuran and methanol were Omnisolv grade and obtained from EMD Biosciences (San Diego, CA). Methods were adapted after Dr. J.E. Markham (Markham et al., 2006).

Micro-isolation of algal sphingolipids.

In a 10 mL glass centrifuge tube, 300 mg dry weight (dw) of freeze dried algal sample was placed with 1 mL beads and 3 mL extraction solvent – lower phase (Propan-2-ol/hexane/water, 55:20:25 v:v:v). Samples were vortexed followed by incubation at 60°C for 15 min. After centrifugation at 500 x g for 10 min., the supernatant was collected in a second 10 mL glass tube and the pellet was

extracted twice more with 3 mL extraction solvent, incubated for 15 min at 60°C each time. The supernatants from each extraction were combined and dried under nitrogen.

Solid phase extraction of sphingolipid extract.

The dried lipid extract was dissolved with 3 mL tetrahydrofuran/methanol/water (1:1:1 v:v:v). Sonication and vortexing was used for effective solubilization. A 200-µl aliquot was removed for hydrolysis and analysis (Total Extract). A SepPak Plus C18 cartridge (Waters, Milford, MA) was prepared by fitting a glass 6-ml luer lock syringe with Teflon frit (Supelco, Bellefonte, PA) to the inlet, followed by 500 mg of C18 silica, passing 2 mL of methanol followed by 2 mL of methanol:water (1:1 v:v) through the cartridge, and the addition of an upper frit. To the sample, 2 mL of water was added, vortexed and centrifuged at 500 x g for 10 min. The supernatant was rapidly poured onto the cartridge and allowed to drain by gravity flow. The column was rinsed twice with 2 mL of methanol:water (1:1 v:v). The sample was eluted with 4 mL chloroform:methanol:water (16:16:5 v:v:v) into clean 10 ml glass centrifuge tubes and eluate was dried under nitrogen.

The C18 eluate was dissolved in 2.9 mL chloroform:methanol:water (16:16:5 v:v:v) and applied to 2 mL of AG4X-X4 acetate resin (Bio-Rad) supported in a 6-ml glass luer lock syringe with lower and upper Teflon frit and allowed to flow by gravity. The column was first washed with 4 mL methanol and 4 mL chloroform:methanol:water (16:16:5 v:v:v). The column flow-through (neutral fraction) was dried under nitrogen and re-dissolved in 2.8 mL chloroform:acetic

acid (99:1) and a 100 µl aliquot was removed for analysis. The anionic charged

lipids were eluted from the column with 7 mL

chloroform/methanol/water/ammonia (16:16:4:1 v:v:v:v) containing 0.1%

triethylamine. The eluate (anionic lipids) was dried under nitrogen and re-

dissolved in 280 µl of propan-2-ol:hexane:water (3:1:1 v:v:v) and 100 µl was

removed for analysis. The re-dissolved neutral fraction (above) was applied to a

SepPak Silica cartridge equilibrated with chloroform:acetic acid (99:1 v:v) and

allowed to drain by gravity flow. The cartridge was washed with 15 mL

chloroform:acetic acid (99:1 v:v). Neutral sphingolipids were eluted from the

cartridge with 4 mL acetone and 4 mL methanol, dried under nitrogen, and

redissolved in 270 µl chloroform. Samples were stored at -20°C for HPLC

analysis.

Electrospray Ionization and Mass Spectrometry.

The charged (anionic) lipid fraction was dried under N_2 and re-suspended in 270

µl of 50% Solvent B (Propan-2-ol:water:formic acid, 60:40:0.1) + 50 mM

ammonium formate. Charged lipid extracts were then introduced by direct

infusion into the TurboV electrospray source of an API 4000 Q TRAP LC/MS/MS

Mass Spectrometer (Applied Biosystems, Foster City, CA) using the flow from a

KDS100 syringe pump (KD Scientific Inc., Holliston, MA), at 10 µl/min with a

source temperature of 650°C and collision energy (CE) of 60. All data were

collected and analyzed using Analyst 1.6.1 (AB Sciex Instruments). Following

data acquisition, the highest signal from the mass spectrum was taken as 100%

abundance and other signals are represented as a percentage of total abundance.

Results

Choice of plant material. Four algal species from the division *Chlorophyta* were selected in order to assess GIPC structural diversity among unicellular, freshwater algae. Algal model organisms used by the scientific community were chosen: *C. variabilis,* a well-known algal model for viral-host interactions as both host and viral genomes have been sequenced (Blanc et al., 2010; Van Etten and Dunigan, 2012); *C. sorokiniana*, recently sequenced and annotated (Cerutti et al., manuscript in preparation), is currently a prime model for the utilization of microalgae biomass for biotechnological studies in the development of biofuel production. The high productivity, high lipid content, and resistance to high light conditions of *C. sorokiniana* make it a suitable candidate for the advancement of increasing algal biomass in photobioreactors (Cazzaniga et al., 2014); *Chlamydomonas* is a haploid, motile organism and has proved to be an excellent system in the study of mutations, as well as flagellar assembly (Harris, 2001; Siaut et al., 2011)*; Coccomyxa*, used in pioneering studies on green algal chromosomal architecture is still widely used in current research on chromosome repair (Darienko et al., 2015). Due to its morphological and physiological plasticity, *Coccomyxa* is an ecological and evolutionary complex alga applicable for a wide array of biological research (Blanc et al., 2012).

Bioinformatics and identification of sphingolipid biosynthetic genes. The enzymatic genes involved in sphingolipid biosynthesis in *Arabidopsis thaliana*

were used to identify homologs in the genomes of the four algal *Chlorophytes*.

A. thaliana (*Brassicaceae, Cruciferae*) is a model organism for the study of

different aspects of plant biology and has been used for more than 50 years to

study plant mutations and classical genetic analysis (Rhee et al., 2003). Here we

have listed the *A. thaliana* gene specific abbreviation, gene identification (ID)

number, the predicted or characterized function and subcellular location of each

enzyme (Table 1). Our initial search was against the *C. variabilis* genome and

along with gene ID, we included percent (%) query coverage, e-value, and

percent (%) identity. As the *C. sorokiniana* genome has not been released with

gene IDs, we have used the available and corresponding scaffold numbers. E-

values are reported for homologs found in *C. sorokiniana*, *Chlamydomonas*, and

Coccomyxa (Table 1). Homologs of the major enzymes involved in sphingolipid

biosynthesis were identified in *Chlorella* with the exception of the long-chain base

(LCB) delta 8 desaturase, putative condensing enzyme for very long chain fatty

acid (VLCFA) synthesis and the omega 9 desaturase (Table 1). Interestingly, the

VLCFA condensing enzyme was identified in *Coccomyxa* exclusively. Several

enzymes have yet to be identified in many species of the plant kingdom and have

been listed as unknowns (Table 1). Several homologs within the *C. sorokiniana*

genome were unidentified which we contribute to the relatively new annotation

and our pre-release genome blast. Two genes of interest were present in

Chlorella, Inositol phosphorylceramide glucuronosyl transferase 1 (IPUT1) and

the Long-Chain Base (LCB)-1-phosphate phosphatase, which were not found in

the genomes of either *Chlamydomonas* or *Coccomyxa* (Table 1).

Characterization and comparison of Chlorophyte LCB and FA.

Through sphingolipid hydrolysis and LC-MS analysis we were able to

characterize the algal long-chain base (LCB). The major LCB composition

among the *Chlorophytes* in this study were tri-hydroxylated, 18-carbon (C),

saturated (t18:0) and monounsaturated (t18:1) phytosphingosine. In *C. variabilis*,

the LCB t18:0 was present at almost 100%, *C. sorokiniana* at 55%,

Chlamydomonas at 70% of total LCB (Fig. 1A). In *Coccomyxa*, both t18:0 and

t18:1, at 55% and 40%, respectively, were identified (Fig. 1A). Fatty acid analysis

by GC-MS was achieved through TMS-deriativization of hydroxyl fatty acid

methyl esters (hFAMEs). Each algal species had a composition of very long

chain fatty acids (VLCFAs), which were hydroxylated at position 2. In *C.

variabilis*, the major hFAME, present at 95%, consisted of a 24-C chain with a

monounsaturation (h24:1) (Fig. 1B). *C. sorokiniana* and *Chlamydomonas*

contained a mixture of the saturated hFAMEs 24:0 and 26:0 in roughly the same

amounts, 40% and 50%, respectively (Fig. 1B). The major hFAME in

Coccomyxa, present at 75%, was the saturated hFAME 24:0 (Fig. 1B). The

major LCB and hFA composition from each of the algae was used to characterize

and compare the major phytoceramides present among the *Chlorophytes* as well

as a comparison with the major ceramide structure found in fungi and higher

plants (Table 2).

Electrospray Ionization-Mass Spectrometry of algal GIPCs.

GIPCs were detected in *m/z* 1200 - 1800 mass range. In *C. variabilis* and *C.

sorokiniana*, the major parent ions detected were *m/z* 1249 [M + H]+ and *m/z*

1251 [M + H]$^+$, respectively (Fig. 2-3). Product ion scans of these ions created

the major product ions of *m/z* 665.0, with lesser fragments of *m/z* 925.2 and *m/z*

1087.0 in *C. variabilis* and m/z 667.2, with fragments of *m/z* 927.0 and *m/z*

1089.4 in *C. sorokiniana*. The fragmentation of *m/z* 1249.0 to *m/z* 665.0

represents a neutral loss of 584 Daltons (Da) in *C. variabilis* which corresponds

to the molecular weight of t18:0/h24:1 phytoceramide (Fig. 1A-B; Fig. 2). In *C.*

sorokiniana a neutral loss of 586 Da results from the fragmentation of *m/z* 1251

to *m/z* 667 corresponding to the molecular weight of t18:0/h24:0 phytoceramide

(Fig. 1A-B; Fig. 3). The *m/z* 2 difference between these two species is explained

by the unsaturated hFA (h24:1) of *C. variabilis* compared to the saturated hFA

(h24:0) of *C. sorokiniana* (Fig. 1B). This pattern difference in *m/z* 2 is seen

among each fragment in both *Chlorella* mass spectra. Additional fragments in

the product ion scan of *C. sorokiniana*, *m/z* 1848.4, *m/z* 761.1 and *m/z* 576.0, will

require further analysis for characterization (Fig. 3). Having an exact mass of

260.03 Da, inositol phosphate groups were detected as fragments of *m/z* 925

and *m/z* 927 from *m/z* 1249 and *m/z* 1251 in *C. variabilis* and *C. sorokiniana*,

respectively (Fig. 2-3). The loss of *m/z* 162 is representative of a hexose which

we identified as occurring twice from each of the species GIPC exact masses

(Fig. 2-3). Hexuronic acid (HexA), having an exact mass of 194.04 Da and m/z

176, was not detected as a fragment in either product or precursor ion scans;

therefore, we suggest *Chlorella* lacks HexA in its GIPC composition. Thus, the

combination of the GC-MS, LC-MS and ESI-MS (direct infusion) allowed us to

elucidate the chemical composition of the ceramide backbone and polar head

group of the major GIPC in the *Chlorella* species as having the structure Hex(2)-

IPC (Fig. 2).

Mass spectrometry analysis of the algae *Chlamydomonas* and

Coccomyxa revealed that the major GIPC differs from *Chlorella*. In

Chlamydomonas, the major peak of the precursor scan was at *m/z* 1802 [M +

H]$^+$. A product ion scan showed a major product ion at *m/z* 695.3 which

corresponds with the molecular weight of the phytoceramide t18:0/h26:0 (Fig.

1A-B; Fig. 4). A precursor ion scan of *m/z* 695.5 detected an inositol

phosphoceramide (IPC) group at *m/z* 977 as a Na+ adduct (Fig. 4). The neutral

loss of *m/z* 176 from *m/z* 1153.5 identified the presence of HexA in the final GIPC

structure (Fig. 4). The fragmentation pattern of four 162 Da hexoses from *m/z*

1802 was identified at *m/z* 1639.9, *m/z* 1477.4, *m/z* 1315.5 and *m/z* 1153.5 (Fig.

4). A complete GIPC structure for *Chlamydomonas* is proposed as Hex(4)-HexA-

IPC (Fig. 4). GIPC characterization in *Coccomyxa* was more complex with

several major peaks of the precursor scan at m/z 1956.2, *m/z* 1623.8, *m/z* 1161,

m/z 665 and *m/z* 552 (Fig. 5). Previous analysis by LC- and GC-MS, identified

the *Coccomyxa* LCB t18:1 and hFA 24:0, respectively (Fig. 1A-B). A precursor

ion scan of *m/z* 665, the molecular weight of the phytoceramide t18:1/h24:0,

allowed the identification of the IPC at *m/z* 926. Lesser peaks at *m/z* 1102, *m/z*

1264, and *m/z* 1426 reflected the loss of HexA and two hexoses, respectively.

We, therefore, propose the major GIPC structure in *Coccomyxa* as Hex(2)-HexA-

IPC (Fig. 5). Conclusive identification of additional hexoses to the polar head

group of *Coccomyxa* will require further analysis.   Using the information provided

from mass spectrometry analysis, the proposed molecular structure of the major

GIPC in *C. variabilis* and *C. sorokiniana* as Hex$_{(2)}$-IPC, in contrast to that of

Chlamydomonas and *Coccomyxa* as Hex$_{(n)}$-HexA-IPC (where n = number of

hexose moieties) (Fig. 2-5). The exact identity of the hexoses could not be

assigned based on the mass spectrum. The GIPC composition of the

Chlorophytes in this study were then compared with the major GIPC structure

found in fungi and higher plants (Table 2).

Biosynthetic pathway of the atypical GIPC in Chlorella variabilis.

Chlorella contains an unusual GIPC not common to most algae or plants and

more similar to fungi in its lack of a HexA (Fig. 2; Table 2). Through the use of

bioinformatics, *i.e.* gene mining, blasts, and alignments, within the C. variabilis

genome we identified the enzyme, IPUT1, thought to be responsible for the

addition of HexA; however, its function will require further research (Table 1).

Based on identification of biosynthetic enzymes involved and complete GIPC

structure, we propose a sphingolipid biosynthetic pathway for the GIPC dihexose

inositol-phosphate found in *Chlorella* (Fig. 6).

Discussion

In comparing the phytoceramide portion of GIPCs among the Chlorophytes in

this study, we found slight variations in long chain base and fatty acid acyl

chains.   Long chain bases from all four algae were found to be trihydroxylated

and 18 carbons (C) in length; however, only *Coccomyxa* LCBs (t18:1) were

monounsaturated compared to the saturated LCBs (t18:0) of *C. variabilis*, *C.*

sorokiniana, *Chlamydomonas* (Fig. 1A-B; Table 2). Algal fatty acids were composed of 2-hydroxy Very Long Chain Fatty Acids (hVLCFA) with slight variation in number of carbons and saturation; *C. variabilis* having a monounsaturated, 24 C hVLCFA (h24:1) and *Chlamydomonas* with a saturated, 26 C hVLCFA (h26:0), *C. sorokiniana* and *Coccomyxa* both having saturated 24 C hVLCFA (Fig. 1A-B; Table 2). The major composition of phytoceramides found in fungi and plants are t18:0/h24:0 and t18:1/h24:0, respectively (Markham et al., 2006; Blaas and Humpf, 2013; Bure et al., 2014). Based on these results, algal phytoceramide structures of *Chlorella* and *Chlamydomonas* are more similar to fungi whereas *Coccomyxa* has a composition similar to plants (Table 2).

GIPC structure among *Chlorophytes* is similar with respect to acyl chain length and degree of saturation; however, differences between *Chlorella* species and the other algae are notable i.e., the presence or absence of HexA in the polar head groups. Until recently, a glucuronosyl transferase involved in the addition of glucuronic acid to the IPC acceptor for GIPC synthesis was difficult to identify due to the variability of glycosylation patterns between kingdoms (Rennie et al., 2014). Current research has identified the plant protein inositol phosphorylceramide glucuronosyl-transferase 1 (IPUT1), showing IPC glucuronosyl transferase activity and is associated with this activity in *A. thaliana* (Rennie et al., 2014). Interestingly, we have identified the IPUT1 homolog within the Chlorella genomes; however, our research has shown the absence of a glucuronic acid in the GIPC sphingolipids of this species (Table1; Fig. 2-3). More intriguing, is the absence of IPUT1 homologs in the genomes of *Chlamydomonas*

and *Coccomyxa* which we have shown to synthesize glucuronic acid-containing GIPCs (Table 1; Fig. 4-5). In *Saccharomyces cerevisiae*, the mannosyl transferase protein SUR1 is responsible for the addition of the mannose to the IPC acceptor in the GIPC biosynthesis (Bennion et al., 2003). Given the similarity of sterol composition between *Chlorella* and fungi, we included a Blastp of SUR1 (GenBank: AAA68909) to the *Chlorella* genomes. A homolog within *C. variabilis* was identified (CHLNCDRAFT 10358) with a greater percent query coverage (57%), e-value (2 e-59), and percent identity (45%) than that of IPUT1 (Table 1). As mentioned previously, the exact identity of the hexoses of the GIPCs could not be assigned, this along with the lack of HexA, we speculate whether the GIPCs in the species *Chlorella* may contain mannose as its sugar moieties using SUR1 for the glycosylation of its GIPCs.

With previous characterization of GIPC structures, ceramide and polar head groups, in fungi and plants along with our comparison within the *Chlorophytes*, we suggest that *Chlorella* species have a fungal-like membrane and the algae *Chlamydomonas* and *Coccomyxa* more closely resemble those of higher plants. These differences were also found and described in our current research on sterol composition of algal membranes; *Chlorella* have the fungal sterol ergosterol, *Chlamydomonas* has ergosterol and a phytosterol, and *Coccomyxa* has the plant-specific phytosterols. We suggest a possible sphingolipid-sterol interaction between these two lipid species. The characterization and comparison of *Chlorophyta* GIPCs provides insight to and framework for a more detailed evolutionary distinction within all branches of algae.

Conclusions

The biological lipid membrane and its complexity in composition, structure and functional roles is a major area of research. Studies of eukaryotic model membranes, fungi and plants, have shown the presence of liquid-ordered (L_o) domains rich in lipids with relatively saturated acyl chains (i.e. GIPCs) (Xu et al., 2001). These domains, described as lipid rafts, are stabilized through their association with sterols and are enriched with proteins that interact and anchor to saturated acyl chain lipids (Guan et al., 2009). The formation of these lipid rafts is dependent on the ability to tightly-pack with their natural sterol partners leading to their detergent-resistant, insoluble characteristic (Eisenkolb et al., 2002; Guan et al., 2009). Given the prevalence of GIPCs having saturated acyl chains within the *Chlorophytes* and our current characterization of sterol composition in algae, we suggest the presence of lipid rafts within algal membranes.   Relatively understudied, the functional roles and the protein composition of these domains among algae is an important area of research. Here we have provided substantial evidence for the presence of lipids with the composition required for lipid raft formation in algae; however, the differences in GIPC polar head groups and their subsequent functions and roles in lipid rafts will require further research.

References

Bennion, B., Park, C., Fuller, M., Lindsey, R., Momany, M., Jennemann, R., and Levery, S.B. (2003). Glycosphingolipids of the model fungus Aspergillus nidulans: characterization of GIPCs with oligo-a-mannose-type glycans. Journal of Lipid Research 44.

Blaas, N., and Humpf, H. (2013). Structural profiling and quantitation of glycosyl inositol phosphoceramides in plants with Fourier transform mass spectrometry. Journal of Agriculture and Food Chemistry 61, 4257-4269.

Blanc, G., Duncan, G., Agarkova, I., Borodovsky, M., Gurnon, J., Kuo, A., Lindquist, E., Pangilinan, J., Polle, J., Salamov, A., Terry, A., Yamada, T., Dunigan, D.D., Grigoriev, I.V., Claverie, J.-M., and Van Etten, J.L. (2010). The Chlorella variabilis NC64A genome reveals adaptation to photosymbiosis, coevolution with viruses, and cryptic sex. Plant Cell 22, 2943-2955.

Blanc, G., Agarkova, I., Grimwood, J., Kuo, A., Bruegeman, A., Dunigan, D.D., Gurnon, J., Ladunga, I., Lindquist, E., Lucas, S., Pangilinan, J., Proschold, T., Salamov, A., Schmutz, J., Weeks, D., Yamada, T., Lomsadze, A., Borodovsky, M., Claverie, J.-M., Grigoriev, I.V., and Van Etten, J.L. (2012). The genome of the polar eukaryotic microalgo Coccomyxa subellipsoidea reveals traits of cold adaptation. Genome Biology 13.

Breslow, D.K., and Weissman, J.S. (2010). Membranes in Balance: Mechanisms of Sphingolipid Homeostasis. Molecular Cell 40.

Bure, C., Cacas, J.-L., and Mongrand, S. (2014). Characterization of glycosyl inositol phosphoryl ceramides from plants and fungi by mass spectrometry. Analytical and Bioanalytical Chemistry 406, 995-1010.

Cacas, J.-L., Bure, C., Furt, F., Maalouf, J.-P., Badoc, A., Cluzet, S., Schmitter, J.-M., Antajan, E., and Mongrand, S. (2013). Biochemical survey of the polar head of plant glycosylinositolphosphoceramides unravels broad diversity. Phytochemistry 96, 191-200.

Cazzaniga, S., Dalli'Osto, L., Szaub, J., Scibilia, L., Ballottani, M., Purton, S., and Bassi, R. (2014). Domestication of the green alga Chlorella: reduction of antenna size improves light-use efficiency in a photobioreactor. Biotechnology for Biofuels 7, 13.

Darienko, T., Gustavs, L., Eggert, A., Wolf, W., and Proschold, T. (2015). Evaluating the species boundaries of green microalgae (Coccomyxa, Trebouxiophyceae, Chlorophyta) using integrative taxonomy and DNA barcoding with further implications for the species identification in environmental samples. PLoS ONE 10.

Eisenkolb, M., Zenzmaier, C., Leitner, E., and Schneiter, R. (2002). A Specific Structural Requirement for Ergosterol in Long-chain Fatty Acid Synthesis Mutants Important for Maintaining Raft Domains in Yeast. Molecular Biology of the Cell 13, 4414-4428.

Guan, X.L., Souza, C.M., Pichler, H., Dewhurst, G., Schaad, O., Kajiwara, K., Wakabayashi, H., Ivanova, T., Castillon, G.A., Piccolis, M., Abe, F., Loewith, R., Funato, K., Wenk, M.R., and Riezman, H. (2009). Functional

Interactions between Sphingolipids and Sterols in Biological Membranes Regulating Cell Physiology. Molecular Biology of the Cell 20, 2083-2095.

Harris, E. (2001). Chlamydomonas as a model organism. Annual Review of Plant Physiology and Plant Molecular Biology 52, 363-406.

Markham, J.E. (2013). Acyl-Lipid Metabolism. In The Arabidopsis Book 11.e0161 (The American Society of Plant Biologists.

Markham, J.E., Li, J., Cahoon, E.B., and Jaworski, J.G. (2006). Separation and Identification of Major Plant Sphingolipid Classes from Leaves. The Journal of Biological Chemistry 281, 22684-22694.

Rennie, E., Ebert, B., Miles, G., Cahoon, R.E., Christiansen, K., Stonebloom, S., Khatab, H., Twell, D., Petzold, C., Adams, P., Dupree, P., Heazlewood, J., Cahoon, E.B., and Scheller, H. (2014). Identification of a sphingolipid alpha-glucuronosyltransferase that is essential for pollen function in Arabidopsis. Plant Cell 26, 3314-3325.

Rhee, S., Beavis, W., Berardini, T., Chen, G., Dixon, D., Doyle, A., Garcia-Hernandez, M., Huala, E., Lander, G., Montoya, M., Miller, N., Mueller, L., Mundodi, S., Tacklind, J., Weems, D., Wu, Y., Xu, I., Yoo, D., Yoon, J., and Zhang, P. (2003). The Arabidopsis Information Resource (TAIR): a model organism database providing a centralized, curated gateway to Arabidopsis biology, research materials and community. Nucleic Acids Research 31, 224-228.

Siaut, M., Cuine, S., Cagnon, C., Fessler, B., Nguyen, M., Carrier, P., Beyly, A., Beisson, F., Triantaphylides, C., Li-Beisson, Y., and Peltier, G. (2011). Oil accumulation in the model green alga Chlamydomonas reinhardtii: characterization, variability between common laboratory strains and relationship with starch reserves. BMC Biotechnology 11.

Van Etten, J.L., and Dunigan, D.D. (2012). Chloroviruses: Not your everyday plant virus. Trends in Plant Science 17, 1-8.

Xu, X., Bittman, R., Duportail, G., Heissler, D., Vilcheze, C., and London, E. (2001). Effect of the Structure of Natural Sterols and Sphingolipids on the Formation of Ordered Sphingolipid/Sterol Domains (Rafts). The Journal of Biological Chemistry 276, 33540-33546.

Table 1. Putative and characterized sphingolipid biosynthetic genes among *Chlorophyta*. (NF = not found, PM = plasma membrane, ER = endoplasmic

| Function (characterized or predicted)	*Arabidopsis thaliana* (Gene ID)	Gene specific abbreviation	*Chlorella variabilis* (CHLNCDRAFT)	% Query coverage	e-value	% Identity	*Chlorella sorokiniana* (Scaffold)	e-value	*Chlamydomonas reinhardtii* (NCBI Accession)	e-value	*Coccomyxa* C169 (COCSUDRAFT)	e-value	Subcellular location
Subunit of serine palmitoyltransferase	At4g36480	LCB1	138531	90	1e-127	45	215_g33	0	XP_001695193	7e-108	17160	8e-132	ER
Subunit of serine palmitoyltransferase	At5g23670/At3g68780	LCB2a/b	144864	96	0	59	172_g166	0	XP_001692248	0	53835	0	ER
Small subunit SPT	At1g06515/At3g30942	ssSPT1/2	NF				NF		NF		NF		ER
3-Ketosphinganine reductase	At3g06060	KSR1	57682	82	2e-42	34	12_g52	1e-154	XP_001691588	3e-35	57609	7e-18	ER
	At5g19200	KSR2	58302		1e-16								ER
Sphingobase C4-hydroxylase	At1g69640	SBH1	57760	68	5e-05	27	222_g20	2e-133	XP_001699995	3e-63	11014	1e-05	ER
	At1g14290	SBH2	142325	59	3e-04	25	NF		XP_001699995	5e-65	11014	7e-06	ER
LCB delta 8 desaturase	At3g61580/At2g46210	SLD1/SLD2	NF				NF		XP_001690117	6e-12	47604	2e-76	ER
Fatty Acid alpha(2) hydroxylase	At2g34770/At4g20870	FAH1/2	144683	92	3e-45	41	127_g49	2e-137	XP_001702396	7e-28	39420	7e-47	ER
Dihydrosphingosine-delta 4 desaturase	At4g04930	DES1	57665	95	9e-96	45	12_g97	0	NF		12493	7e-101	ER
Ceramide synthase	At1g25540/At1g13580	LOH1/LOH3	50975	89	5e-47	33	61_g123	2e-09	XP_001697632	2e-41	37754	5e-46	ER
	At3g19260	LOH2							XP_001697161	1e-40	66904	5e-52	ER
IPC synthase	At3g54020/At2g37940/At2g29525	IPCS1/IPCS2/IPCS3	17179	76	6e-69	46	274_g25	1e-138	XP_001696665	2e-71	11455	5e-70	Golgi
IPUT1	At5g18480	IPUT1	138328	49	8e-71	40	57_g13	6e-174	NF		NF		Golgi
GONST1	At2g13650	GONST-1	32701	89	5e-87	46	104_g74	1e-174	XP_001690031	2e-73	64566	2e-93	Golgi ?
Glucosylceramide Glucosidase	Unknown	GCG	Unknown				Unknown		Unknown		Unknown		PM
Glucosylceramide synthase	At2g19880	GCS	133847	71	1e-71	32	22_g78	0	XP_001696683	9e-24	NF		ER ?
Glycosylinositolphosphorylceramide synthase	Unknown	GIPCS	Unknown				Unknown		Unknown		Unknown		Golgi
Ceramide kinase	At5g51290	ACD5/AtCERK	54812	83	7e-61	29	7_g24	0	XP_001694757	3e-33	56197	3e-51	PM
LCB kinase	At5g23450/At4g21540	AtLCBK1/SPHK1	134482	35	2e-13	26	75_g108	1e-172	XP_001693043	1e-15	56197	1e-25	ER
LCB-1phosphate lyase	At1g27980	AtDPL1	144988	95	9e-161	46	12_g222	3e-178	XP_001697463	9e-68	64705	3e-161	ER
LCB1 phosphate phosphatase	At3g58490	LCB-PP1	138478	66	3e-42	34	177_g19	0	NF		NF		ER
3-Ketoacyl-CoA synthase	At1g01120	KCS1-21	48950	89	8e-173	55	139_g135	0	XP_001697210	8e-169	58877	2e-178	ER
3-Ketoacyl-CoA reductase	At1g67730	KCR	56728	84	4e-72	41	89_g307	3e-146	XP_001693094	4e-18	48005	2e-86	ER
3-Hydroxyacyl-CoA dehydratase	At5g10480	HCD/PAS2	143333	94	3e-51	42	44_g17	6e-108	XP_001696106	1e-25	16404	1e-42	ER
Enoyl-CoA reductase	At3g55360	ECR/CER10	20573	99	2e-111	53	8_g75	0	XP_001699001	1e-104	36177	6e-106	ER
Putative condensing enzyme for VLCFA synthesis	At3g06460	AtELO6	NF				NF		NF		83573	3e-32	ER
omega 9-desaturase	At3g21080	ADS2	NF				NF		NF		NF		ER ?
Alkaline ceramidase	At4g22330	AtCES1	NF				NF		NF		NF		PM ?
Neutral ceramidase	At1g07380/At2g38010/At5g58980	AtNCASE	139234	94	0	48	NF		XP_001697801	0	43643	0	PM ?
Phospholipase C	Unknown	PLC	Unknown				Unknown		Unknown		Unknown		PM
ORMDL family protein	At1g01230/At5g42000	ORM1/2	29488	96	1e-43	52	89_g182	1e-91	XP_001703235	4e-40	54383	1e-42	?

A
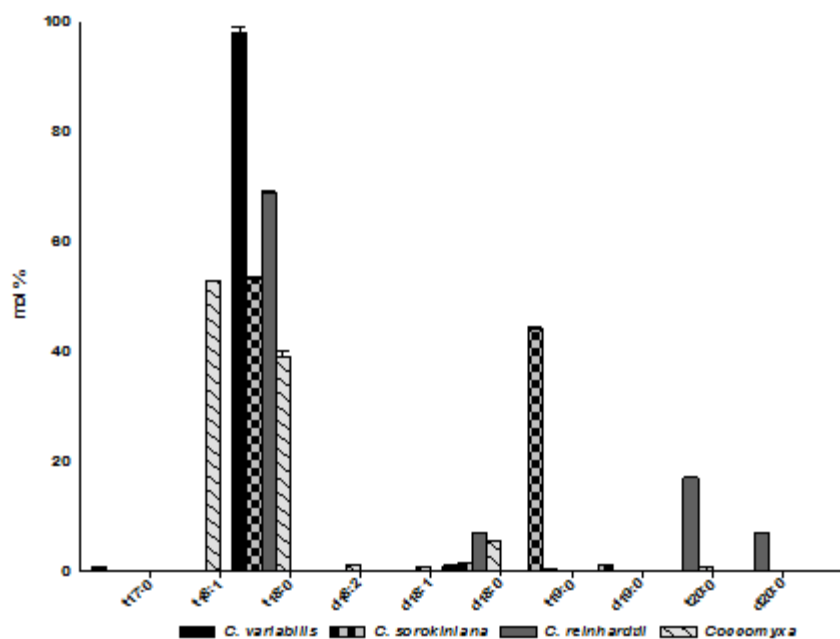
B
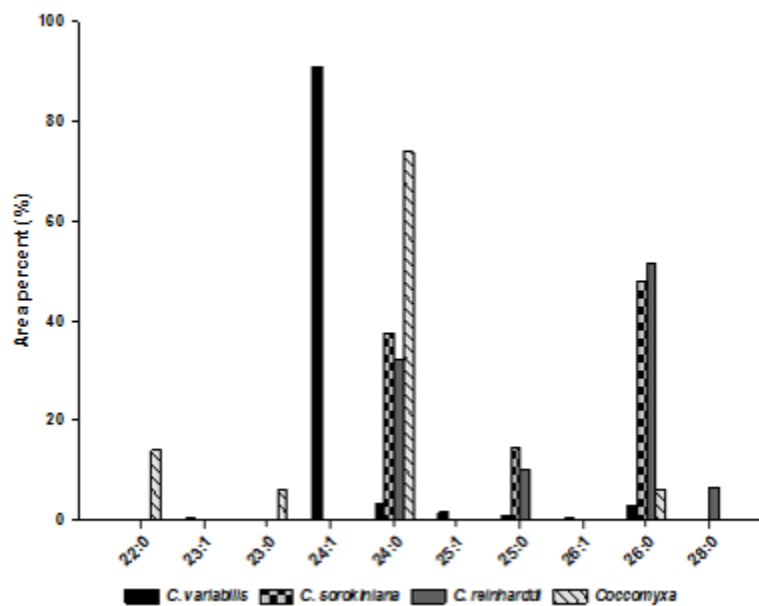
Figure 1 A-B. Characterization and comparison of ceramide components among
Chlorophytes. A) Long chain base (LCB) and B) hydroxyl fatty acid methyl esters
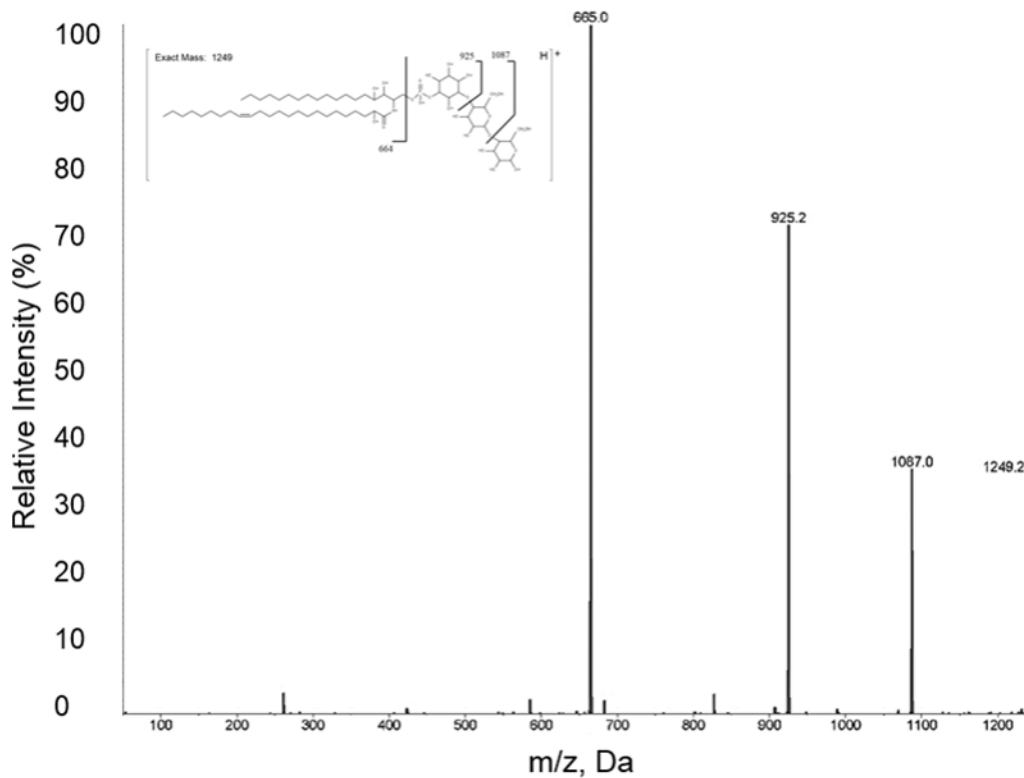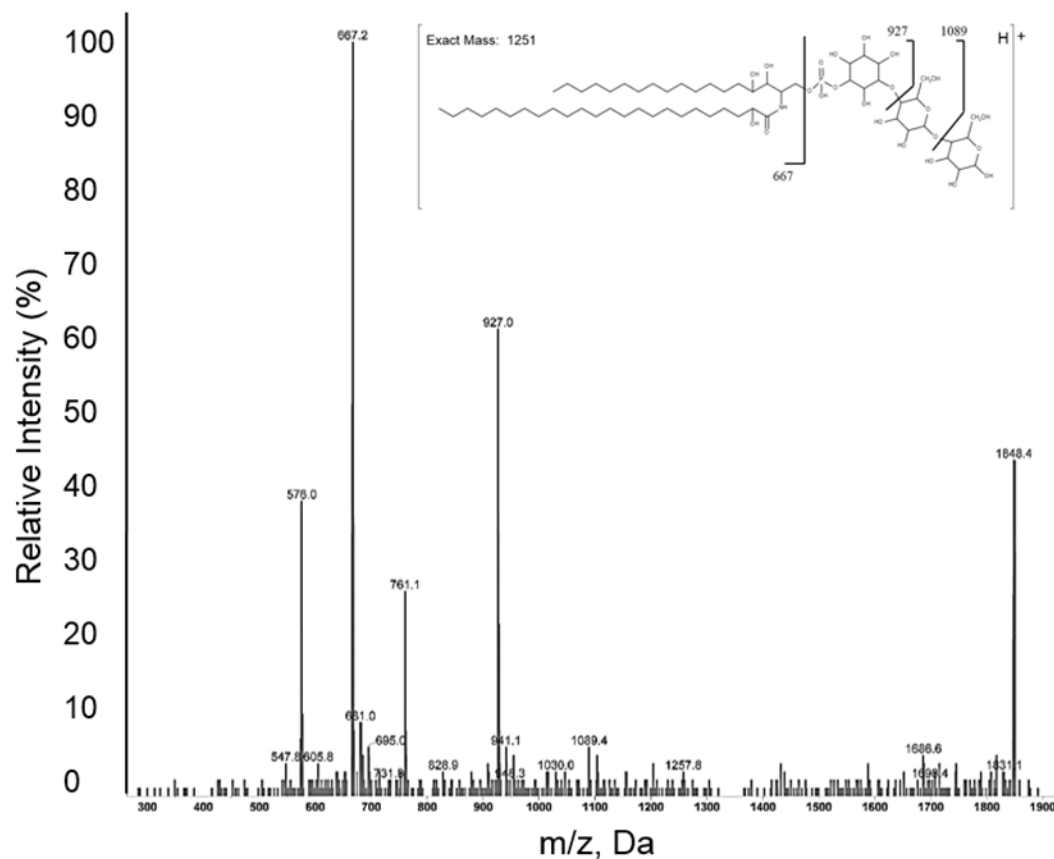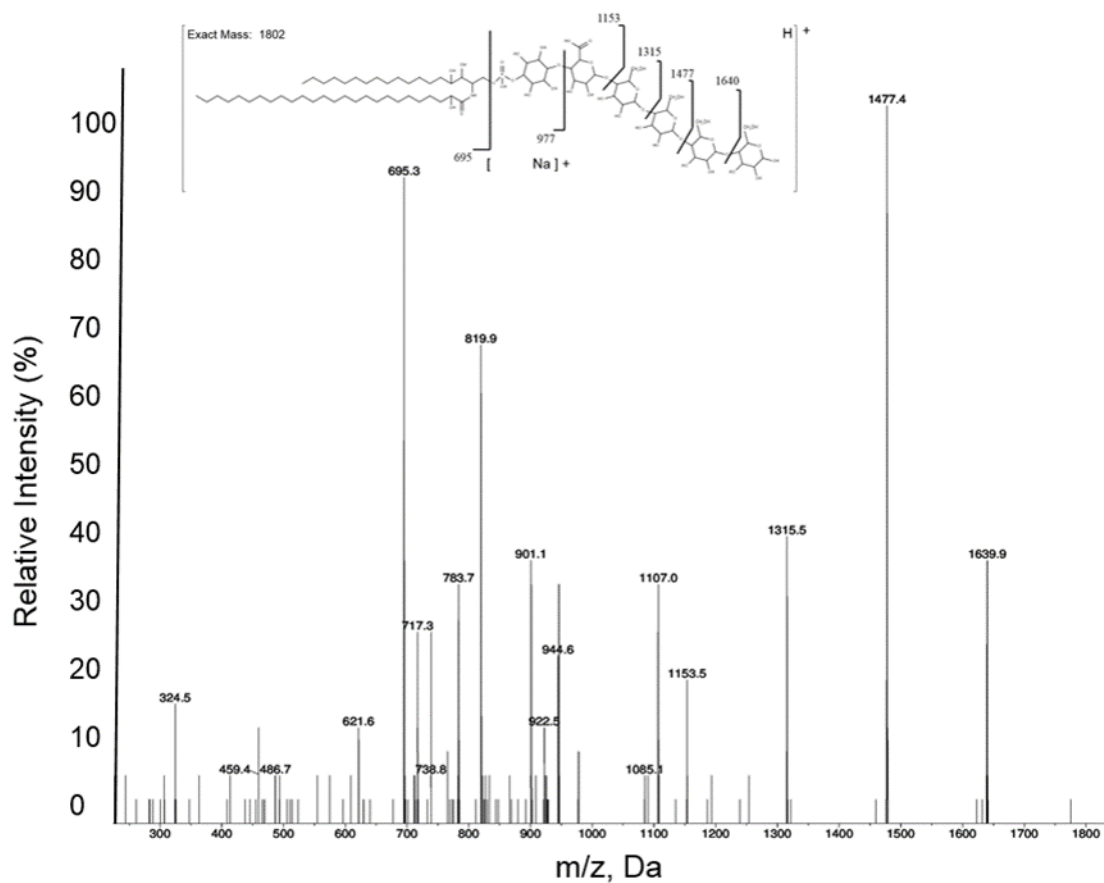(hFAME) profiles of four unicellular algae.

Figure 2. ESI-MS analysis of *Chlorella variabilis* GIPC. The +MS2 scan of the

phytoceramide m/z 665 shows the fragmentation pattern of the major GIPC

structure Hex(2)-IPC with exact mass of 1249 Daltons (Da). Panel insert of the

complete GIPC with its phytoceramide t18:0/h24:1. Hex = hexose, IPC =

inositolphosphorylceramide.

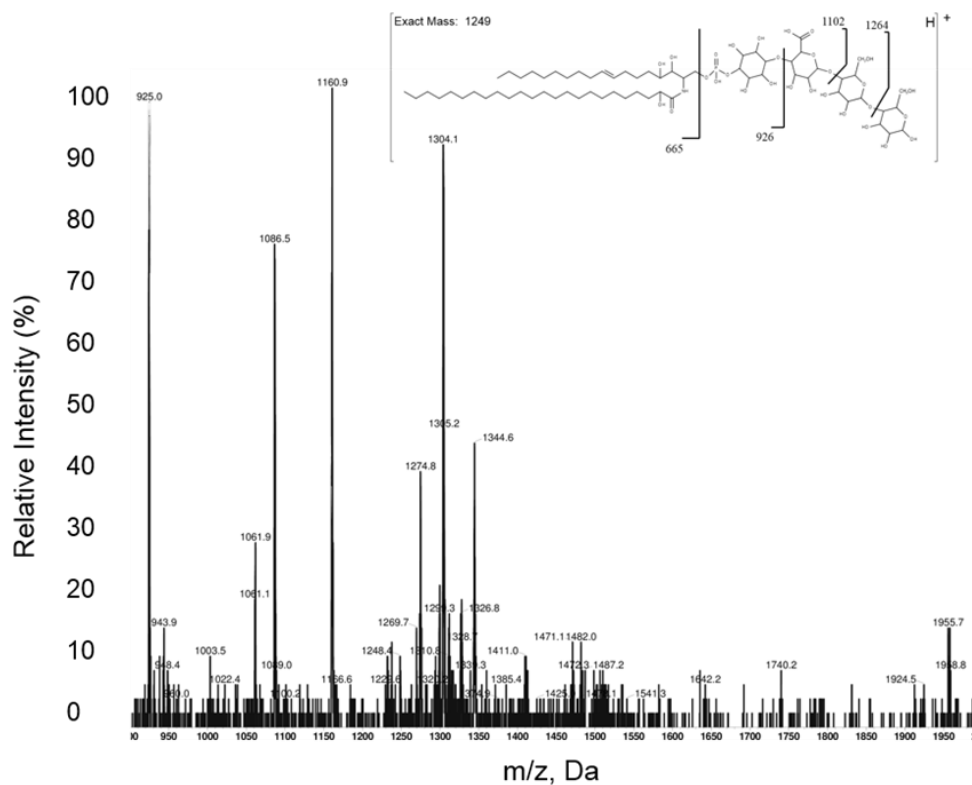Figure 3. ESI-MS analysis of *Chlorella sorokiniana* GIPC. The +MS2 scan of the phytoceramide m/z 667 shows the fragmentation pattern of the major GIPC structure Hex(2)-IPC with exact mass of 1251 Daltons (Da). Panel insert of the complete GIPC with its phytoceramide t18:0/h24:0. Hex = hexose, IPC = inositolphosphorylceramide.

Figure 4.   Figure 3. ESI-MS analysis of *Chlamydomonas reinhardtii* GIPC. The +MS2 scan of the phytoceramide m/z 695 shows the fragmentation pattern of the major GIPC structure Hex(4)-HexA-IPC with exact mass of 1802 Daltons (Da). Panel insert of the complete GIPC with its phytoceramide t18:0/h26:0. Hex = hexose, HexA = hexuronic acid, IPC = inositolphosphorylceramide.

Figure 5. ESI-MS analysis of *Coccomyxa subellipsoidea C-169* GIPC. The precursor scan of the phytoceramide m/z 665 shows the fragmentation pattern of the major GIPC structure Hex(n)-HexA-IPC with exact mass of 1426 Daltons (Da). Panel insert of the complete GIPC with its phytoceramide t18:0/h24:1. Hex = hexose, HexA = hexuronic acid, IPC = inositolphosphorylceramide.

Table 2. Characterization and comparison of ceramide backbone and GIPC

structure among algae, fungi and plants. (f = fungi, a = algae, p = plant; n =

variable number of hexoses, Hex = hexose, HexA = hexuronic acid, IPC =

inositolphosphoceramide)

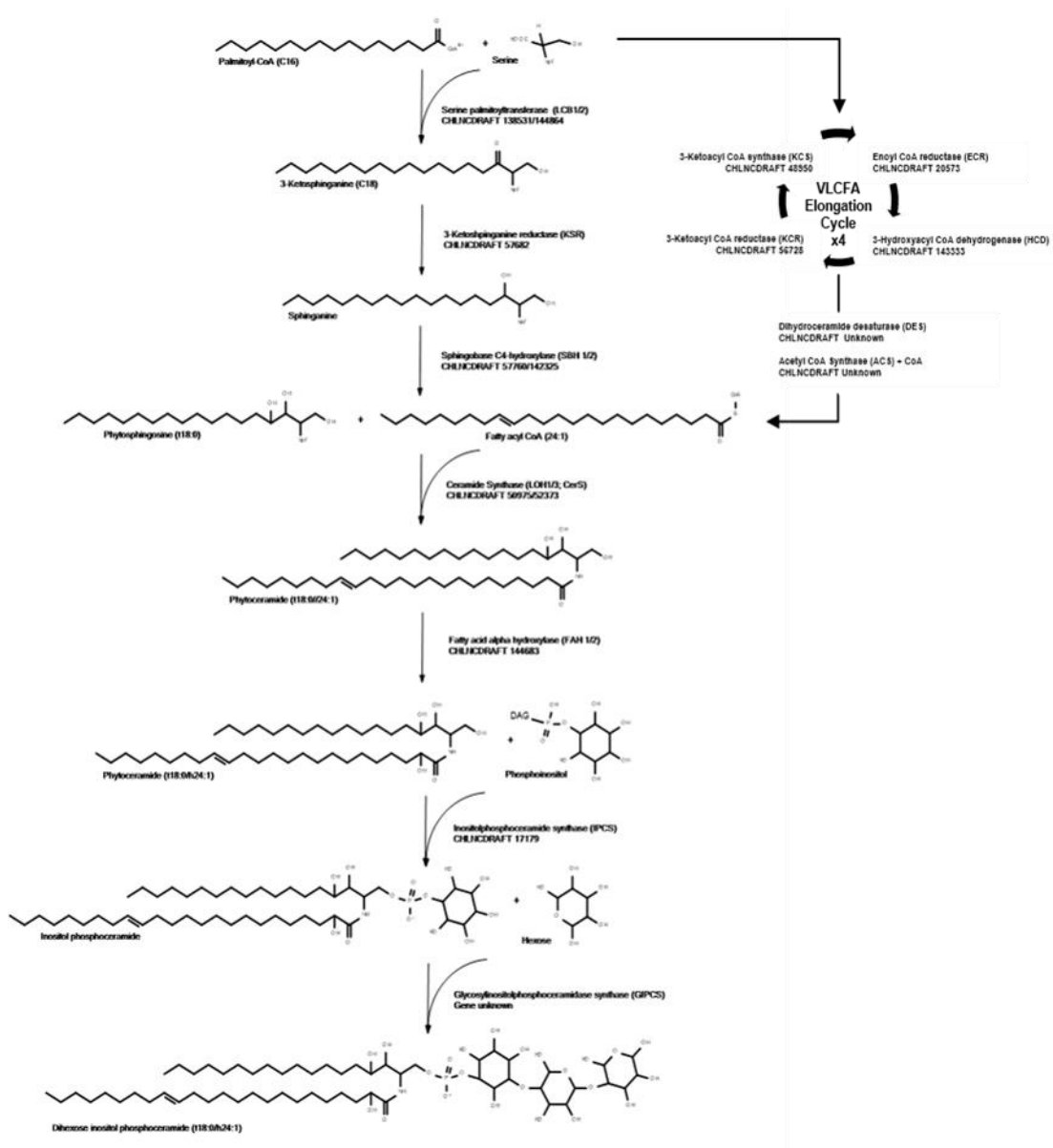| MODEL ORGANISM	MAJOR CERAMIDE		MAJOR GIPC STRUCTURE	REFERENCE
	LCB	hFA		
A. fumigatus (f)	t18:0	h24:0	Man-IPC	(Bennion et al., 2003)
C. variabilis (a)	t18:0	h24:1	Hex(2)-IPC	
C. sorokiniana (a)	t18:0	h24:0	Hex(2)-IPC	
Chlamydomonas (a)	t18:0	h26:0	Hex(4)-HexA-IPC	
Coccomyxa (a)	t18:1	h24:0	Hex(n)-HexA-IPC	
A. thaliana (p)	t18:1	h24:0	Hex(n)-HexA-IPC	(Markham et al., 2006; Blaas and Humpf, 2013)

Figure 6. GIPC sphingolipid biosynthetic pathway in *Chlorella variabilis* of dihexose inositol phosphoceramide (t18:0/h24:1).

CHAPTER 4

Lipid Analysis of the Chlorovirus PBCV-1 Internal Membrane and the Effect of Viral Infection on Lipid Biogenesis in the Alga *Chlorella variabilis*

Suzanne L. Rose[1,2], James R. Gurnon[3], Janet Rowe[2], Jennifer Markham[4,5], James L. Van Etten[2,3,5]

[1]School of Biological Sciences, University of Nebraska, Lincoln, NE 68588-0118

[2]Nebraska Center for Virology, University of Nebraska, Lincoln, NE 68583-0900

[3]Department of Plant Pathology, University of Nebraska, Lincoln, NE 68583-0722

[4]Department of Biochemistry, University of Nebraska, Lincoln, NE 68558-0664

[5]Center for Plant Science Innovation, University of Nebraska, Lincoln, NE 68558

Corresponding author: James L. Van Etten

Abstract

Paramecium bursaria chlorella virus 1 (PBCV-1) is the type member of the *Chlorovirus* genus. PBCV-1 is a lytic, double-strand (ds) DNA virus with a 331-kb genome enclosed in an internal, single bilayered membrane surrounded by an icosahedral outer capsid containing a spike structure at one vertex. Its fresh-water host, *Chlorella variabilis*, is a unicellular, eukaryotic green alga and an endosymbiont of *Paramecium bursaria*. PBCV-1 has a 6 to 8 h life cycle with DNA synthesis starting at 60 – 90 min post infection (p.i.). Virus assembly centers are visible in the cytoplasm at 2 to 5 h p.i. followed by localized lysis and release of infectious progeny at 6 to 8 h p.i. Viral DNA packaging is the culminating step in virion assembly leading to the production of infectious progeny inside the cell. In this study we describe the lipid composition of the PBCV-1 internal membrane and the effect of viral infection on lipid biogenesis in *C. variabilis*. The increased levels of ergosterol, long chain bases and hydroxy fatty acid methyl esters change very little during viral infection. There is an increase in mRNAs involved in sphingolipid biosynthesis and a decrease in sterol biosynthetic mRNAs during PBCV-1 replication. Electrospray Ionization-Mass Spectrometry of the PBCV-1 internal membrane detected diacylglycerol, ceramide, phospholipids, cardiolipin, and several unidentified peaks indicating that new lipid species were present in the virion that might result from viral lipid-modification proteins.

Introduction

The compositional changes of lipids during viral infection are relatively under studied. To further algal lipidomic research and elucidate the host-derived cellular origin and composition of the viral internal bilayered membrane of *Paramecium bursaria Chlorella* Virus (PBCV-1), we determined the sterol and sphingolipid composition, metabolic lipid biosynthetic pathways, and the relevant genes and enzymes during PBCV-1 infection of *Chlorella variabilis*. Previously, we identified the major sterol ergosterol and characterized the sphingolipid glycosylinositolphosphorylceramide (GIPC) in uninfected *C. variabilis* (Rose et al., manuscript in preparation). GIPC was formed from inositolphosphorylceramide (IPC) and contained palmitic acid – phytosphinganine (t18:0) in its acyl chains, monounsaturated hydroxyl fatty acids (MUFAs) (h24:1) and a head group consisting of two sugars – dihexoseinositolphosphoceramide (Rose et al., manuscript in preparation). Interestingly, *C. variabilis* lacks the glucuronic acid that is typically present in GIPCs of other algae and higher plants.

Lipids are essential components of many viruses, the majority of which are found in viral membranes (Roine and Bamford, 2012). Viruses in the family *Phycodnaviridae* have an internal membrane, underneath an icosahedral protein capsid, and one representative the marine coccolithovirus *Emiliania huxleyi* virus – 86 (EhV86), also has an external envelope (Table 1) (Castberg et al., 2002; Wilson et al., 2009). Viruses containing internal membranes are usually lytic in nature, whereas external enveloped viruses usually obtain their membrane

through budding during release from their host (Roine and Bamford, 2012). Host cytoplasmic membranes are the primary source of viral internal membranes and at least some membranes serve as a scaffold for capsid protein assembly (Roine and Bamford, 2012; Milrot et al., 2015).

Viruses with internal membranes are not limited to the *Phycodnaviridae* family; e.g., the *Tectiviridae* archaeal *Sulfolubus* Turreted Icosahedral Virus (STIV), the eukaryotic *Mimiviridae Acanthamoeba polyphaga* mimivirus, and the Bacteriophage PRD1 all have internal membranes (Bamford et al., 1995; Rice et al., 2004; Raoult et al., 2007; Roine and Bamford, 2012). These viruses share common features: an icosahedral protein capsid structure, an internal lipid membrane, dsDNA genomes, and the presence of cytoplasmic viral factories (VF) during replication in their hosts. The fact that these 3 viruses infect members of all 3 domains of life, Archaea, Eukarya, and Bacteria, suggests a deep-rooted evolutionary relationship in which a common viral ancestor might have preceded the divergence of the domains more than 3 billion years ago (Rice et al., 2004).

As host membrane acquisition is central to the production of successful viral progeny, recent research has focused on the generation, structure and functional features of cytoplasmic VFs among internal membrane containing viruses. To-date VFs have been described as coordinating the spatial and temporal assembly of viral progeny; however, the lipid composition of the internal viral bilayered membrane is relatively unstudied among the *Phycodnaviridae* (Wilson et al., 2009; Milrot et al., 2015). Belonging to the nucleocytoplasmic large DNA

viruses (NCLDV) group (Iyer et al., 2006), both PBCV-1 and Mimivirus VFs and virion assembly have recently been investigated and found to differ (Mutsafi et al., 2013; Milrot et al., 2015). In contrast to Mimivirus VFs, where replicated and transcribed genomes are located in the factory center with membrane accumulation and capsid assembly occurring at the boundary, PBCV-1 viral genomes are localized at the boundary with the membrane and capsid region located in the factory center (Kuznetsov et al., 2013; Milrot et al., 2015). PBCV-1 VFs first appear in the host cytoplasm at ~2 h p.i. and their appearance is associated with significant accumulation of host membrane cisternae which bud from the rough endoplasmic reticulum (ER) located near the outer membrane of host nuclei (Milrot et al., 2015). As cisternae are translocated into the VF center the double membrane bilayers are converted into open single-bilayer sheets which then act as templates for the formation of the outer icosahedral capsid structures (Milrot et al., 2015). Our research takes a closer look into membrane biogenesis during PBCV-1 infection of *C. variabilis* by characterizing the lipid composition of the viral internal membrane.

Materials and Methods

Viral preparation and purification of PBCV-1.

C. variabilis cultures were grown in Modified Basal Broth Medium (MBBM) under constant shaking at 100 RPM, 22°C and light intensity of 30 μmol m^{-2}s^{-1} (μE). Cells were grown to mid-log phase (2 x 10^7 cells/ml), inoculated with PBCV-1 at an MOI of 0.01 and allowed to lyse for two days. Trition X-100 was added to the lysates at a final concentration of 0.1% and the lysates were centrifuged in a

Sorvall GSA rotor at 5,000 rpm for 5 min at 4°C to remove debris. The viral-containing supernatant was centrifuged in a Beckman Type 19 rotor for 50 min at 17,000 rpm at 4°C to pellet virus. The virus pellets were re-suspended in 50 mM Tris, pH 7.8 and 10 mM $MgCl_2$ and then layered on 10-40% sucrose gradients. Gradients were centrifuged in a Beckman SW-32 rotor at 20,000 rpm for 20 min at 4°C. The band containing virus was collected, slowly diluted with 50 mM Tris, pH 7.8 and 10 mM $MgCl_2$ and pelleted in the GSA rotor for 60 min at 17,000 rpm. To obtain purer preparations, the virus was subjected to a second sucrose density gradient and pelleted. The final virus pellet was re-suspended in 50 mM Tris, pH 7.8 and 10 mM $MgCl_2$. Viral concentrations were determined by measuring absorbance at 260 nm and virus titer was determined by plaque assay (Van Etten et al., 1983).

Algal culture conditions and PBCV-1 infection of C. variabilis.

C. variabilis cultures were grown as described above and purified PBCV-1 was added to actively growing cultures (2×10^7 cells/ml) at a MOI of 5. A control culture of *C. variabilis* was harvested at time = 0 h p.i (T=0) and then at every h for six h p.i. (T=1, 2, 3, 4, 5, 6). Harvested cultures were centrifuged at 4,000 x g for 10 min at 4°C, the pellet washed with fresh MBBM and centrifuged again before placing in the freeze dryer overnight. Freeze dried pellets were stored at -80°C until used for sterol, LCB and hFAME analyses.

Data analysis of mRNA transcription levels during viral infection.

The *C. variabilis* genome (taxid: 554065) [http://genome.jgi-psf.org/NC64A; (Blanc et al., 2010)] used to identify and characterize the sterol and sphingolipid biosynthetic pathway genes has been described (Rose et al., manuscript in preparation). Genes involved in sterol and sphingolipid biosynthesis were used to characterize up- or down-regulation of these pathways during virus infection (Rowe et al., 2014). The PBCV-1 genome (taxid: 10506) was accessed through the National Center for Biotechnology Information (NCBI; www.ncbi.nlm.nih.gov). Messenger RNA sequence data from PBCV-1 infected *C. variabilis* was obtained from Rowe et al (2014). Messenger RNA transcription levels at 0 min p.i (T=0) were standardized to 0% and mRNA transcripts at T= 7, 14, 20, 40, 60 min p.i. were calculated as a percentage of up- or down-regulation using the equation $(v[tX]/v[t0]-1)*100$; v= number of transcripts, tX = time.

Sterol analysis of PBCV-1 infected C. variabilis.

Sterol extraction followed a modified version of the Bligh and Dyer (1959) chloroform-methanol. One mg/ml of cholestanol standard (Matreya, Pleasant Gap, PA) was added to freeze dried algal pellets. Total sterols were extracted three times with chloroform:methanol (1:1, v:v), loaded onto silica SPE columns and eluted with 30% 2-propanol. Purified sterol extracts were dried under nitrogen at 37°C and then converted to trimethylsilyl ether (TMS-ether) derivatives using bis (trimethylsilyl) trifluoracetamide (BSFTA-TMCS 99:1) (Sigma, St. Louis, MO). Dried sterol samples were suspended in 100 µl hexane for GC/MS analysis. Initial gas chromatographic analysis was carried out using the Agilent 6890 Series Gas Chromatograph System equipped with a DB-5ms

capillary column (30.0 m x 250.00 μm, 0.25 μm, J&W 122-5532, J&W Scientific, Inc., Folsom, USA).   Helium was used as the carrier gas at a linear velocity of 48 cm/sec and constant flow of 1.5 mL min^{-1}.   A dual ramp temperature program was used with the oven heated from 250 to 270°C for 30 min and then from 270 – 280°C for 3.30 min. A detector temperature of 270°C was used. Sterols were initially identified using the *NIST98 library* (Scientific Instrument Services, Inc., Ringoes, USA) followed by comparisons based on their mass fragmentation patterns and retention times. Peak areas of identified sterols were quantified relative to the cholestanol standard. Sterol extraction and analyses were run in triplicate for each time point.

LCB analysis of C. variabilis during PBCV-1 infection by HPLC/MS.

Long chain base samples were obtained by sphingolipid hydrolysis. To freeze dried pellets (mentioned above), 0.1 nmol/μL of the d16:0 standard, 1 ml dioxane and 1 ml Ba(OH)$_2$ was added and hydrolysis allowed to proceed overnight at 110°C. To cooled samples, 2 ml of both 2%-ammonium sulphate and diethylether were added, vortexed and then centrifuged at 500 x g for 10 min. The upper phase was collected in a glass tube and dried under N$_2$. The samples were allowed to derivatize at room temperature for 20 min following the addition of o-phthalaldehyde (OPA) reagent. OPA diluent was added and samples were run on HPLC/MS (C18 HPLC column). Sphingolipid hydrolysis and LCB analysis were run in triplicate for each time point.

hFAME analysis of C. variabilis during PBCV-1 infection.

Analysis of 2-hydroxy fatty acids was achieved by producing TMS-derivatives of hydroxy fatty acid methyl esters for GC/MS. Hydrolysis with 2 ml methanolic HCL (Fluka 17935) added to freeze dried pellets was allowed to proceed overnight at 75°C. Hexane extractions of the cooled hydrolysis reaction were done in triplicate and the upper phase from each collected, combined into a tube and dried under N_2. Extracts were purified on a silica acid column and hFAMEs eluted with hexane:ethyl acetate (6:1, v:v). TMS-derivatives of hFAMEs, using BSFTA +TMCS 99:1 (Supelco, 33154-U), were analyzed by GC/MS. Hydrolysis and production of hFAMEs were run in triplicate for each time point.

Lipid extraction of the PBCV-1 internal membrane.

Methanol was added to the purified PBCV-1 sample (1.3×10^{12} pfu/ml) in a 1:1 (v:v) and vortexed. To this suspension, 5 mL of MTBE was added and incubated for 60 min at 60°C with intermittent vortexing every 15 min. The viral suspension was then centrifuged at 1,000 x g for 10 min and the upper (organic) phase was collected in a glass tube. The lower phase was re-extracted with 2 mL of MTBE: MeOH: H_2O (10:3:2.5 v:v:v), vortexed and centrifuged at 1,000 x g for 10 min. The upper phase was collected, combined with the previously collected upper phase and dried under N_2. Extracted viral lipids were dissolved in 200 µl of chloroform: MeOH: H_2O (60:30:4.5 v:v:v) and stored at -20°C.

Gas chromatography-Flame Ionization Detection (GC-FID) analysis of the PBCV-1 internal membrane. Five µl of the dissolved extracted viral lipid (described above) was placed in a glass tube together with 2 µg of the standard, heptadecanoic acid (17:0) (NU-CHEK Prep Inc., Elysian, MN) and dried under

N_2. Two mL methanolic HCL (Fluka #17935) was added to the dried sample and refluxed overnight at 75°C. To the cooled hydrolysis reaction, 2 mL of MilliQ H_2O and 2 mL of hexane was added, vortexed and centrifuged at 3,000 x g for 5 min. The upper hexane phase was removed and placed in a glass tube, and the lower phase was washed twice with hexane, and the upper phases were combined. The hexane extract was then dried under N_2 followed by resuspension in 100 µl fresh hexane. Injection of 5 µl of sample was used for detection of hFAMES and quantitation of total lipid by running on an Agilent 7890A GC system. The sample was injected and maintained at 185°C for 1 min and then at 7°C/min to 235°C for 4 min for a total run time of 12.14 min. Peaks were analyzed and viral fatty acids were calculated by area percent in relation to the internal standard.

Electrospray ionization and mass spectrometry.

A 200 µl aliquot of PBCV-1 extracted lipids (described above) was dried under N_2 and re-suspended in 200 µl THF: MeOH: H_2O (5:2:3 v:v:v) plus 0.1% formic acid. The viral lipid extract was then introduced by continuous infusion into the TurboV electrospray source of an API 4000 Q Trap Mass Spectrometer (Applied Biosystems, Foster City, CA) using the flow from a KDS100 syringe pump (KD Scientific Inc., Holliston, MA), source temperature of 550°C and collision energy (CE) of 60. After data acquisition the highest signal from the mass spectrum was taken as 100% abundance and other signals are represented as a percentage of this value.

Results

Sterol levels during viral infection. Cultures of infected *C. variabilis* were harvested every hour over the course of six h followed by sterol analysis by GC-MS. Compared to the control, ergosterol levels increased about 50% during the first h of infection and then decreased to near control levels between 4 and 5 h p.i. followed by a slight increase at 6 h p.i. (Fig. 1). Ergosta-5,8-dienol levels steadily increased over the course of the infection cycle (Fig. 1).

LCB and hFAME levels during viral infection. Analysis of long chain bases (LCBs) (t18:0) by LC-MS and 2-hydroxy fatty acid methyl esters (hFAMEs) (h24:1) by GC-MS were determined at 2 h and 6 h p.i. Compared to uninfected *C. variabilis*, no significant change occurred in either LCB or hFAME levels (Fig. 2).

Expression of sterol and sphingolipid biosynthetic genes during viral infection. Host genes involved in the biosynthesis of sterol and sphingolipids were previously identified and reported (Rose et al., manuscript in preparation). A study identifying gene transcript levels during the first 60 min p.i. of PBCV-1 infected *C. variabilis* was recently published (Rowe et al., 2014). Therefore, we examined the mRNA levels of both the identified sterol (Table 2) and sphingolipid (Table 3) biosynthetic genes in order to characterize the regulation of lipids involved in membrane biogenesis. mRNA levels were standardized to percentages where at time 0 min p.i (T=0) transcription levels were 0% (Fig. 3). At 7 min p.i (T=7), transcripts involved in sterol biosynthesis were similar to those at T=0 and then they decreased about 2 fold by 60 min p.i. (T=60) (Table 2; Fig.

3A). There were several exceptions, acetoacetyl-CoA thiolase and HMGS

transcripts, which by 60 min p.i (T=60) were up-regulated ~2 fold and Delta-14,

24-reductase ~3 fold from T=0 (Table 2; Fig. 3A). In contrast, genes involved in

sphingolipid biosynthesis were up-regulated 2 to 3 fold at 7 min p.i (T=7) and

then slowly decreased by T=60, yet remained at levels above T=0 (Table 3; Fig.

3B). Three transcripts slowly increased during infection, GONST1, ORM, and

neutral ceramidase, and were present at 1 to 3 fold higher levels by T=60 (Table

3; Fig. 3B). Both sphingobase-C4-hydroxylases and LCB-1-phosphate lyase

mRNA transcripts were below control levels at 60 min p.i. (Table 3; Fig. 3B).

Total viral fatty acids.

The PBCV-1 fatty acid composition was determined by GC-FID and peaks

calculated by area percent in relation to an internal standard (IS) (Fig.4). Four

peaks of unknown fatty acid chain lengths were identified with chain lengths

shorter than the 17:0 IS and two peaks occurred between 18:2 and 18:3 of

unknown length. Both 18:0 and 18:1 fatty acids were identified and comprised

about 12% and 15% of the total fatty acids, respectively. Total viral lipid fatty acid

were calculated at 12 µg of lipid fatty acid/1ml virus ($1x10^{12}$ pfu/ml).

PBCV-1 lipidome.

PBCV-1 total lipid extract, directly infused by ESI/MS, was analyzed with an initial

Q1 scan (Fig. 5). Diacylglycerol (DAG) at 576 m/z, Da, ceramide at 664 m/z, Da,

phosphatidylcholine (PC) at 780 m/z, Da, phosphatidylinositol (PI) at 835 m/z,

Da, and cardiolipin at 1510 m/z, Da were identified (Fig. 5). Unidentified lipids

were present between 1160 and 1200 m/z, Da and at 1300 m/z, Da. (Fig.5). A +MS2 scan of the fragment at 576 m/z, Da showed the fragmentation pattern of DAG 18:3-18:3 into its constitutive acyl m/z and glycerol m/z, Da fragments (Fig. 6). A precursor ion scan of host t18:1/h24:0 ceramide m/z 665 identified the major GIPC found in *C. variabilis* in the viral membrane (Fig. 7). The fragmentation pattern of host GIPC dihexose-inositolphosphoceramide 1248 m/z shows loss of two hexose at 1088 and 924 m/z. The loss of the inositolphosphate fragment of 260 Da from 924 m/z results in the precursor ion of 665 m/z (Fig. 7). The most abundant signal of the Q1 scan lies between 725 and 825 m/z (Fig. 5). Precursor ion scans were run for the phosphoglycerides phosphatidylcholine (PC) 184 m/z and phosphatidylinositol (PI) 261 m/z (Fig. 8). A +MS2 scan of 1510 m/z identified the phosphoglyceride cardiolipin (Fig. 9). In an effort to identify unknown lipids, a +MS2 ion scan of the prominent peak1171 m/z was run (Fig. 10). Fragmentation of this peak is complex and further mass spectrometry research on the unknown lipids will need to be carried out. The host sterol ergosterol 396 m/z was not detected in the PBCV-1 virion.

Discussion

Sterol and sphingolipid distribution and levels during PBCV-1 infection.

The sterol and sphingolipid pathways each have a unique set of enzymatic steps; however, they both use the endoplasmic reticulum (ER) for initial biosynthesis. Synthesis and concentration of these lipids typically increase along the secretory pathway; they begin with a low concentration in the ER, are modified and increase in abundance in the Golgi, and then they are shuttled to the plasma

membrane where they reach their highest concentrations (Gulati et al., 2010; Hannich et al., 2011).   The presence and co-affinity of sterols and sphingolipids as binding partners in the plasma membrane are essential for cell homeostasis and an imbalance of one disrupts the specialized lipid microdomains, lipid rafts, and cell membrane stability (Gulati et al., 2010). Biosynthetic co-regulation of sterol and sphingolipid metabolism in algae is not well known and the master regulator of sterol transcription found in most eukaryotes, sterol regulatory element binding protein (SREBP), is absent in *C. variabilis*. Of interest is the down-regulation of the sterol MEP pathway in the chloroplast and an up-regulation of the first two genes in the MVA pathway in the cytosol. Lacking the complete biosynthetic pathway for IPP production via the MVA pathway in the cytosol, *C. variabilis* mRNA transcripts for the first two enzymes in the pathway, acetoacetyl-CoA thiolase and HMGS, increased 2-fold during viral infection (Table 2).   Down-regulation of sterol biosynthesis as a host defense mechanism during viral infection has been reported in many host-viral systems (Blanc et al., 2011). Given the down-regulation of sterol mRNAs within the first 7 min of infection and the inability to detect sterols in PBCV-1, we conclude that sterols are nonessential components in the PBCV-1 internal membrane. The presence of an intricate, yet unknown innate immune response to viral infection involving sterol down-regulation in *C. variabilis* is hypothesized.

In contrast, sphingolipid biosynthesis gene transcripts are up-regulated 2- to 3-fold within minutes of PBCV-1 infection and remain above control levels over the course of 60 min (Table 3). This up-regulation along with the presence of

phospholipids, glycerolipids, GIPCs, and DAGs as components of the viral internal membrane suggests the relative importance of these lipids in an effort to maintain cell membrane and organelle stability and an innate defense response.

PBCV-1 internal membrane lipid composition and VFs.

Initial analysis of the purified PBCV-1 lipid extract by GC-FID revealed six lipid fatty acid species with unknown chain lengths, four of which were shorter than the 17:0 internal standard (Fig.4). One unknown was the highest detected fatty acid, 40% of the total fatty acids, with a chain length shorter than 16:0 (Fig. 4).

For analysis of viral membrane we employed "Shotgun lipidomics", developed by Han and Gross (2005), an ESI-MS method involving direct infusion of total lipid extract into an ESI source, separation of lipids based on electrical properties, and detection according to their mass to charge ratio (m/z) (Han and Gross, 2005; Gross and Han, 2007). Data acquisition using Q1, precursor ion, product ion and neutral loss ion scans of the viral lipid extract allowed the identification of groups of lipid classes.

Diacylglycerols (DAGs) are glycerides with two covalently bonded fatty acid chains to a glycerol molecule through ester linkages. As a product or precursor of triacylglycerol (TAG) metabolism and synthesis, DAGs function as second messengers, initiating components of intracellular signal transduction cascades involved in proliferation, migration, survival and apoptosis. DAG 18:3-18:3 (two linolenic fatty acid chains) was an abundant component of the viral internal membrane (Fig.6). *C. variabilis* TAG lipase (CHLNCDRAFT 142167) mRNA

transcription levels increased during PBCV-1 infection and was 2-fold higher than the control at 60 min p.i.   As a membrane-associated, hydrophobic molecule and intermediate in phospholipid biosynthesis along with undetectable levels of TAG and an increase in TAG lipase mRNA transcripts, we predict that the conversion of TAG to DAG is a critical part of the cell response to viral infection, membrane biosynthesis and the role of DAG in triggering apoptosis as a second messenger, respectively.

Sphingolipids are essential components of all eukaryotic cell membranes. The most abundant class of sphingolipids in plants are GIPCs. Currently sphingolipid research in algae is limited. In an effort to characterize sphingolipid structures and their biodiversity in microalgae, we previously reported the GIPC composition - phytoceramide structure and polar head group - of four, freshwater algal species, including *C. variabilis* (Rose et al., manuscript in preparation). The major GIPC in *C. variabilis*, dihexoseinositolphosphate, has a phytoceramide structure consisting of a LCB t18:0 and 2-hydroxy fatty acid h24:1. Previous research shows VFs sequestering a single bilayered membrane from the rough ER located near the nuclear membrane; since, sphingolipid biosynthesis begins in the ER, we expected the GIPC precursor phytoceramide to be present in the viral membrane. Unexpectedly, host GIPC, which is produced in the Golgi, was in the viral membrane, suggesting that the virus membrane also has some association with the smooth ER and Golgi or transport lipid vesicles.

Phospholipids, the main constituents of all cellular membranes are synthesized in localized regions of the ER. Phospholipids consist of a hydrophobic region – two

fatty acids attached to a glycerol unit – and a hydrophilic region – a phosphate

group and a polar molecule (Lagace and Ridgway, 2013). The properties of

these regions are responsible for the orientation of phospholipids into the lipid

bilayered membrane. In our analysis of the viral internal membrane, we

expected phospholipids to be the most abundant lipid; therefore, a precursor ion

scan of the choline polar head group of phosphatidylcholine (PC), 184 m/z was

run (Fig. 8A). PC was identified as having 18:3/18:3 fatty acid chains with a 780

m/z (Fig. 8A). Phosphatidylinositol (PI), with an inositol headgroup, forms a

minor component of the cell membrane; however, its ability to be phosphorylated

to phosphatidylinositol phosphate (PIP), phosphatidylinositol biphosphate (PIP_2),

and phosphatidylinositol triphosphate (PIP_3), and their subsequent role(s) in the

activation of cell signal cascades make it a prominent molecule involved in cell

stress and the defense response (Gamper and Shapiro, 2007). Specifically,

membrane bound PIP_2 is cleaved by phospholipase C (PLC) into the products

IP3 and DAG, both functioning as second messengers in cell signal cascades

(Weernink et al., 2007). DAG remains membrane-bound, activating protein

kinase C (PKC), whereas IP3 is released into the cytosol which binds to IP3

receptors on the smooth ER, opening calcium channels and allowing the release

of Ca^{2+} into the cytosol (Gamper and Shapiro, 2007; Weernink et al., 2007). We

found PLC mRNA transcription levels in *C. variabilis* (CHLNCDRAFT 143477)

were 2-fold higher during viral infection by 60 min p.i. Relatively low levels of PI

were detected in the viral membrane as expected, supporting current findings

that most PI is phosphorylated and present as PIP_2 in the plasma membrane and its hydrolysis results in increased levels of membrane DAG (Fig. 6,8B).

Cardiolipin (CL), also known as diphosphatidylglycerol, is found predominantly in the inner mitochondrial membrane (IMM), is a unique phospholipid that plays a crucial role in mitochondrial bioenergetics and as a launch site for programmed cell death, or apoptosis, of host cells (Schug and Gottlieb, 2009). CL is a highly acidic phospholipid in which two phosphatidic acid moieties connect to a central glycerol backbone resulting in four distinct alkyl groups allowing for a high complexity molecule (Paradies et al., 2014). It has been reported that CL also resides in the outer mitochondrial membrane (OMM) and is enriched at sites where the IMM and OMM are connected (Schug and Gottlieb, 2009; Paradies et al., 2014). CL plays a major role in the production of ATP through its known association with energy-transducing membranes, as well as a signaling platform for various death-inducing proteins involved in PCD processes – the release of cytochrome c, autoprocessing of caspases, cristae remodeling and mitochondrial fragmentation (Schug and Gottlieb, 2009; Paradies et al., 2014). Apoptosis is known to occur during viral infection as a defense mechanism. The presence of this anionic mitochondrial phospholipid in the viral internal membrane suggests the possible sequestration of lipid membrane fragments from various other organelles to the VF during viral DNA packaging. Surprisingly, we detected glycerolipid CL in the PBCV-1 membrane.

Conclusions

A recent study on VFs formed during PBCV-1 replication along with our lipid

analyses indicates that the viral internal membrane is derived from host

cytoplasmic membranes (Milrot et al., 2015). Given the current model on PBCV-1

VFs, where in the PBCV-1 genome is located throughout the cytoplasm, along

with our findings of some putative organelle-specific lipids suggest that the

internal bilayered PBCV-1 membrane is acquired not only from the rough ER but

components also come from other organelle membranes (Milrot et al., 2015).

This conclusion would explain the presence of CL from the mitochondrial

membrane and GIPCs from the Golgi and smooth ER in the viral membrane.

The normally low abundance of sterols in the ER and the reported down-

regulation of sterol biosynthesis during viral infection is consistent with the

inability to detect sterols in the viral internal membrane. Lipid analysis by ESI/MS

and GC/FID of the highly purified virions detected several unknown lipid species,

suggestive of possible viral-encoded lipid modification mechanism of host lipids

or acquisition of other classes of lipids required for viral assembly. Given the

structure of PBCV-1 icosahedral capsid, with both planar tri- and vertex penta-

symmetrons, constraints of the inner membrane curvature at the vertices may

require lipid selectivity from available host membranes (Zhang et al., 2011; Roine

and Bamford, 2012). Lipids are known to vary widely in structure – hydrocarbon

chain length, degree of saturation and head group structure – therefore,

sequestration by viral proteins which attract certain types of lipids for different

positions in the curved internal membrane may explain the presence of unknown

compounds in the PBCV-1 lipid membrane.

Acknowledgements

References

Abe, I. (2007). Enzymatic synthesis of cyclic triterpenes. Natural Product Reports 24, 1311-1331.

Ackman, R., and Sipos, J. (1964). Application of specific response factors in the gas chromatographic analysis of methyl esters of fatty acis with flame ionization detectors. Journal of the American Oil Chemists Society 41, 377-378.

Agarkova, I., Dunnigan, D., and Van Etten, J. (2006). Virion-associated restriction endonucleases of chloroviruses. Journal of Virology 80, 8114-8123.

Alcazar-Fuoli, L., Mellado, E., Garcia-Effron, G., Lopez, J.F., Grimalt, J.O., Cuenca-Estrella, J.M., and Rodriguez-Tudela, J.L. (2008). Ergosterol biosynthesis pathway in Aspergillus fumigatus. Steroids 73, 339-347.

Altschul, S., Gish, W., Miller, W., Myers, E., and Lipman, D. (1990). Basic local alignment search tool. Journal of Molecular Biology 215, 403-410.

Alverson, A.J., Beszteri, B., Julius, M.L., and Theriot, E.C. (2011). The model marine diatom Thalassiosira pseudonana likely descended from a freshwater ancestor in the genus Cyclotella. BMC Evolutionary Biology 11.

Armbrust, E.V.e.a. (2004). The Genome of the Diatom Thlassiosira Pseudonana: Ecology, Evolution, and Metabolism. Science 306.

Bamford, D., Caldentey, J., and Bamford, J. (1995). Bacteriophage PRD1: a broad host range dsDNA tectivirus with an internal membrane. Advances in Virus Research 45, 281-319.

Bennion, B., Park, C., Fuller, M., Lindsey, R., Momany, M., Jennemann, R., and Levery, S.B. (2003). Glycosphingolipids of the model fungus Aspergillus nidulans: characterization of GIPCs with oligo-a-mannose-type glycans. Journal of Lipid Research 44.

Benveniste, P. (2004). Biosynthesis and Accumulation of Sterols. Annual Review of Plant Biology 55, 429-457.

Berg, D., Plempel, M., Buchel, K.-H., Holmwood, G., and Stroech, K. (1988). Sterol Biosynthesis Inhibitors. Secondary effects and enhanced in vivo efficacy. Annals of the New York Academy of Sciences 544, 338-347.

Berkey, R., Bendigeri, D., and Xiao, S. (2012). Sphingolipids and plant defense/dis3ease: the "death" connection and beyond. Frontiers in Plant Science 3.

Blaas, N., and Humpf, H. (2013). Structural profiling and quantitation of glycosyl inositol phosphoceramides in plants with Fourier transform mass spectrometry. Journal of Agriculture and Food Chemistry 61, 4257-4269.

Blanc, G., Mozar, M., Agarkova, I., Gurnon, J., Yanai-Balser, G.M., Rowe, J.M., Xia, Y., Riethoven, J.-J., Dunigan, D.D., and Van Etten, J.L. (2014). Deep RNA sequencing reveals hidden features and dynamics of early gene transcription in Paramecium bursaria Chlorella Virus 1. PLoS ONE 9.

Blanc, G., Duncan, G., Agarkova, I., Borodovsky, M., Gurnon, J., Kuo, A., Lindquist, E., Pangilinan, J., Polle, J., Salamov, A., Terry, A., Yamada, T., Dunigan, D.D., Grigoriev, I.V., Claverie, J.-M., and Van Etten, J.L. (2010). The Chlorella variabilis NC64A genome reveals adaptation to photosymbiosis, coevolution with viruses, and cryptic sex. Plant Cell 22, 2943-2955.

Blanc, G., Agarkova, I., Grimwood, J., Kuo, A., Bruegeman, A., Dunigan, D.D., Gurnon, J., Ladunga, I., Lindquist, E., Lucas, S., Pangilinan, J., Proschold, T., Salamov, A., Schmutz, J., Weeks, D., Yamada, T., Lomsadze, A., Borodovsky, M., Claverie, J.-M., Grigoriev, I.V., and Van Etten, J.L. (2012). The genome of the polar eukaryotic microalgo Coccomyxa subellipsoidea reveals traits of cold adaptation. Genome Biology 13.

Blanc, M., Hsieh, W.Y., Robertson, K.A., Watterson, S., Shui, G., Lacaze, P., Khondoker, M., Dickinson, P., Sing, G., Rodriguez-Martin, S., Phelan, P., Forster, T., Strobl, B., Muller, M., Riemersma, R., Osborne, T., Wenk, M.R., Angulo, A., and Ghazal, P. (2011). Host Defense against Viral Infection Involves Interferon Mediated Down-Regulation of Sterol Biosynthesis. PLoS Biology 9.

Bligh, E.G., and Dyer, W.J. (1959). A rapid method for total lipid extraction and purification. Canadian Journal of Biochemistry and Physiology 37, 911-917.

Bodey, G. (1992). Azole antifungal agents. Clinical infectious diseases: An official publication of the Infectious Diseases Society of America 14, S161-169.

Bou Khalil, M., Hou, W., Zhou, H., Elisma, F., Swayne, L., Blanchard, A., Yao, Z., Bennett, S., and Figeys, D. (2010). Lipidomics era: accomplishments and challenges. Mass Spectrometry Reviews 29, 877-929.

Bratbak, G., Egge, J., and Heldal, M. (1993). Viral mortality of the marine alga Emiliania huxleyi (Haptophyceae) and termination of algal blooms. Marine Ecology Progress Series 93, 39-48.

Breslow, D.K., and Weissman, J.S. (2010). Membranes in Balance: Mechanisms of Sphingolipid Homeostasis. Molecular Cell 40.

Brown, A., and Galea, A. (2010). Cholesterol as an evolutionary response to living with oxygen. Evolution 64, 2179-2183.

Brugger, B. (2014). Lipidomics: Analysis of the lipid composition of cells and subcellular organelles by electrospray ionization mass spectrometry. Annual Review of Biochemistry 83, 79-98.

Brussard, C.P.D., Kempers, R., Kop, A., Riegman, R., and Heldal, M. (1996). Virus-like particles in a summer bloom of Emiliania huxleyi in the North Sea. Aquatic Microbial Ecology 10, 105-113.

Burden, R.S., Cooke, D.T., and Carter, G.A. (1989). Inhibitors of Sterol Biosynthesis and Growth in Plants and Fungi. Phytochemistry 28, 1791-1804.

Bure, C., Cacas, J.-L., and Mongrand, S. (2014). Characterization of glycosyl inositol phosphoryl ceramides from plants and fungi by mass spectrometry. Analytical and Bioanalytical Chemistry 406, 995-1010.

Cacas, J.-L., Melser, S., Domergue, F., Joubes, J., Bourdeux, B., Schmitter, J.-M., and Mongrand, S. (2012). Rapid nanoscale quantitative analysis of plant sphingolipid long-chain bases by GC-MS. Analytical and Bioanalytical Chemistry 403, 2745-2755.

Cacas, J.-L., Bure, C., Furt, F., Maalouf, J.-P., Badoc, A., Cluzet, S., Schmitter, J.-M., Antajan, E., and Mongrand, S. (2013). Biochemical survey of the polar head of plant glycosylinositolphosphoceramides unravels broad diversity. Phytochemistry 96, 191-200.

Castberg, T., Thyrhaug, R., Larsen, A., Sandaa, R.-A., Heldal, M., Van Etten, J., and Bratbak, G. (2002). Isolation and characterization of a virus that infects Emiliania huxleyi (Haptophyta). Journal of Phycology 38, 767-774.

Cazzaniga, S., Dalli'Osto, L., Szaub, J., Scibilia, L., Ballottani, M., Purton, S., and Bassi, R. (2014). Domestication of the green alga Chlorella: reduction of antenna size improves light-use efficiency in a photobioreactor. Biotechnology for Biofuels 7, 13.

Chemler, J.A., Yan, Y., and Koffas, M.A. (2006). Biosynthesis of isoprenoids, polyunsaturated fatty acids, and favenoids in Saccromyces cerevisiae. Microbial Cell Factories 5.

Chen, L., Wang, G., and Zhang, H. (2007). Sterol biosynthesis and prokaryotes-to-eukaryotes evolution. Biochemical and Biophysical Research Communications 363, 885-888.

Cherrier, M.V., Kostyuchenko, V.A., Xiao, C., Bowman, V.D., Battisti, A.J., Yan, X., Chipman, P.R., Baker, T.S., Van Etten, J.L., and Rossmann, M.G. (2009). An icosahedral algal virus has a complex unique vertex decorated by a spike. PNAS 106, 11085-11089.

Chuchrid, N., Hiramatsu, S., Sugimoto, I., Fujie, M., Usami, S., and Yamada, T. (2001). Digestion of Chlorella cells by Chlorovirus-encoded polysaccharide degrading enzymes. Microbes and Environments 16, 206-212.

Chugh, A., Ray, A., and Gupta, J. (2003). Squalene epoxidase as hypercholesterolemic drug target revisted. Progress in Lipid Research 42, 37-50.

Cottrell, M., and Suttle, C. (1991). Wide-spread occurrence and clonal variation in viruses which cause lysis of a cosmopolitan, eukaryotic marine

phytoplankton, Micromonas pusilla. Marine Ecology Progress Series 78, 1-9.

Crowley, P.D., and Gallagher, H.C. (2014). Clotrimazole as a pharmaceutical: past, present and future. Journal of Applied Microbiology 117, 611-617.

Darienko, T., Gustavs, L., Eggert, A., Wolf, W., and Proschold, T. (2015). Evaluating the species boundaries of green microalgae (Coccomyxa, Trebouxiophyceae, Chlorophyta) using integrative taxonomy and DNA barcoding with further implications for the species identification in environmental samples. PLoS ONE 10.

Devarenne, T.P., Ghosh, A., and Chappell, J. (2002). Regulation of Squalene Synthase, a Key Enzyme of Sterol Biosynthesis, in Tobacco. Plant Physiology 129, 1095-1106.

Dhar, M.K., Koul, A., and Kaul, S. (2013). Farnesyl pyrophosphate synthase: a key enzyme in isoprenoid biosynthetic pathway and potential molecular target for drug development. New Biotechnology 30.

Dunigan, D.D., Cerny, R.L., Bauman, A.T., Roach, J.C., Lane, L.C., Agarkova, I., Wulser, K., Yanai-Balser, G.M., Gurnon, J., Vitek, J.C., Kronschnabel, B.J., Jeanniard, A., Blanc, G., Upton, C., Duncan, G.A., McClung, O.W., Ma, F., and Van Etten, J.L. (2012). Paramecium bursaria Chlorella Virus 1 proteome reveals novel architectural and regulatory features of a giant virus. Journal of Virology 86, 8821-8834.

Eisenkolb, M., Zenzmaier, C., Leitner, E., and Schneiter, R. (2002). A Specific Structural Requirement for Ergosterol in Long-chain Fatty Acid Synthesis Mutants Important for Maintaining Raft Domains in Yeast. Molecular Biology of the Cell 13, 4414-4428.

Fenn, J., Mann, M., Meng, C., Wong, S., and Whitehouse, C. (1989). Electrospray ionization for mass spectrometry of large biomolecules. Science 246, 64-71.

Frohns, F., Kasmann, A., Kramer, D., Schafer, B., Mehmel, M., Kang, M., Van Etten, J., Gazzarrini, S., Moroni, A., and Thiel, G. (2006). Potassium ion channels of Chlorella viruses cause rapid depolarization of host cells during infection. Journal of Virology 80, 2437-2444.

Gamper, K., and Shapiro, M. (2007). Target-specific PIP2 signalling: how it might work. Journal of Physiology 582, 967-975.

Gazzarrini, S., Severino, M., Lombardi, M., Morandi, M., DiFrancesco, D., Van Etten, J.L., Thiel, G., and Moroni, A. (2003). The viral postassium channel Kcv: structural and functional features. FEBS Letters 552, 12-16.

German, J., Gillies, L., Smilowitz, J., Zivkovic, A., and Watkins, S. (2007). Lipidomics and lipid profiling in metabolomics. Current Opinion in Lipidology 18, 66-71.

Graybill, J., Burgess, D., and Hardin, T. (1997). Key issues concerning fungistatic versus fungicidal drugs. European Journal of Clinical Microbiology and Infectious Dieseases 16, 42-50.

Gross, R., and Han, X. (2007). Lipidomics in diabetes and the metabolic syndrome. Methods in Enzymology 433, 73-90.

Guan, X.L., Souza, C.M., Pichler, H., Dewhurst, G., Schaad, O., Kajiwara, K., Wakabayashi, H., Ivanova, T., Castillon, G.A., Piccolis, M., Abe, F., Loewith, R., Funato, K., Wenk, M.R., and Riezman, H. (2009). Functional Interactions between Sphingolipids and Sterols in Biological Membranes Regulating Cell Physiology. Molecular Biology of the Cell 20, 2083-2095.

Guindon, S., Dufayard, J., Lefort, V., Anisimova, M., Hordijk, W., and Gascuel, O. (2010). New algorithms and methods to estimate maximum-likelihood phylogenies: assessing the performance of PhyML 3.0. Systems Biology 59, 307-321.

Gulati, S., Munkacsi, A.B., Wilcox, L., and Sturley, S.L. (2010). Sterols and sphingolipids: Dynamic duo or partners in crime? Progress in Lipid Research 49, 353-365.

Han, X., and Gross, R. (2005). Shotgun lipidomics: electrospray ionization mass spectrometric analysis and quantitation of cellular lipidomes directly from crude extracts of biological samples. Mass Spectrometry Reviews 24, 367-412.

Han, X., and Christie, W.W. (2010). Lipid Analysis: Isolation, Separation, Identification and Lipidomic Analysis. (Bridgewater, England: The Oily Press).

Han, Y.-B., Wu, L., Rich, J.R., Huang, F.-T., Withers, S.G., Feng, Y., and Yang, G.-Y. (2015). Comprehensive characterization of sphingolipid ceramide N-deacylase for the synthesis and fatty acid remodeling of glycosphingolipids. Applied Microbiology and Biotechnology 99, 6715-6726.

Hannich, J.T., Umebayashi, K., and Riezman, H. (2011). Distribution and Functions of Sterols and Sphingolipids. Cold Spring Harbor Perspectives in Biology 3, a004762.

Harris, E. (2001). Chlamydomonas as a model organism. Annual Review of Plant Physiology and Plant Molecular Biology 52, 363-406.

He, J.-X., Fujioka, S., Li, T.-C., Kang, S.G., Seto, H., Takatsuto, S., Yoshida, S., and Jang, J.-C. (2003). Sterols Regulate Development and Gene Expression in Arabidopsis. Plant Physiology 131, 1258-1269.

Ho, C., Lam, C., Chan, M., Cheung, L., Law, L., Lit, L., Ng, K., Suen, M., and Tai, H. (2003). Electrospray ionisation mass spectrometry: principles and clinical applications. Clinical Biochemistry Review 24, 3-12.

Holm-Hanson, O. (1964). Isolation and culture of terrestrial and fresh-water algae of Antartica. Phycologia 4, 43-51.

Holmberg, N., Harker, M., Gibbard, C.L., Wallace, A.D., Clayton, J.C., Rawlins, S., Hellyer, A., and Safford, R. (2002). Sterol C-24 methyltransferase type 1 controls the flux of carbon into sterol biosynthesis in tobacco seed. Plant Physiology 130, 303-311.

Hoshina, R., Iwataki, M., and Imamura, N. (2010). Chlorella variabilis and Micractinium reisseri sp. nov. (Chlorellaceae, Trebouxiophyceae): Redscription of the endosymbiotic green algae of Paramecium bursaria (Peniculia, Oligohymenophorea) in the 120th year. Phycological Research 58, 188-201.

Hunter, W.N. (2007). The Non-mevalonate Pathway of isoprenoid Precursor Biosynthesis. The Journal of Biological Chemistry 282, 21573-21577.

ICTV. (2012). Virus taxonomy: Classification and nomenclature of viruses: Ninth Report of the International Committee on Taxonomy of Viruses, A. King, M. Adams, E. Carstens, and E. Lefkowitz, eds (San Diego: Elsevier Academic Press).

Istvan, E.S., and Deisenhofer, J. (2001a). Structural mechanism for statin inhibition of HMG-CoA reductase. Science 292, 1160-1164.

Istvan, E.S., and Deisenhofer, J. (2001b). The structure of the catalytic portion of human HMG-CoA reductase. Biochimica et Biophysica Acta 1529, 9-18.

Iyer, L., Balaji, S., Koonin, E., and Aravind, L. (2006). Evolutionary genomics of nucleo-cytoplasmic large DNA viruses. Virus Research 117, 156-184.

Jordan, R.W., and Chamberlain, A.H.L. (1997). Biodiversity among haptophyte algae. Biodiversity Conservation 6, 131-152.

Kapaun, E., and Reisser, W. (1995). A chitin-like glycan in the cell wall of a Chlorella sp. (Chlorococcales, Chlorophyceae). Planta 197, 577-582.

Katoh, K., and Standley, D. (2013). MAFFT multiple sequence alignment software version 7: improvements in performance and usability. Molecular Biology and Evolution 30, 772-780.

Kennedy, M., and Bard, M. (2001). Positive and negative regulation of squalene synthase (erg9), an ergosterol biosynthetic gene, in Saccromyces cerevisiae. Biochimica et Biophysica Acta 1517, 177-189.

Kodner, R.B., Pearson, A., Summons, R.E., and Knoll, A.H. (2008). Sterols in red and green algae: quantification, phylogeny, and relevance for the interpretation of geologic steranes. Geobiology 6, 411-420.

Koonin, E.V., and Yutin, N. (2001). Nucleo-cytoplasmic Large DNA Viruses (NCLDV) of Eukaryotes. In eLS (John Wiley & Sons, Ltd.

Kumari, P., Kumar, M., Reddy, C., and Jha, B. (2012). Algal lipids, fatty acids and sterols. In Functional ingredients from algae for foods and nutraceuticals, H. Dominguez, ed (Woodhead Publishing Ltd.), pp. 87-134.

Kuznetsov, Y., Klose, T., Rossmann, M.G., and McPherson, A. (2013). Morphogenesis of Mimivirus and its viral factories: an atomic force microscopy study of infected cells. Journal of Virology 87, 11200-11213.

Kuzuyama, T. (2002). Mevalonate and Nonmevalonate Pathways for the Biosynthesis of Isoprene Units. Bioscience Biotechnology Biochemistry 66, 1619-1627.

Lagace, T., and Ridgway, N. (2013). The role of phospholipids in the biological activty and structure of the endoplasmic reticulum. Biochemical and Biophysical Acta 1833, 2499-2510.

Leonardsen, L., Stromstedt, M., and Byskov, A. (2000). Effect of inhibition of sterol delta 14-reductase on accumulation of meiosis-activating sterol and meiotic resumption in cumulus-enclosed mouse oocytes in vitro. Journal of Reproduction and Fertility 118, 171-179.

Lewis, J., and Graybill, J. (2008). Fungicidal versus fungistatic: What's in a word? Expert opinion on pharmacotherapy 9, 927-935.

Lombard, J., and Moreira, D. (2011). Origins and Early Evolution of the Mevalonate Pathway of isoprenoid Biosynthesis in the Three Domains of Life. Molecular Biology and Evolution 28, 87-99.

Maier, I., Muller, D., and Katsaros, C. (2002). Entry of the DNA virus, Ectocarpus fasciculatus type 1 (Phycodnaviridae), into host cell cytosol and nucleus. Phycology Research 50, 227-231.

Malhotra, H., and Goa, K. (2001). Atorvastatin: an updated review of its pharmacological properties and use in dyslipidemia. Drugs 61, 1835-1881.

Malin, G., Wilson, W., Bratbak, G., Liss, P., and Mann, N. (1998). Elevated production of dimethylsulfide resulting from viral infection of cultures of Phaeocystis pouchetti. Limnology and Oceanography 43, 1389-1393.

Markham, J.E. (2013). Acyl-Lipid Metabolism. In The Arabidopsis Book 11.e0161 (The American Society of Plant Biologists.

Markham, J.E., Li, J., Cahoon, E.B., and Jaworski, J.G. (2006). Separation and Identification of Major Plant Sphingolipid Classes from Leaves. The Journal of Biological Chemistry 281, 22684-22694.

Marques, J.T., Cordeiro, A.M., Viana, A.S., Herrmann, A., Marinho, H.S., and de Almeida, R.F. (2015). Formation and Properties of Membrane-Ordered Domains by Phytoceramide: Role of Sphingoid Base Hydroxylation. In ACS Publications - Langmuir, pp. 12.

Mayer, J., and Taylor, F. (1979). A virus which lyses the marine nanoflagellate Micromonas pusilla. Nature 281, 299-301.

Meints, R.H., Lee, K., and Van Etten, J.L. (1986). Assembly site of the virus PBCV-1 in a Chlorella-like green alga: ultrastructural studies. Virology 154, 240-245.

Meints, R.H., Lee, K., Burbank, D.E., and Van Etten, J.L. (1984). Infection of a chlorella-like alga with the virus, PBCV-1: Ultrastructural studies. Virology 138, 341-346.

Mercer, E. (1993). Inhibitors of sterol biosynthesis and their applications. Progress in Lipid Research 32, 357-416.

Merchant, S.S.e.a. (2007). The Chlamydomonas Genome Reveals the Evolution of Key Animal and Plant Functions. Science 318.

Miller, M.B., Haubrich, B.A., Wang, Q., Snell, W.J., and Nes, D. (2012). Evolutionarily conserved delta 25(27)-olefin ergosterol biosynthesis pathway in the alga Chlamydomonas reinhardtii. Journal of Lipid Research 53, 1636-1645.

Miller, S.M. (2010). Volox, Chlamydomonas, and the Evolution of Multicellularity. Nature Education 3, 65.

Milrot, E., Mutsafi, Y., Fridmann-Sirkis, Y., Shimoni, E., Rechav, K., Gurnon, J., Van Etten, J.L., and Minsky, A. (2015). Virus-host interactions: insights from the replication cycle of the large Paramecium bursaria Chlorella virus. Cellular Microbiology.

Mo, C., and Bard, M. (2005). A systematic study of yeast sterol biosynthetic protein-protein interactions using the split-ubiquitin system. Biochemical and Biophysical Acta 1737, 152-160.

Morita, M., Watanabe, Y., and Saiki, H. (2000). High photosynthetic productivity of green microalga Chlorella sorokiniana. Applied Biochemistry and Biotechnology 87, 203-218.

Murphy, R., Fiedler, J., and Hevco, J. (2001). Analysis of nonvolatile lipids by mass spectrometry. Chemical Reviews 101, 479-526.

Mutsafi, Y., Shimoni, E., Shimon, A., and Minsky, A. (2013). Membrane assembly during the infection cycle of the giant Mimivirus. PlOS Pathogens 9.

Nagasaki, K., and Yamaguchi, M. (1998a). Isolation of a virus infectious to the harmful bloom causing microalga Heterosigma akashiwo virus. Aquatic Microbial Ecology 15.

Nes, W.R., and New, W.D. (1980). Lipids in Evolution (New York: Plenum), pp. 157-197.

Paradies, G., Paradies, V., De Benedictis, V., Ruggiero, F.M., and Petrosillo, G. (2014). Functional role of cardiolipin in mitochondrial bioenergetics. Biochemical and Biophysical Acta 1837, 408-417.

Patterson, G.W. (1991). Physiology and Biochemistry of Sterols. (American Oil Chemists' Society).

Plugge, B., Gazzarrini, S., Nelson, M., Cerana, R., Van Etten, J.L., Derst, C., DiFrancesco, D., Moroni, A., and Thiel, G. (2000). A potassium channel protein encoded by chlorella virus PBCV-1. Science 287.

Porsbring, T., Blanck, H., Tjellstrom, H., and Backhaus, T. (2009). Toxicity of the pharmaceutical clotrimazole to marine microalgal communities. Aquatic toxicology 91, 203-211.

Rahier, A., and Taton, M. (1997). Fungicides as Tools in Studying Postsqualene Sterol Synthesis in Plants. Pesticide Biochemistry and Physiology 57, 1-27.

Rao, V., and Feiss, M. (2008). The bacteriophage DNA packaging motor. Annual Review Genetics 42, 647-681.

Raoult, D., La Scola, B., and Birtles, R. (2007). The discovery and characterization of Mimivirus, the largest known virus and putative pneumonia agent. Clinical Infectious Diseases 45, 95-102.

Read, B.A., Kegel, J., Klute, M.J., Kuo, A., Lefebvre, S.C., Maumus, F., Mayer, C., Miller, J., Monier, A., Salamov, A., Young, J., Aguilar, M., Claverie, J.-M., Frickenhaus, S., Gonzalez, K., Herman, E.K., Lin, Y.-C., Napier, J., Ogata, H., Sarno, A.F., Shmutz, J., Schroeder, D., de Vargas, C., Verret, F., von Dassow, P., Valentin, K., Van de Peer, Y., Wheeler, G., Emiliania huxleyi Annotation, C., Dacks, J.B., Delwiche, C.F., Dyhrman, S.T., Glockner, G., John, U., Richards, T., Worden, A.Z., Zhang, X., and Grigoriev, I.V. (2013). Pan genome of the phytoplankton Emiliania underpins its global distribution. Nature 499, 209-213.

Rennie, E., Ebert, B., Miles, G., Cahoon, R.E., Christiansen, K., Stonebloom, S., Khatab, H., Twell, D., Petzold, C., Adams, P., Dupree, P., Heazlewood, J., Cahoon, E.B., and Scheller, H. (2014). Identification of a sphingolipid alpha-glucuronosyltransferase that is essential for pollen function in Arabidopsis. Plant Cell 26, 3314-3325.

Rhee, S., Beavis, W., Berardini, T., Chen, G., Dixon, D., Doyle, A., Garcia-Hernandez, M., Huala, E., Lander, G., Montoya, M., Miller, N., Mueller, L., Mundodi, S., Tacklind, J., Weems, D., Wu, Y., Xu, I., Yoo, D., Yoon, J., and Zhang, P. (2003). The Arabidopsis Information Resource (TAIR): a model organism database providing a centralized, curated gateway to Arabidopsis biology, research materials and community. Nucleic Acids Research 31, 224-228.

Rice, G., Tang, L., Stedman, K., Roberto, F., Spuhler, J., Gillitzer, E., Johnson, J., Douglas, T., and Young, M. (2004). The structure of a thermophilic archaeal virus shows a double-stranded DNA viral capsid type that spans all domains of life. PNAS 101, 7716-7720.

Roberts, S.C. (2007). Production and engineering of terpenoids in plant cell culture. Nature Chemical Biology 3, 387-395.

Robinson, G., Tsay, Y., Kienzle, B., Smithmonroy, C., and Bishop, R. (1993). Conservation between human and fungal squalene synthetases: similarities in structure, function, and regulation. Molecular Cell Biology 13, 2706-2717.

Roine, E., and Bamford, D.H. (2012). Lipids of Archaeal Viruses. Archaea, 8.

Romani, G., Piotrowski, A., Hillmer, S., Gurnon, J., Van Etten, J., Moroni, A., Thiel, G., and Hertel, B. (2013). A virus-encoded potassium ion channel is a structural protein in the chlorovirus Paramecium bursaria Chlorella virus 1 virion. Journal of General Virology 94, 2549-2556.

Rossard, S., Roblin, G., and Atanassova, R. (2010). Ergosterol triggers characteristic elicitation steps in Beta vulgaris leaf tissues. Journal of Experimental Botany 61, 1807-1816.

Rowe, J.M., Jeanniard, A., Gurnon, J., Xia, Y., Dunigan, D.D., Van Etten, J.L., and Blanc, G. (2014). Global analysis of Chlorella variabilis NC64A mRNA profiles during the early phase of Paramecium bursaria Chlorella Virus-1 infection. PLoS ONE 9.

Ryder, N. (1992). Terbinafine: mode of action and properties of the squalene epoxidase inhibition. The British Journal of Dermatology 126, 2-7.

Schug, Z.T., and Gottlieb, E. (2009). Cardiolipin acts as a mitochondrial signalling platform to launch apoptosis. Biochemical and Biophysical Acta, 2022-2031.

Schuster, A., Girton, L., Burbank, D.E., and Van Etten, J.L. (1986). Infection of a Chlorella-like alga with the virus PBCV-1: Transcriptional studies. Virology 148, 181-189.

Segura, M., Lodeiro, S., Meyer, M., Patel, A., and Matsuda, S. (2002). Directed evolution experiments reveal mutations at cycloartenol synthase residue His477 that dramatically alter catalysis. Organic Letters 4, 4459-4462.

Seppanen-Laakso, T., and Oresic, M. (2009). How to study lipidomes. Journal of Molecular Endocrinology 42, 185-190.

Siaut, M., Cuine, S., Cagnon, C., Fessler, B., Nguyen, M., Carrier, P., Beyly, A., Beisson, F., Triantaphylides, C., Li-Beisson, Y., and Peltier, G. (2011). Oil accumulation in the model green alga Chlamydomonas reinhardtii:

characterization, variability between common laboratory strains and relationship with starch reserves. BMC Biotechnology 11.

Song, Z., and Nes, D. (2007). Sterol biosynthesis inhibitors: potential for transition state analogs and mechanism-based inactivators targeted at sterol methyltransferase. Lipids 42, 15-33.

Sun, L., Adams, B., Gurnon, J., Ye, Y., and Van Etten, J.L. (1999). Characterization of two chitinase genes and one chitosanase gene encoded by Chlorella virus PBCV-1. Virology 263, 376-387.

Suzuki, M., and Muranaka, T. (2007). Molecular Genetics of Plant Sterol Backbone Synthesis. Lipids 42, 47-54.

Taramino, S., Valachovic, M., Oliaro-Bosso, S., Viola, F., Teske, B., Bard, M., and Balliano, G. (2010). Interactions of oxidosqualene cyclase (Erg7p) with 3-keto reductase (Erg27p) and other enzymes of sterol biosynthesis in yeast. Biochimica et Biophysica Acta 1801.

Teske, B., Taramino, S., Bhuiyan, M.S.A., Kumaraswarmi, N.S., Randall, S.K., Barbuch, R., Eckstein, J., Balliano, G., and Bard, M. (2008). Genetic analyses involving interactions between the ergosterol biosynthetic enzymes, lanosterol synthase (Erg7p) and 3-ketoreductase (Erg27p), in the yeast Saccromyces cerevisiae. Biochemical and Biophysical Acta 1781, 359-366.

Vago, T., Baldi, G., Colombo, D., Barbareschi, M., Norbiato, G., Dallegri, F., and Bevilacqua, M. (1994). Effects of Naftifine and Terbinafine, Two Allylamine Antifungal Drugs, on Selected Functions of Human Polymorphonuclear Leukocytes. Antimicrobial Agents and Chemotherapy 38, 2605-2611.

Van Etten, J.L. (2003). Unusual life style of giant Chlorella viruses. Annual Review Genetics 37, 153-195.

Van Etten, J.L., and Dunigan, D.D. (2012). Chloroviruses: Not your everyday plant virus. Trends in Plant Science 17, 1-8.

Van Etten, J.L., Burbank, D.E., Kuczmarski, D., and Meints, R.H. (1983). Virus infection of culturable Chlorella-like algae and development of a plaque assay. Science 219, 994-996.

Van Etten, J.L., Burbank, D.E., Joshi, J., and Meints, R.H. (1984). DNA synthesis in a chlorella-like alga following infection with the virus PBCV-1. Virology 134, 443-449.

Van Etten, J.L., Graves, M., Muller, D., Boland, W., and Delaroque, N. (2002). Phycodnaviridae - large DNA algal viruses. Archives of Virology 147, 1479-1516.

Van Etten, J.L.G., MV; Muller, DG; Boland, W; Delaroque, N. (2002). Phycodnaviridae -- large DNA algal viruses. Archives of Virology 147, 1479-1516.

Van Meer, G., Voelker, D.R., and Feignson, G.W. (2008). Membrane lipids: where they are and how they behave. Nature Reviews Molecular Cell Biology 9.

Veen, M., Stahl, U., and Lang, C. (2003). Combined overexpression of genes of the ergosterol biosynthetic pathway leads to accumulation of sterols in Saccharamomyces cerevisiae. FEMS Yeast Research 4, 87-95.

von Dassow, P., Ogata, H., Probert, I., Wincker, P., Da Silva, C., Audic, S., Claverie, J.-M., and de Vargas, C. (2009). Transcriptome analysis of functional differentiation between haploid and diploid cells of Emiliania huxleyi, a globally significant photosynthetic calcifying cell. Genome Biology 10, R114.

Weernink, P., Han, L., Jakobs, K., and Schmidt, M. (2007). Dynamic phospholipid signaling by G protein-coupled receptors. Biochemical and Biophysical Acta - Biomembranes 1768, 888-900.

Wenk, M. (2005). The emerging field of lipidomics. Nature Reviews Drug Discovery 4, 594-610.

Wilson, W., Van Etten, J., and Allen, M. (2009). "The Phycodnaviridae: the story how tiny giants rule the world". Current Topics in Microbiology and Immunology 328, 1-42.

Winkel, B.S.J. (2009). Multi-enzyme Complexes. In Plant-derived natural products: Synthesis, function and application, A.E. Osbourn and V. Lanzotti, eds (New York: Springer), pp. 195.

Xu, X., Bittman, R., Duportail, G., Heissler, D., Vilcheze, C., and London, E. (2001). Effect of the Structure of Natural Sterols and Sphingolipids on the Formation of Ordered Sphingolipid/Sterol Domains (Rafts). The Journal of Biological Chemistry 276, 33540-33546.

Yanai-Balser, G.M., Duncan, G., Eudy, J.D., Wang, D., Li, X., Agarkova, I., Dunigan, D.D., and Van Etten, J.L. (2010). Microarray analysis of Paramecium bursaria Chlorella Virus 1 transcription. Journal of Virology 84, 532-542.

Yashchenko, V.V., Gavrilova, O.V., Rautian, M.S., and Jakobsen, K. (2012). Association of Paramecium bursaria Chlorella viruses with Paramecium bursaria cells: Ultrastructural studies. European Journal of Protistology 48, 149-159.

Zhang, X., Xiang, Y., Duncan, G., Klose, T., Chipman, P.R., Van Etten, J.L., and Rossmann, M.G. (2011). Three-dimensional structure and function of the Paramecium bursaria chlorella virus capsid. PNAS 108, 14837-14842.

Zhou, W., Lepesheva, G.I., Waterman, M.R., and Nes, D. (2006). Enzyme Catalysis and Regulation: Mechanistic Analysis of a Multiple Product Sterol Methyltransferase Implicated in Ergosterol Biosynthesis in Trypanosoma brucei. The Journal of Biological Chemistry 281, 6290-6296.

Table 1. Type species of known membrane-containing *Phycodnaviridae* viruses from each of the six genera, their exit strategies and presence of internal membrane or outer lipid envelope. *Paramecium bursaria* virus 1 (PBCV-1), *Emiliania huxleyi* virus 86 (EhV-86), *Micromonas pusilla* virus (MpV-SP1), *Phaeocystis pouchetti* virus (PPV01), *Ectocarpus siliculousus* (EsV-1), *Heterosigma akashiwo* virus (HaV-01).

GENERA	TYPE SPECIES	EXIT STRATEGY	LIPID MEMBRANE	REFERENCES
Chlorovirus	PBCV-1	Lytic	Internal	(Meints et al., 1984; Van Etten et al., 2002)
Coccolithovirus	EhV-86	Virion budding	Double enveloped	(Bratbak et al., 1993; Brussard et al., 1996; Castberg et al., 2002)
Prasinovirus	MpV-SP1	Lytic	Internal	(Mayer and Taylor, 1979; Cottrell and Suttle, 1991)
Prymnesiovirus	PPV01	Lytic	Internal	(Malin et al., 1998)
Phaeovirus	ESV-1	Lysogenic/latent	Internal	(Maier et al., 2002)
Raphidovirus	HaV-01	Lytic	Internal	(Nagasaki and Yamaguchi, 1998a)
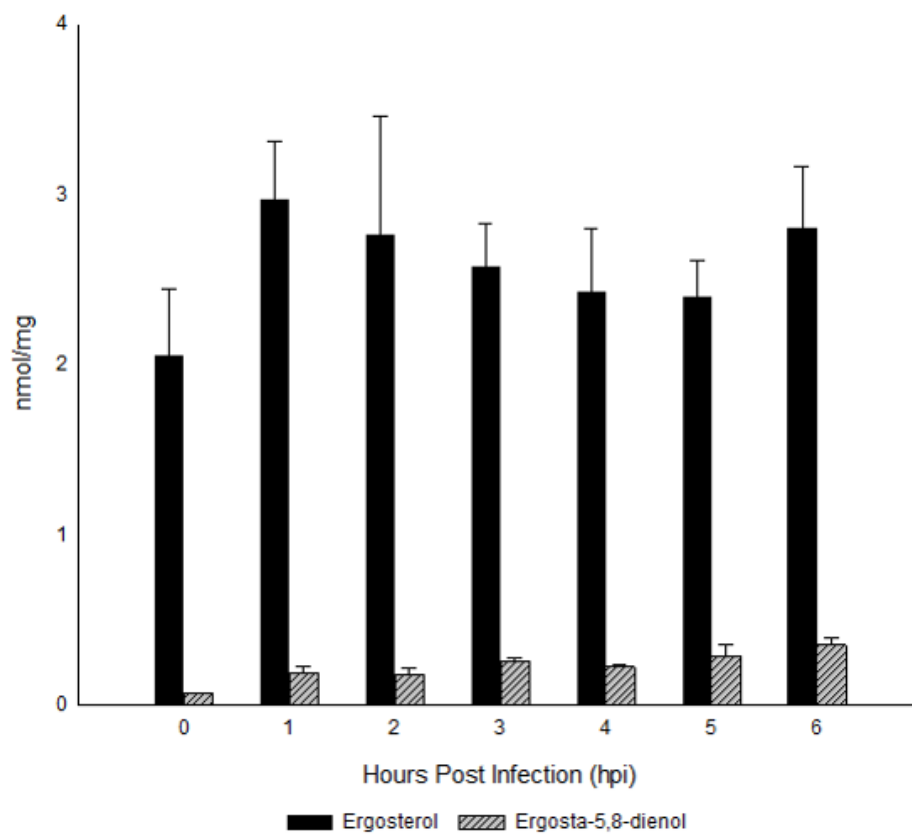
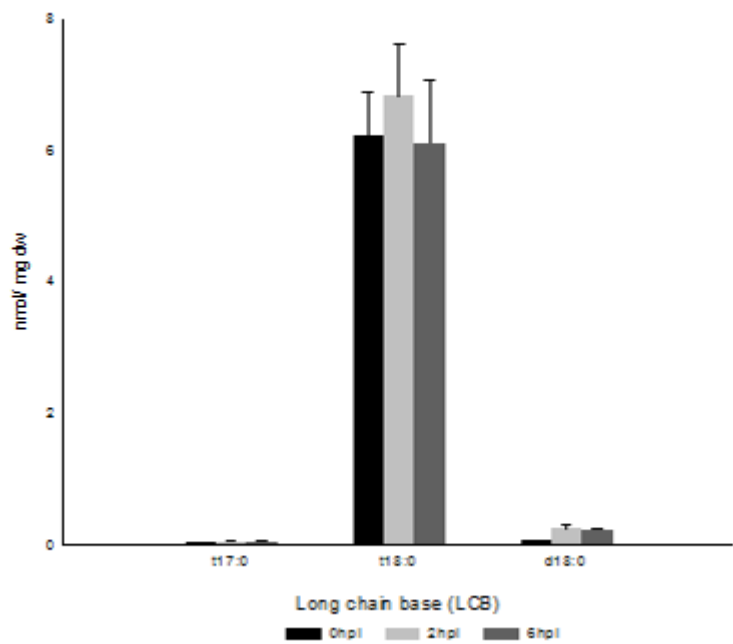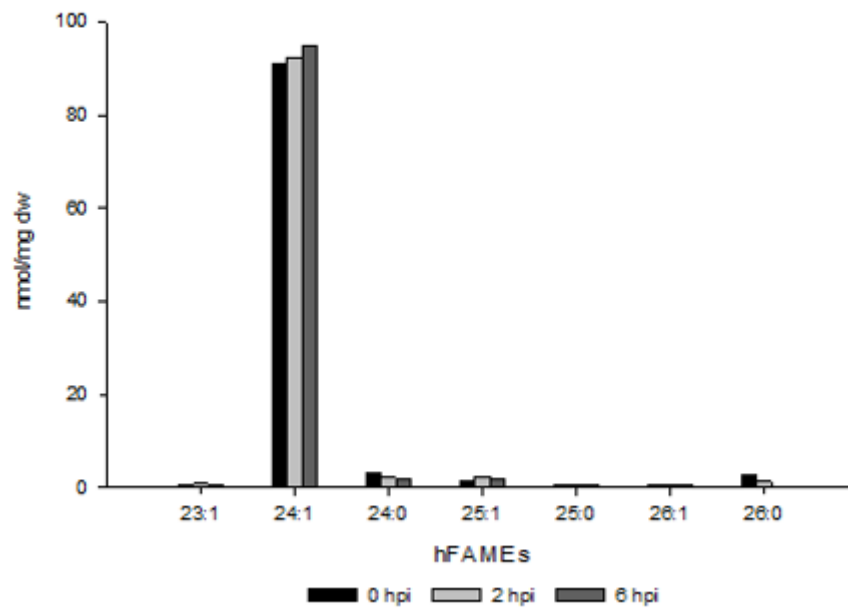Figure 1. Ergosterol levels in host *Chlorella variabilis* during PBCV-1 viral infection.

A

B

Figure 2 A-B. A) Long chain base (LCB) and B) hydroxy fatty acid methyl ester (hFAMEs) levels during PBCV-1 infection of *Chlorella variabilis*.

Table 2. Host mRNA transcription levels of genes involved in sterol biosynthesis during PBCV-1 infection.

Function (characterized or predicted)	*Chlorella variabilis* (CHLNCDRAFT)	Host mRNA transcripts (mpi)					
		0	7	14	20	40	60
1-deoxy-D-xylulose 5-phosphate synthase	59788	4104.4	4113.5	3568.8	2605.8	2246.0	2744.3
1-deoxy-D-xylulose 5-phosphate reductoisomerase	29723	633.5	682.4	666.9	419.0	306.0	327.8
2-C-methyl-D-erythritol 4-phospate cytidyltransferase	141910	60.4	71.5	57.5	55.6	47.3	34.9
4-diphosphocytidyl-2-C-methyl-D-erythritol kinase	33454	36.1	50.3	49.5	37.4	34.8	33.6
2-C-methyl-D-erythritol 2,4-cyclo-diphosphate synthase	53457	NF					
1-hydroxy-2-methyl-2E-butenyl-4-diphosphate synthase	144676	965.9	981.2	936.7	697.9	645.3	660.9
4-hydroxy-3-methyl-2E-butenyl-4-diphosphate reductase	59658	2400.7	2424.7	2515.4	2275.0	1749.5	1685.8
Isopentenyl pyrophosphate isomerase	53578	644.5	620.3	449.3	281.9	258.7	270.0
Acetoacetyl-CoA thiolase	27161	1018.5	1060.6	1236.5	1345.1	1674.4	2079.4
3-Hydroxy-3-methylglutaryl-CoA synthase	138158	41.6	29.1	32.7	42.2	40.3	71.2
3-Hydroxy-3-methylglutaryl-CoA reductase	N/A						
Mevalonate kinase	N/A						
Phosphomevalonate kinase	N/A						
Mevalonate diphosphate decarboxylase	N/A						
Farnesyl pyrophosphate synthase	33543	4192.2	3853.3	4440.0	4626.7	4102.6	2807.4
Squalene synthase	18492	NF					
2,3-oxidosqualene	137251	1464.6	1320.1	997.7	970.2	717.6	621.9
Cycloartenol/Lanosterol Synthase	22200	2314.4	2469.5	2663.1	2104.4	1400.5	1144.5
C14-alpha-demethylase/ C22-desaturase	56217	1766.4	1708.5	1879.5	1842.6	1312.8	961.8
Delta-14/24-reductase	136479	11.8	13.4	14.2	8.6	22.3	33.6
C4-demethylase/ Delta7-Sterol-C5-desaturase	37407	699.4	668.3	705.8	623.2	442.3	339.8
C4-decarboxylase/C3-dehydrogenase	49861	534.7	540.9	530.7	459.2	424.2	393.6
3-ketoreductase	56728	700.1	643.9	667.8	602.1	399.1	347.9
S-AdoMet-C24-methyltransferase	37067	1855.8	2106.3	2056.4	1801.4	1091.7	947.0
Delta-8-delta-7-sterol isomerase	34496	358.3	286.2	276.0	227.2	258.7	240.4

Table 3. Host mRNA transcription levels of genes involved in sphingolipid biosynthesis during PBCV-1 infection.

| Function (characterized or predicted)	Chlorella variabilis (CHLNCDRAFT)	Host mRNA transcripts (mpi)					
		0	7	14	20	40	60
Subunit of serine palmitoyltransferase	138531	415.0	829.5	816.9	745.6	820.7	719.0
Subunit of serine palmitoyltransferase	144864	165.0	656.2	577.9	439.6	294.3	207.2
Small subunit SPT	NF						
3-Ketosphinganine reductase	57682	104.0	152.1	128.2	101.7	74.8	105.7
	58302	30.0	40.8	43.2	41.6	30.7	29.2
Sphingobase C4-hydroxylase	57760	12.0	31.4	28.3	29.2	21.1	9.7
	142325	53.0	0.5	0.8	2.7	9.6	33.4
LCB delta 8 desaturase	NF						
Fatty Acid alpha(2)-hydroxylase	144683	268.0	874.2	773.6	650.1	623.2	472.8
Dihydrosphingosine-delta 4 desaturase	57665	301.0	1401.8	1295.7	1021.6	862.8	538.2
Ceramide synthase	50975	283.0	416.3	418.3	429.9	383.5	364.4
IPC synthase	17179	158.0	406.9	378.2	325.5	272.3	222.5
IPUT1	138328	200.7	268.9	219.3	245.4	257.3	221.6
GONST1	32701	152.1	153.3	171.6	169.7	233.6	239.1
Glucosylceramide Glucosidase	Unknown						
Glucosylceramide synthase	133847	132.0	249.3	232.7	219.3	220.5	203.0
Glycosylinositolphosphorylceramide synthase	Unknown						
Ceramide kinase	54812	592.0	910.3	735.9	782.8	741.1	726.0
LCB kinase	134482	180.0	300.3	287.0	229.1	234.9	193.3
LCB-1-phosphate lyase	144988	88.0	127.0	122.6	112.3	86.3	69.5
LCB-1-phosphate phosphatase	138478	164.0	214.8	224.1	168.0	201.3	222.5
3-Ketoacyl-CoA synthase	48950	2993.0	8389.9	8621.7	9119.8	8139.4	4966.3
		392.0	1315.6	1235.1	1179.0	985.6	717.6
3-Ketoacyl-CoA reductase	56728	259.0	700.1	643.9	667.8	602.1	399.1
3-Hydroxylacyl-CoA dehydratase	143333	213.0	729.9	719.4	588.2	352.8	280.9
Enoyl-CoA reductase	20573	55.0	109.8	74.7	85.8	90.1	58.4
Putative condensing enzyme for VLCFA synthesis	NF						
omega 9 desaturase	NF						
Alkaline ceramidase	NF						
Neutral ceramidase	139234	21.2	14.2	31.0	67.1	51.5	76.6
ORMDL family protein	29488	225.0	246.9	261.8	303.9	321.3	307.6
Phospholipase C	Unknown						

A

B

mRNA transcript levels (%)
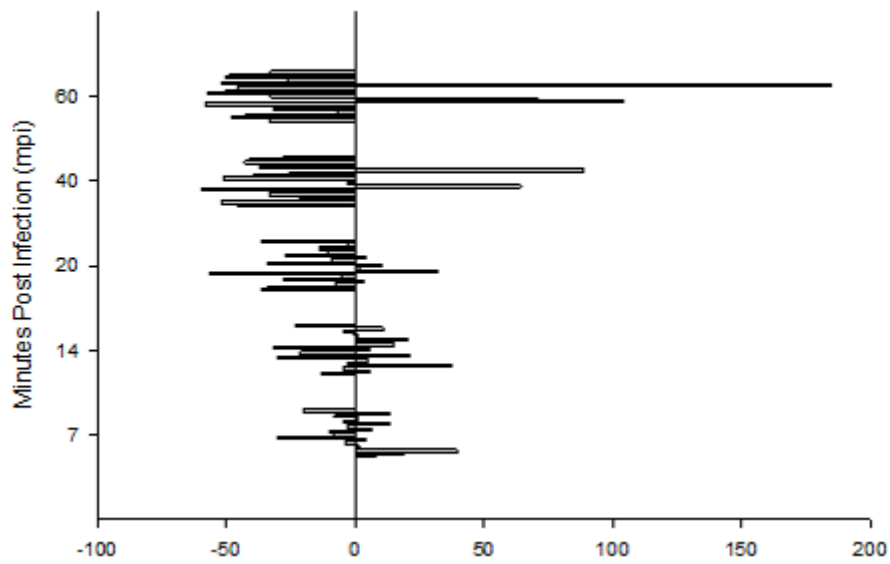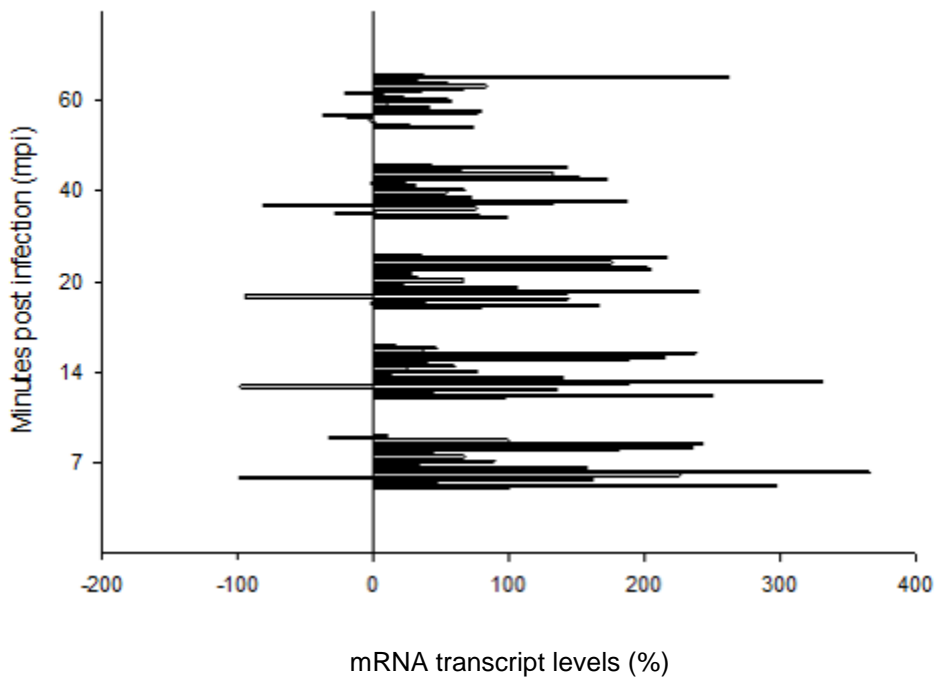
Figure 3A-B.   Messenger RNA transcription levels during PBCV-1 infection A) Sterol biosynthesis mRNA transcripts and B) Sphingolipid biosynthesis mRNA transcripts.
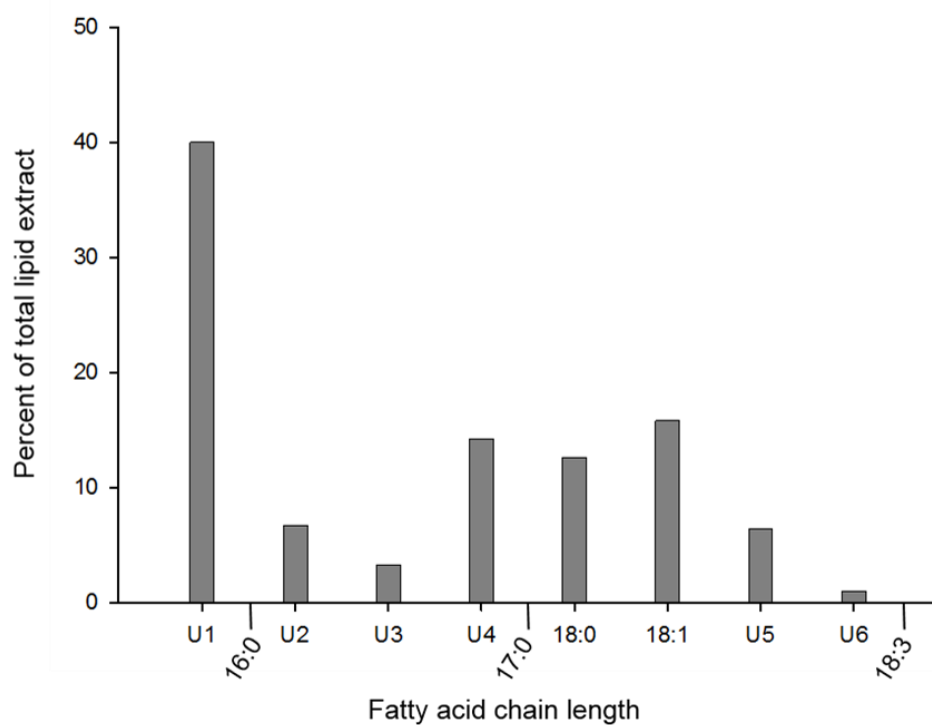
Figure 4. GC-FID analysis of fatty acid chain lengths present in highly purified PBCV-1 total lipid extract. *U denotes unknown fatty acid chain length.
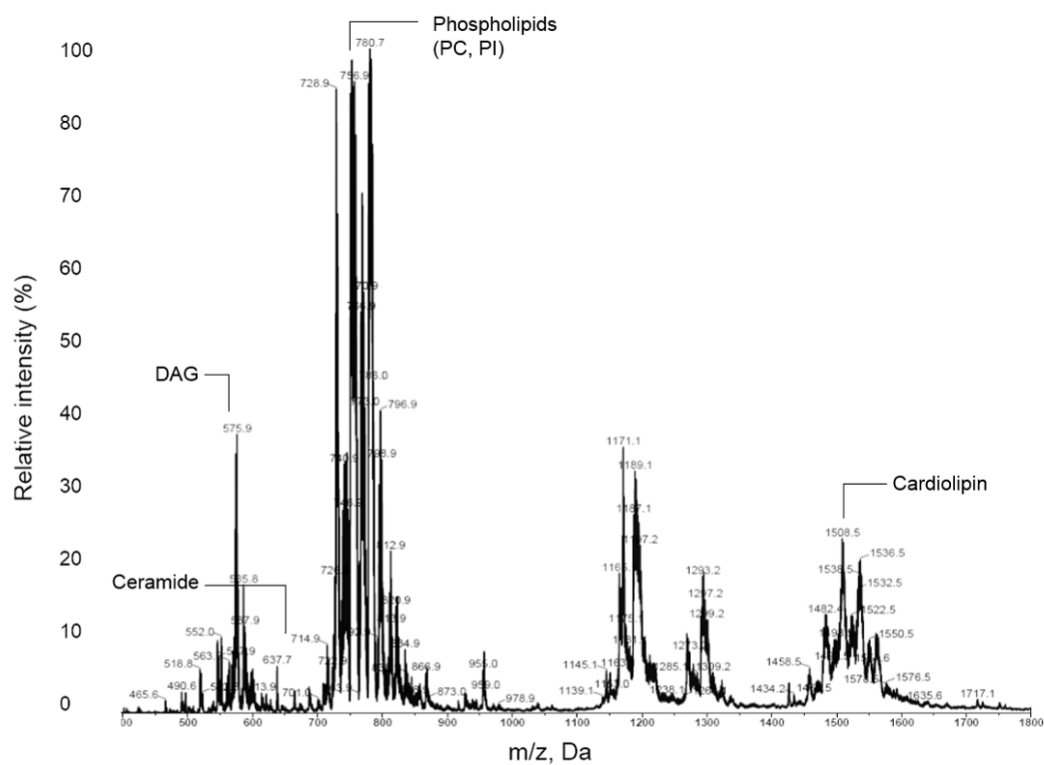
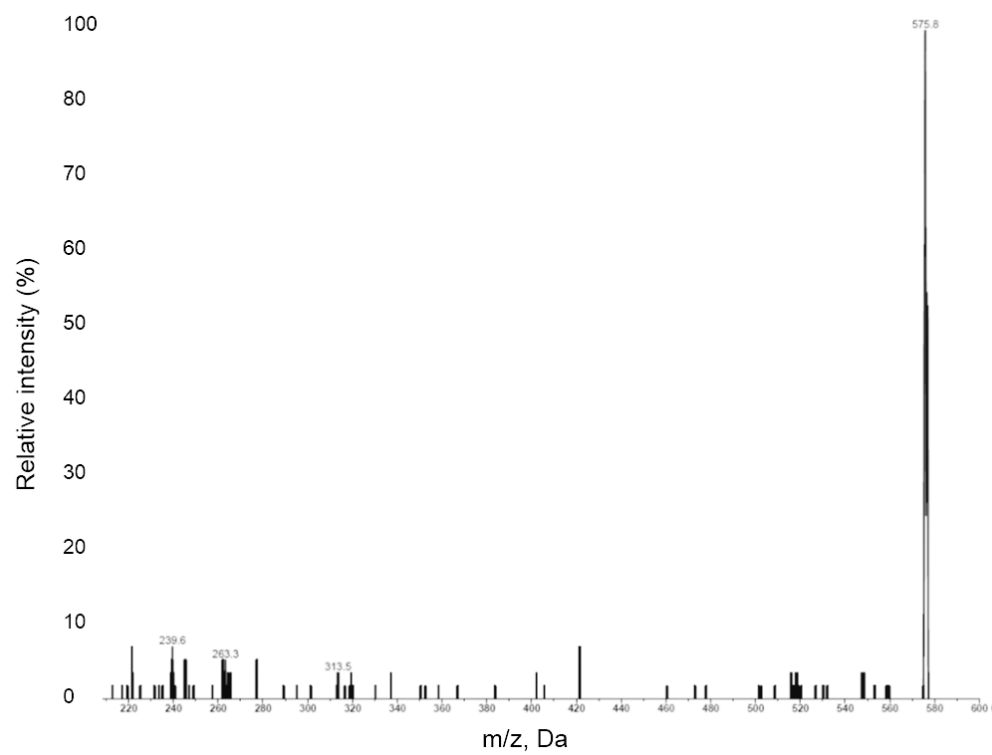Figure 5. Q1 scan of PBCV-1 internal membrane lipid extraction by ESI/MS.
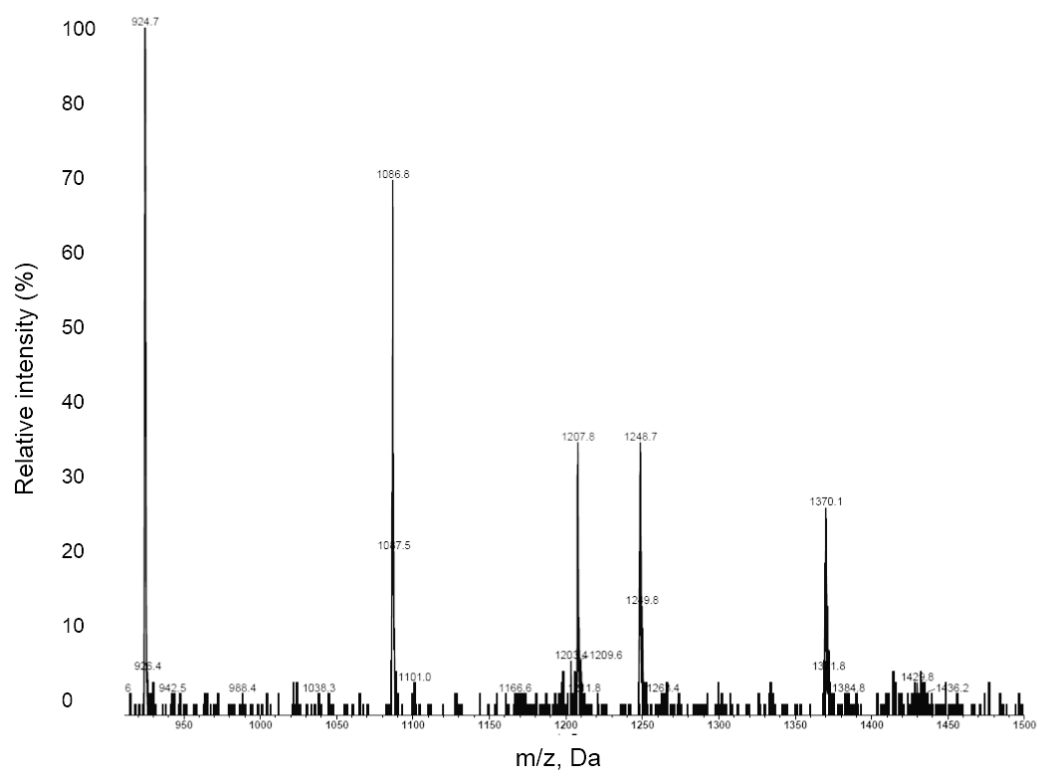
Figure 6. MS2 ion scan of diacylglycerol (DAG).

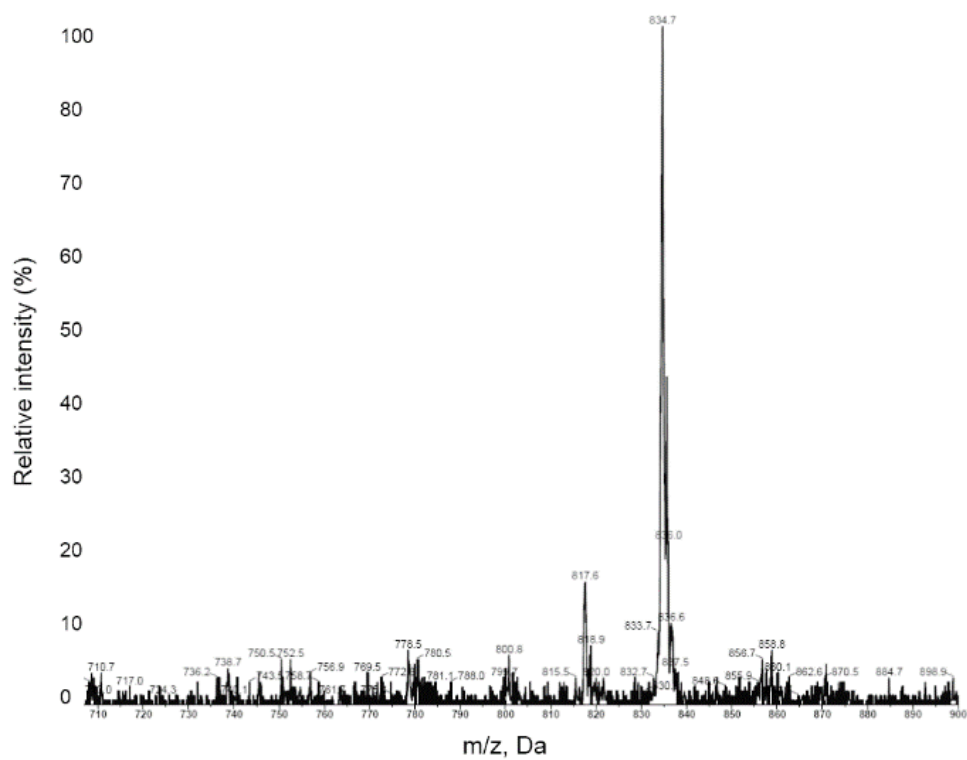Figure 7. Precursor ion scan of GIPC
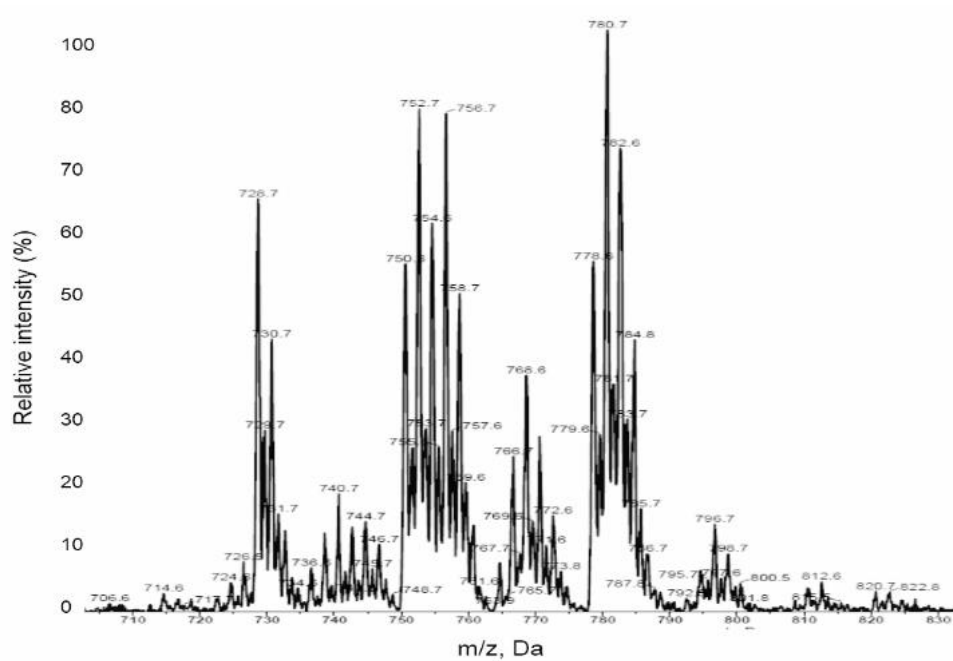
Figure 8A-B. Phospholilpids A. Precursor ion scan of phosphatidylcholine B. Precursor ion scan of phosphatidylinositol
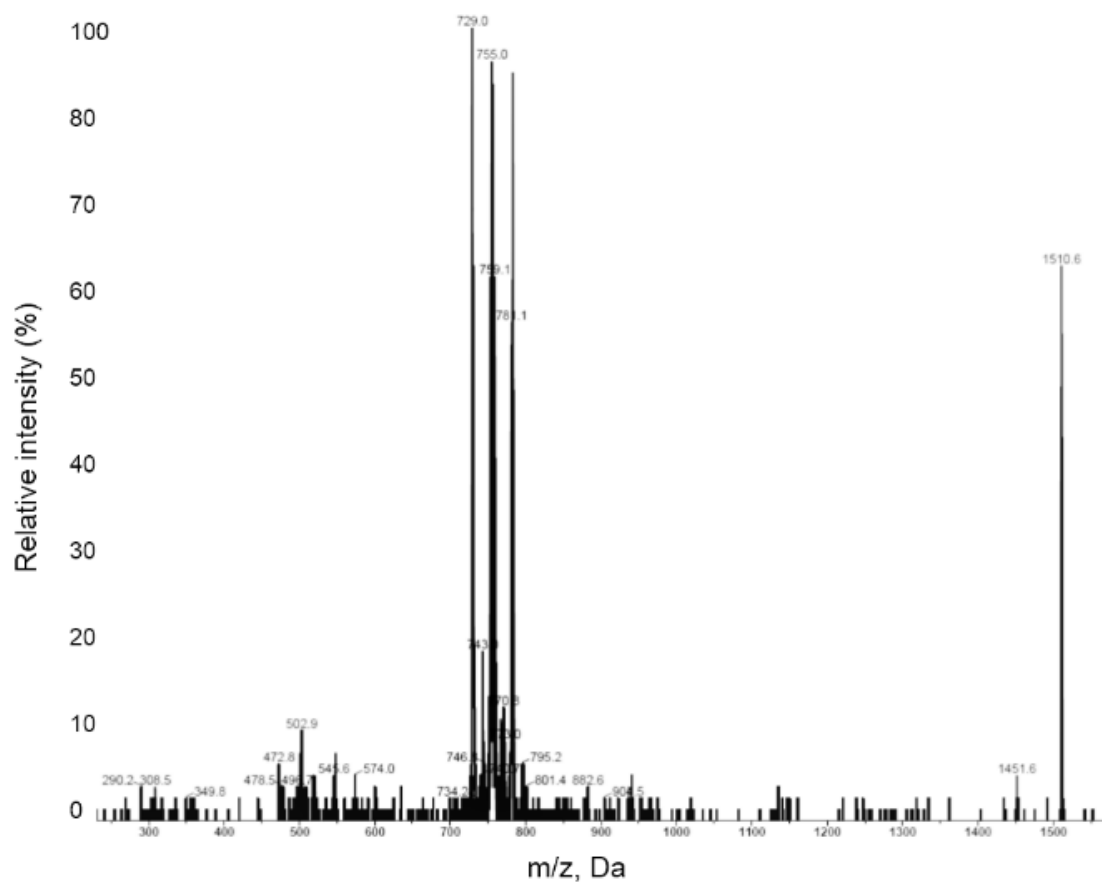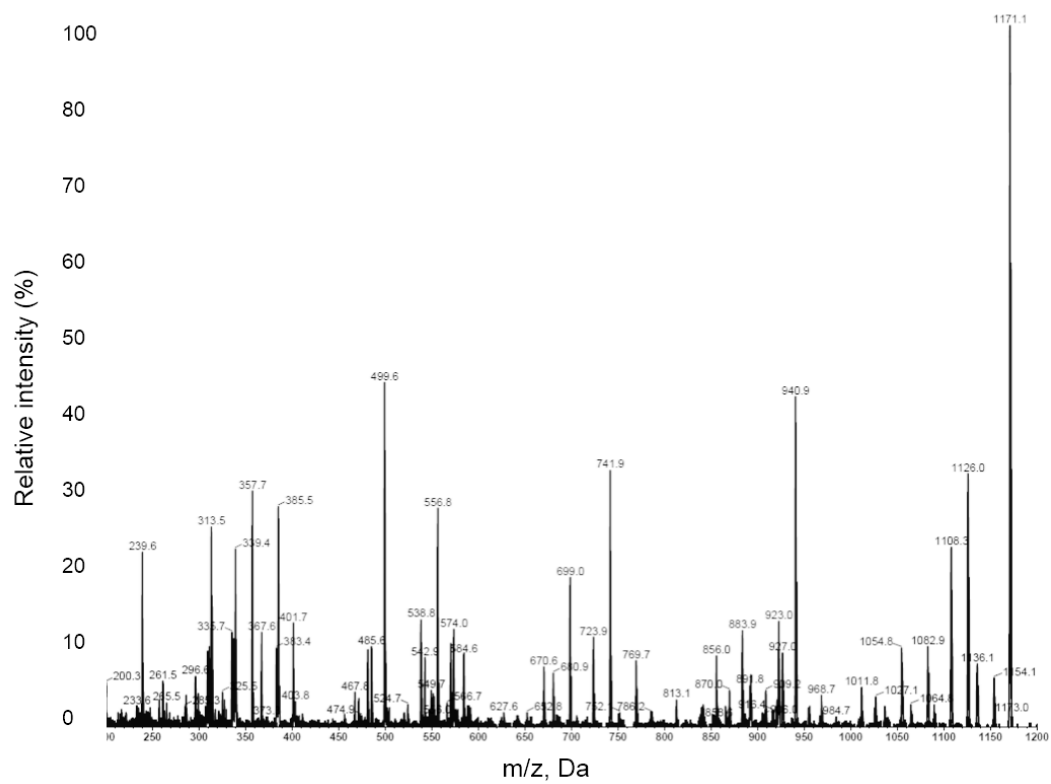
Figure 9. MS2 ion scan of cardiolipin

Figure 10. MS2 ion scan of unknown lipids.